MEASUREMENT OF STABLE CARBON ISOTOPE RATIOS OF NON-METHANE HYDROCARBONS AND HALOCARBONS

Adriaan Tiemen Zuiderweg

2012

Cover design: Proefschriftmaken.nl || Uitgeverij BOXPress

Printed by: Proefschriftmaken.nl || Uitgeverij BOXPress

Published by: Uitgeverij BOXPress, 's-Hertogenbosch

ISBN: 978-90-8891-452-2

Cover photo: Adapted from ‘Shining through clouds’ by Wing-chi Poon (free use Wikimedia Commons) with molecular structures by Ben Mills (public domain)

MEASUREMENT OF STABLE CARBON ISOTOPE RATIOS OF NON-METHANE HYDROCARBONS AND HALOCARBONS

Metingen van Verhoudingen van Stabielekoolstofisotopen: Niet-Methaan Koolwaterstoffen en Chloorfluoorkoolstoffen

(met een samenvatting in het Nederlands)

Proefschrift

ter verkrijging van de graad van doctor aan de Universiteit Utrecht op gezag van de rector magnificus, prof.dr. G.J. van der Zwaan, ingevolge het besluit van het college voor promoties in het openbaar te verdedigen op woensdag 5 september 2012 des ochtends te 10.30 uur

door

Adriaan Tiemen Zuiderweg

geboren op 27 mei 1979
te Nijmegen

Promotor: Prof. dr. Th. Röckmann

Co-promotor: Dr. R. Holzinger

Table of Contents

Samenvatting in het Nederlands

In de klasse “vluchtige organische verbindingen” vormen (halogeen)koolwaterstoffen een aanzienlijke bijdrage aan de hoeveelheid koolstof in de atmosfeer. Daarbinnen zijn de lichte niet-methaan koolwaterstoffen (NMHC: *Non-Methane HydroCarbons*, 2 tot 7 koolstof- en meerdere waterstofatomen) en eenvoudige chloorfluorkoolstoffen (CFK, één koolstof atoom en meerdere chloor- en/of fluoratomen) speciaal van belang omdat zij in zeer belangrijke mate, en vaak zelfs exclusief bronnen hebben die zijn gekoppeld aan menselijke activiteiten. Met concentraties die doorgaans liggen in het gebied van parts-per-trillion (10^{-12} mol/mol) tot parts-per-billion (10^{-9} mol/mol) hebben deze spoorgassen, hoewel zij ondergeschikte bestanddelen zijn van de atmosfeer, diverse gevolgen zowel door hun aanwezigheid als door hun verwijderingsprocessen. Deze betreffen onder andere het veroorzaken van luchtverontreininging aan het aardoppervlak en de daaruit voorkomende gezondheidsrisico’s, het bijdragen aan antropogene klimaatverandering, en het afbreken van de ozonlaag in de stratosfeer.

Het bestaan van stabiele isotopen (atomen met een gelijk aantal protonen die slechts verschillen wat betreft hun aantallen neutronen, en niet radioactief vervallen) van verscheidene elementen die een rol spelen in de chemie en de fysica van de atmosfeer is een zegen voor het onderzoek daarnaar. Hun aanwezigheid in moleculen is waarneembaar via de massa en veroorzaakt minuscule veranderingen in intra- en intermoleculaire eigenschappen. Dit betreft fysische veranderingen (bijv. in het kookpunt) en chemische veranderingen (bijv. reactiesnelheid); ook externe interacties kunnen worden beïnvloed. Meting van de verhouding tussen een stabiele isotoop met een relatief lage abundantie en een isotoop met hoge abundantie (de stabiele-

isotoopverhouding) kan dienen voor bronherkenning, om wisselwerkingen te traceren, en om de kennis te verfijnen van diverse individule bijdragen van bronnen en "putten" (plaatsen van verwijdering uit de atmosfeer, *sinks)* aan de atmosfeer als geheel .

De stabiele koolstofisotoop ^{13}C heeft een natuurlijke abundantie van ongeveer 1,1 % en heeft voldoende fractioneel massaverschil met ^{12}C (abundantie ~ 98.9%) om relevante effecten te veroorzaken. Deze eigenschappen maken ^{13}C tot een ideale isotoop om de verhoudingen tussen en de eigenschappen van NMHC's en CFK's te onderzoeken.

Om de wetenschappelijke kennis van de bronnen, de *sinks*, en de intra- en intermoleculaire processen van deze spoorgassen te verbeteren, werd in 2006 besloten om een instrument te bouwen voor het selectief meten van NMHC concentraties en hun verhoudingen tussen de stabiele C-isotopen. Dit was bestemd voor voor gebruik in het laboratorium van de Atmospheric Physics and Chemistry Group van de Universiteit Utrecht.

Dit proefschrift beschrijft de successvolle ontwikkeling, bouw, beproeving, en de eerste toepassingen van dit koolstofisotoopverhoudingsmeetinstrument. Het is opgedeeld in vijf hoofdstukken met als afsluiting een sectie over toekomstperpectieven.

Hoofdstuk 1 bevat een algemene introductie tot de NMHC's en CFK's in kader van dit onderzoek, met inbegrip van een overzicht van de betrokken bronnen en verwijderingsprocessen, en de gevolgen van hun aanwezigheid in de atmosfeer en hun verwijdering. Verder wordt het begrip "stabiele isotopen" hier geïntroduceerd, inclusief de normatieve conventies voor rapportage daarover. Details van de effecten van isotopische substitutie in termen van variaties in fysische, chemische en

biologische wisselwerkingen (bekend onder de naam fractionering) en het gebruik daarvan in de wetenschap van de atmosfeer worden hier ook gepresenteerd. Dit wordt gevolgd door een overzicht van de technische achtergrond van de instrumentontwikkeling voor isotoopmetingen, met inbegrip van een discussie over het gebruik van standaarden voor het eenduidig presenteren van resultaten. Dit hoofdstuk wordt afgesloten met een overzicht van de daaropvolgende vier hoofdstukken, en de belangrijkste vondsten daarin.

Hoodfstuk 2 beschrijft de ontwikkeling van het Utrecht NHMC stabiele-koolstofisotoopverhoudingsmeetinstrument. Technishe details worden beschreven van de terzake doende meetconcepten, en het ontwerp, het testen en de validatie tegen internationale standaarden. Hierop volgt de eerste toepassing: de analyse van NMHC in buitenlucht bemonsterd op de campus van de universiteit. De interpretatie van de resultaten wat betreft mogelijke bronnen, en vergelijking met voorgaande metingen volgt hierop.

Hoofdstuk 3 beschrijft de eerste metingen (voor zover wij weten) van fractionering bij de UV-fotolytische splitsing van CFK-11 en -12 (de meest voorkomende CFK's). De relevantie, beperkingen, en betekenis van deze metingen, en de implicaties hiervan voor de atmosferische metingen van deze CFK's worden in detail uiteengezet.

Vervolgens beschrijft hoofdstuk 4 de onverwacht ver uiteenlopende resultaten van metingen van koolstofisotoopverhoudingen van CFK-12 in luchtmonsters uit niet-geconsolideerde monsters van samengepakte sneeuw (zogeheten *firn*) uit Groenland. Een onverwacht grote verschuiving in de isotoopverhouding werd gevonden op grote diepte (overeenkomend met oude lucht). Interpretatie door middel van modelering van de eigenschappen van de *firn* geeft aan dat deze in het midden van de 20^{e} eeuw

moet hebben plaatsgevonden. Modelering door middel van massabalansen, gecombineerd met metingen aan het exclusieve atmosferische verwijderingsproces van deze verbinding, wijst erop dat de isotoopverhouding van de bron van CFK-12 in de loop der tijd aanzienlijk moet zijn veranderd. De vermoedelijke oorzaak ligt in technologische veranderingen in de synthese van CFK's in de afgelopen eeuw, die inderdaad hebben plaatsgevonden.

Hoofdstuk vijf (in twee delen) presenteert aanvullende data voor (voornamelijk) hoofdstuk 4. Het eerste deel meldt metingen van CFK-12 koolstofisotoopverhoudingen uit luchtmonsters van het CARIBIC project. Deze werden op 9-11 km hoogte per vliegtuig bemonsterd en dienen daarom als referentiepunt voor verhoudingswaardes in de verafgelegen atmosfeer.

Het tweede deel van hoofdstuk 5 betreft 7 volledige concentratie- en isotoopverhoudingsmetingen van niet-methaan koolwaterstoffen uit *firn* monsters uit Groenland, dezelfde monsters als in hoofdstuk 4. Deze metingen zijn tot nu toe niet gepubliceerd, maar zij zijn van betekenis voor de context van NMHC metingen omdat ze een ruwgeschatte recente atmosferische geschiedenis presenteren van deze stoffen op het noordelijk halfrond.

In het laatste hoofdstuk worden mogelijkheden voor toekomstige metingen en mogelijke technische verbeteringen van het instrument besproken. Onder andere: doorlopende metingen van buitenlucht om dagelijkse en seizoensgebonden cycli te bepalen; (verder) onderzoek naar de fractionering en isotoopeffecten eigen aan reacties van NMHC en CFK met diverse componenten; het uitbreiden van de kennis van globale isotopenwaardes en gradiënten door het meten van monsters van diverse herkomst; en de mogelijke verbetering van het instrument door de processen te

optimaliseren voor tijdwinst en meetgevoeligheid, om nieuwe mogelijkheden voor onderzoek te openen.

Hartelijk dank aan Tjip Lub voor het nakijken en grondig verbeteren van deze samenvatting.

Summary in English

Within the realm of volatile organic compounds, hydrocarbons and halocarbons form a sizable proportion of carbon input to the atmosphere. Within these compound categories, the light non-methane hydrocarbons (NMHC, two to seven carbon atoms) and monocarbon halocarbons have a special place as these have strong, if not exclusive, anthropogenic (human-caused) sources. With common atmospheric molar mixing ratios in the parts-per-trillion (10^{-12} mole/mole) to parts-per-billion (10^{-9} mole/mole) range, these trace gases, though decidedly minor constituants of the atmosphere, have diverse consequences due to their atmospheric presence and their removal processes. Effects range from causing ground level air pollution and resulting hazards to health, to contributing to anthropogenic climate change and the destruction of the ozone layer in the stratosphere, among many others.

The existance of stable isotopes (otherwise identical atoms with varying amounts of neutrons that do not spontaneously disintegrate) in several elements relevant to atmospheric chemistry and physics is a boon to research. Their presence in molecules is detectable by mass and cause small intra- and intermolecular property changes. These changes range from the physical (e.g. boiling point variation) to the chemical (reaction rate variation) and can influence external interactions as well. The measurement of the ratio of a minor stable isotope of an element to the major one (the stable isotope ratio) can be used to establish source fingerprints, trace the interaction dynamics, and refine the understanding of the relative contribution of sources and sinks to the atmosphere as a whole.

The stable minor stable isotope of carbon, ^{13}C, has a natural abundance of approximately 1.1 %. It has a sufficient fractional mass difference from its major

isotope as to cause significant effects, making it ideal for measuring the ratios and properties of hydro- and halocarbons. In order to enable a better understanding of the behavior of these compounds in terms of their sources, sinks, inter- and intramolecular processes, it was decided in 2006 to develop an instrument capable of selectively measuring NMHC mixing ratios and stable carbon isotope ratios for use in the laboratory of the Atmospheric Physics and Chemistry Group at Universiteit Utrecht.

This thesis documents the successful development, construction, testing and first applications of this stable carbon isotope ratio instrument. It is divided into five chapters plus a section on future perspectives:

Chapter one contains a general introduction to the non-methane hydrocarbons and monocarbon halocarbons in the context of this research, including an overview of their sources, sinks, and effects from their atmospheric presence and removal. Further, stable isotopes are introduced here along with the standard conventions of reporting these. Details of the effects of isotopic substitution in terms of physical, chemical and biological interaction variation (known as fractionations), and the usage of these in atmospheric science are presented here as well. An overview of the technical background in stable isotope instrument development and the standard components used in measurement follows, including a discussion of the use of standards for uniform presentation of findings. The chapter concludes with a summary of the following four chapters and their key findings.

Chapter two documents the development of the Utrecht NMHC stable carbon isotope ratio instrument. Technical details of the relevant measurement concepts, and the design, testing and verification to international standards of the instrument are presented. Following this, a first application: the analysis of hydrocarbons from urban

ambient air sampled at the Universiteit Utrecht campus. Interpretation of the results in terms of possible sources and the comparison with previous measurements follow.

Chapter three reports the first (to our knowledge) measurements of a fractionation in the laboratory ultraviolet photolytic removal of the monocarbon chlorofluorocarbons CFC-11 and -12, the most abundant anthropogenic halocarbons in the atmosphere. The relevance, limitations and significance of these measurements and their implications with regards to atmospheric measurements of these halocarbons is discussed in detail.

Continuing, chapter 4 reports the measurement of an unexpectedly large variation with depth in CFC-12 stable carbon isotope measurements from Greenland unconsolidated snow (firn) samples. Interpretation through modeling of the firn properties places this as having taken place in the middle part of the 20th century, with significant changes since to current atmospheric isotope ratio values. Combined with the measurements of the fractionation in the sole removal process of this compound, as presented in chapter 3, mass balance modeling indicates that the isotope ratio of the source of CFC-12 must have changed substantially with time. This is ascribed to significant technological changes in the synthesis of the compound, which did occur during the course of the the 20th century.

Chapter 5 presents additional measurements for reference and completeness of the previous chapters as appendicies. First, the evaluation of a set of upper troposphere air samples from the CARIBIC I project for CFC-12 mixing ratio and stable carbon isotope ratios gives a reference point for well-mixed remote lower atmosphere values of this compound for chapter 4. Second, the seven most complete non-methane hydrocarbon compound mixing and stable carbon isotope ratio measurements from the same firn samples as in chapter 4 are presented here. These have as yet not been

published, but are relevant to the measurement of NMHC as they present a rough recent northern hemisphere atmospheric history of these compounds as trapped in the unconsolidated snow.

Finally, in Future Perspectives, some possibilities for future measurements in stable isotope ratios with the Utrecht NMHC instrument are discussed. These include the establishment of continuous air sampling for enhancing understanding of diurnal and seasonal cycles; (further) study of fractionations and isotope effects in hydrocarbons and halocarbons; expanding the understanding of global atmospheric stable isotope ratios and gradients through the analysis of samples of diverse sources; and technical enhancements and adaptations to the instrument for opening new avenues of research.

Resumen en Castellano

Dentro del ámbito de los compuestos orgánicos volátiles, hidrocarburos y halocarburos forman una proporción considerable de carbono a la atmósfera. Dentro de estas categorías compuestas, los hidrocarburos livianos con exclusión de metano (en inglés: non-methane hydrocarbons o NMHC, de dos a siete átomos de carbono) y los halocarbonos monocarbonados tienen un lugar especial ya que éstos constituyen fuente antropogénica (causado por el hombre).

Con comunes rangos molares de mezcla atmosférica en partes por trillón (10^{-12} mole/mole) a partes por billón (10^{-9} mole/mole), estos gases traza, aunque sean menores constituyentes de la atmósfera, tienen diversas consecuencias debido a su presencia en la atmósfera y sus procesos de eliminación de compuestos de éste tipo. Los efectos van desde la contaminación del aire (polución) a nivel del suelo y los riesgos resultantes para la salud, hasta la que contribuye al cambio climático antropogénico y la destrucción de la capa de ozono en la estratosfera, entre muchos otros.

La existencia de los isótopos estables (átomos idénticos a excepción de cantidades variables de neutrones que no se desintegran de forma espontánea) en varios elementos relevantes a la química atmosférica y la física es una gran ayuda a la investigación. Su presencia en las moléculas es detectable por la masa y causa pequeños cambios en las propiedades intra-e intermoleculares. Estos cambios van desde la física (por ejemplo, la variación del punto de ebullición) a la química (la variación de velocidad de reacción) y puede influir en las interacciones externas también.

La medición de la proporción de un isótopo estable menor de un elemento a la de uno de mayor abundancia (la proporción de isótopos estables) puede ser utilizado para establecer las huellas dactilares de origen, traza la dinámica de interacción, y refinar la comprensión de la contribución relativa de las fuentes y los suministros para el atmósfera como un todo.

El isótopo estable del carbono, ^{13}C, tiene una abundancia natural de alrededor del 1,1%. Tiene una suficiente diferencia de masa fraccional comparado con el isótopo más abundante, como para causar efectos importantes, por lo que es ideal para medir las relaciones y propiedades de los hidrocarburos y los halocarbonos.

A fin de permitir una mejor comprensión del comportamiento de estos compuestos en términos de sus fuentes, los suministros, los procesos inter e intramolecular, se decidió en 2006 desarrollar un instrumento capaz de medir selectivamente la proporción de mezcla de NMHC y la proporción de isótopos de carbono estables para su uso en el laboratorio de Física y Química de la Atmósfera de la Universidad de Utrecht.

Esta tesis documenta el exitoso desarrollo, construcción, pruebas y las primeras aplicaciones de este instrumento. Se divide en cinco capítulos, además de una sección sobre las perspectivas de futuro:

El primer capítulo contiene una introducción general a los hidrocarburos con exclusión de metano y los halocarburos monocarburados en el contexto de esta investigación, incluyendo una visión general de sus fuentes, los suministros y los efectos de su presencia en la atmósfera y la eliminación de compuestos de éste tipo.

Además, se introducen los isótopos estables, junto con las convenciones estándar. Los detalles de los efectos de sustitución isotópica en términos de propiedades físicas,

químicas y la variación interacción biológica (conocido como fraccionamientos), y el uso de estos en la ciencia atmosférica se presentan aquí también.

Le sigue información técnica general sobre el desarrollo del instrumento y los componentes estándar que se utilizan en la medición de los isótopos estables incluyendo una discusión sobre el uso de normas para la presentación uniforme de los resultados. El capítulo concluye con un resumen de los siguientes cuatro capítulos y sus principales conclusiones.

Capítulo dos documenta el desarrollo del instrumento que mide la relación isotópica de NMHC carbono estable. Los detalles técnicos de los conceptos de medición pertinentes y el diseño, prueba y verificación de las normas internacionales del instrumento se presentan también. Después de esto, una primera aplicación: el análisis de hidrocarburos de la muestra del aire urbano ambiental en el campus de la Universidad de Utrecht. La interpretación de los resultados en términos de las posibles fuentes y la comparación con mediciones anteriores.

El capítulo tres muestra la primera medición en laboratorio de la historia (que nosotros sepamos) de un fraccionamiento en el reacción fotolítica ultravioleta de los clorofluorocarburos CFC-11 monocarburados y -12, el más abundante de los halocarburos antropogénicos en la atmósfera. La relevancia, las limitaciones e importancia de estas mediciones y sus implicaciones con respecto a las mediciones atmosféricas de estos hidrocarburos halogenados se discute en detalle.

Continuando, el capítulo 4 presenta la medición de una gran variación inesperada con profundidad en los mediciones de isótopos de carbono estables en CFC-12 en muestras de nieve no consolidadas “firn” de Groenlandia. Interpretación a través del modelado de las propiedades de “firn” traslada esta mediciones a la parte media del siglo 20, con cambios significativos comparado a los valores isotópicos actuales de la

atmósfera. Combinado con las mediciones del fraccionamiento en el proceso de eliminación de este compuesto único, tal como se presenta en el capítulo 3, el modelado del balance de masas indica que la relación isotópica de la fuente de CFC-12 debe haber cambiado sustancialmente con el tiempo. Esto se atribuye a los cambios tecnológicos significativos en la síntesis del compuesto, que se produjeron durante el curso del siglo el 20.

El capítulo 5 presenta mediciones adicionales para la referencia y la integridad de los capítulos anteriores como apéndices también:

En primer lugar, la evaluación de un conjunto de muestras de la troposfera superior de aire del proyecto CARIBIC I para el CFC-12 proporción de mezcla y proporciones de isótopos de carbono estables da un punto de referencia para los bien mezclados valores de la atmósfera baja de este compuesto para el capítulo 4. En segundo lugar, los siete más completos hidrocarburos con exclusion de metano mezcla e isotopos estables de carbono mediciones de mismas muestras de nieve como en el capítulo 4 se presentan aquí. Estos todavía no se han publicado, pero son relevantes para la medición de NMHC, ya que presentan una sólida y reciente historia de la atmosférica en el hemisferio norte sobre estos compuestos como los atrapados en la nieve no consolidada.

Por último, en perspectivas de futuro, algunas posibilidades para futuras mediciones en las relaciones de isótopos estables con el instrumento de Utrecht NMHC se discuten. Estos incluyen el establecimiento de un continuo muestreo de aire para mejorar la comprensión de los ciclos diurnos y estacionales; (además) el estudio de fraccionamientos y los efectos de los isótopos en los hidrocarburos y halocarburos, ampliar la comprensión de la proporción mundial de isótopos estables de la atmósfera y gradientes a través del análisis de muestras de diversas fuentes, y las mejoras

técnicas y adaptaciones en el instrumento para la apertura de nuevas vías de investigación.

Muchas gracias para Catalina Gómez Álvarez por el traducción de este resumen.

Chapter 1: Introduction

1.1 The atmosphere, non-methane hydrocarbons, and chlorofluorocarbons

The Earth's atmosphere is a complex mixture of many compounds. It is well known that it is composed of majority nitrogen (~78%), approximately 21% oxygen and ~1% argon, but it has many additional species as well, of varying abundance. Those species may be termed trace gases, and it is more practicable to express their abundances in terms of mole fractions[1] than in percent. Among these are carbon-based compounds such as carbon dioxide (mixing ratio ~360 ppm) and methane (~1.8 ppm), which are the basis for much discussion in terms of their aspects with regards to climate change.

However, a significant amount of the total carbon input (estimated as near 1150Tg y^{-1}, Guenther et al. 1995) to the atmosphere consists of reactive non-methane hydrocarbons (NMHCs), which belong to the category of volatile organic compounds (VOC). These are emitted to the atmosphere through many processes, both natural as a product of plant metabolism, decay and natural combustion of plant material, and anthropogenic including biomass burning for land clearing, cooking, agricultural waste burning, fossil fuel combustion, and industrial processes. While they do not have direct climactic impact, non-methane hydrocarbons play important roles in atmospheric chemistry contributing to the production of tropospheric ozone and

[1] Mole fraction mixing ratios e.g. ppm (parts-per-million: 10^{-6} mole per mole), ppb (parts-per-billion: 10^{-9} mole/mole) and ppt (parts-per-trillion: 10^{-12} mole/mole) are the most common ways to present trace gas abundances.

[2] Minor stable isotopes that are useful for measurement should have a large fractional mass difference, (e.g. ^{1}H and ^{2}H fractional mass difference is 100%) The larger this

resultant photochemical pollution, the formation of aerosol particles, and the oxidative capacity of the atmosphere (Warneck 1988, Seinfeld & Pandis 1998, Goldstein and Galbally 2007).

Low molecular weight NMHC, consisting of compounds with 2 to 7 carbon atoms (C_2 to C_7), account for the vast majority of anthropogenic emissions to the troposphere (Middleton, 1995). Acetylene (C_2H_2), ethylene (C_2H_4), propyne (C_3H_4), and propylene (C_3H_6), originate primarily from combustion processes such as fossil fuel combustion and biomass burning. The alkanes, ethane (C_2H_6), propane (C_3H_8), isomers (compositionally identical molecules but with differing structures) of butane (C_4H_{10}), isomers of pentane (C_5H_{12}), and onwards mainly stem from natural gas leakage and petroleum product evaporation, with significant sources from the traffic and transportation as well. Aromatic compounds e.g. benzene (C_6H_6) and toluene (C_7H_8) originate mainly from transportation and solvent evaporation (Goldstein and Shaw 2003; Redeker et al., 2007). Abundance of these volatile compounds is highly variable due to their source distribution and high reactivity. These can have mixing ratios at ppb levels in urban environments or may be of such low level in remote environments that these are virtually undetectable (Seinfeld and Pandis 1998).

The chlorofluorocarbons CFC-11 ($CFCl_3$) and CFC-12 (CF_2Cl_2) are the most abundant anthropogenic halocarbons in the atmosphere with high mixing ratios and very consistent distributions throughout the lower atmosphere due to their stability. Before their production was banned under the Montréal Protocol and its amendments, the usage of these compounds as refrigerants, cleansers, aerosol propellants and foam-blowing agents worldwide resulted in significant atmospheric loading; at their peaks in 1990 and 2003, respectively, mean mixing ratios in the troposphere were approximately 260 ppt for CFC-11 and 550 ppt for CFC-12 (Forster et al., 2007;

AGAGE 2011). Due to the buildup of these and other anthropogenic halocarbons, total organic chlorine levels in the troposphere increased from approximately 600 ppt in 1900 to nearly 3350 ppt in 2008 (Butler et al., 1999; WMO 2010).

Oxidative processes provide the atmospheric removal mechanism of hydrocarbon compounds, mainly through reaction with the hydroxyl molecule (OH). Hydroxyl is a major atmospheric cleaning agent, reacting with diverse species and triggering their removal from the atmosphere. It is produced through the photolysis of ozone by UV wavelengths near 300nm and reaction with water vapor (Warneck 1988):

$$O_3 + h\nu \xrightarrow{\lambda \sim 300\,nm} O_2 + O(^1D) \qquad \text{(R1.1)}$$

The oxygen radical thus produced can react with water vapor in the following reaction:

$$O(^1D) + H_2O \longrightarrow 2OH \qquad \text{(R1.2)}$$

OH reaction is by far the dominant oxidation process of non-methane hydrocarbons. Other oxidative mechanisms include NO_3, Cl, or O_3 (Warneck 1988; Seinfeld and Pandis 1998; Brenninkmeijer 2009). The reaction pathway for ethane (C_2H_6) in an environment where oxides of nitrogen are present (e.g. urban situation) provides a simple example. Hydrogen abstraction from the hydrocarbon by OH is the start of the removal process:

$$C_2H_6 + OH \rightarrow C_2H_5\bullet + H_2O \qquad \text{(R1.3)}$$

and fast reaction with molecular oxygen follows:

$$C_2H_5\bullet + O_2 \rightarrow C_2H_5O_2\bullet \qquad \text{(R1.4)}$$

From this point, $C_2H_5O_2\bullet$ can react in a polluted atmosphere with nitrogen oxide (NO) which is generated at high temperature in combustion engines:

$$N_2 + O_2 \rightarrow 2NO \qquad \text{(R1.5)}$$

$$C_2H_5O_2\bullet + NO \rightarrow C_2H_5O\bullet + NO_2 \quad \text{(R1.6)}$$

In the absence of NO (as is the case in remote environments) HO_2 reacts with $C_2H_5O_2$ to form C_2H_5OOH, which is removed in subsequent steps from the atmosphere.

Continuing, $C_2H_5O\bullet$ reaction with oxygen forms acetaldehyde:

$$C_2H_5O\bullet + O_2 \rightarrow CH_3CHO + HO_2 \quad \text{(R1.7)}$$

Further, CH_3CHO is oxidized in the following net reaction, again in the presence of NO:

$$CH_3CHO + 3NO + 3O_2 \rightarrow HCHO + 3NO_2 + CO_2 + H_2O \quad \text{(R1.8)}$$

and the resulting formaldehyde (HCHO), photolyzed by high energy photons, reacts with oxygen:

$$HCHO + h\nu + 2O_2 \rightarrow 2HO_2 + CO \quad \text{(R1.9)}$$

Thus the initial oxidation by OH of ethane, provided the presence of nitrogen oxides, yields, following several steps, in H_2O, CO_2, CO, NO_2 and HO_2. Other hydrocarbon species have different (and vastly more complicated) reaction chains (Warneck 1988; Conny and Currie, 1996) but they typically yield the same final products.

NO_2 and HO_2 are the starting point for the development of tropospheric ozone by the following reactions, and simultaneously allows for the recycling of OH:

$$NO + HO_2 \rightarrow NO_2 + OH \quad \text{(R1.10)}$$

$$NO_2 + h\nu + O_2 \rightarrow NO + O_3 \quad \text{(R1.11)}$$

As opposed to ozone in the upper atmosphere, which provides an ultraviolet radiation blocking function that is vital for the existence of life on earth, lower atmosphere ozone is a pollutant as it is detrimental to pulmonary health. Further, tropospheric ozone and nitrogen oxides, when combined with oxidized hydrocarbon compounds under the right atmospheric conditions react to begin the development of

photochemical smog. This smog is a major urban nuisance and is a severe irritant to the eyes and lungs. In order to reduce the development of this smog and curtail vehicular emission of carbon monoxide (also hazardous to health), the fitting of catalytic converters to internal combustion engines became commonplace in the 1980s. This has reduced the abundance of emissions markedly, improving air quality in cities (Warneck 1988; Wang et al., 2011).

Fully halogenated halocarbons are removed by altogether different processes than oxidative reactions mentioned above. These have their only significant sinks in the stratosphere, at altitudes where UV-C radiation ($\lambda < 220$nm) is sufficiently abundant to dissociate the C-Cl bond. A minor sink (approximately 3-7 %) is due to Cl abstraction by $O(^1D)$, which is produced from the ozone photolysis reaction mentioned previously (eq. R1.1) (Seinfeld and Pandis, 1998; Laube et al., 2010).

$$CF_mCl_{4-m} + h\nu \xrightarrow{\lambda<220\ nm} CF_mCl_{3-m} + Cl\cdot \qquad (R1.12)$$

$$CF_mCl_{4-m} + O(^1D) \longrightarrow CF_mCl_{3-m} + ClO \qquad (R1.13)$$

The most common, CFC-11 and -12, have very long atmospheric lifetimes of 45 and 100 years respectively, as the removal process is slow (Forster et al., 2007; WMO 2010). The release of chlorine into the stratosphere is the starting point for the catalytic destruction of ozone, which was first theorized by Molina and Rowland in 1974:

$$O_3 + Cl \longrightarrow O_2 + ClO \qquad (R1.14)$$

$$ClO + O \longrightarrow O_2 + Cl \qquad (R1.15)$$

This reaction is responsible for the systematic depletion of ozone in the atmosphere. In combination with high chlorofluorocarbon global warming potential, these wholly anthropogenic compounds have a significant atmospheric impact, which was

sufficient cause for these and other chlorine containing compounds to be banned in the 1987 Montréal protocol and subsequent amendments. As a result, release to atmosphere has been drastically reduced (though not wholly eliminated) and atmospheric mixing ratios have reduced from their peaks. However, as atmospheric chlorine is persistent, ozone depletion will continue despite the decrease of chlorofluorocarbon abundance, and stratospheric ozone will take considerable time to recover to pre-industrial levels (WMO 2010).

1.2 Stable isotopes and isotope fractionation

Isotopes of a species are defined as atoms with an identical number of protons but varying numbers of neutrons. Isotopes of elements generally have identical chemical properties (Breninkmeijer et al., 2009). As the name implies, stable isotopes of species are those that do not disintegrate spontaneously through radioactive decay. The trace gases of major interest in atmospheric chemistry consist mostly of hydrogen, carbon, nitrogen, oxygen, sulfur, chlorine and fluorine. With the exception of fluorine, these have useful[2] minor stable isotopes, the relative abundance of which can be measured to ascertain specific properties of compounds and reactions.

The elements mentioned above have varying numbers of stable isotopes: hydrogen has two (^{1}H and ^{2}H which is also known as deuterium), carbon two (^{12}C and ^{13}C), nitrogen two (^{14}N and ^{15}N), oxygen three (^{16}O, ^{17}O and ^{18}O), sulfur four (^{32}S, ^{33}S, ^{34}S, and ^{36}S) and chlorine two (^{35}Cl and ^{37}Cl). The minor stable isotope of carbon, ^{13}C, which is the stable isotope of concern for this work, has an average natural abundance

[2] Minor stable isotopes that are useful for measurement should have a large fractional mass difference, (e.g. ^{1}H and ^{2}H fractional mass difference is 100%) The larger this difference is, a greater isotope effect can be expected in processes involving the atom concerned. Also, it is important for the minor isotope to have a sufficient abundance to allow for adequate detection.

of approximately 1.1%; other mentioned elements have stable isotope abundances both much larger and smaller (Goldstein and Shaw 2003).

Molecules that differ only in their isotopic composition are referred to as isotopologues. Isotopologues have slightly different physical and chemical properties. The standard method of quantifying the relative abundance of isotopologues in sample is the stable isotope ratio, which is expressed as:

$$\delta^{13}\mathrm{C} = \frac{{}^{13}R_{\text{sample}}}{{}^{13}R_{\text{standard}}} - 1 \qquad (1.1)$$

where ${}^{13}R$ is the ${}^{13}\mathrm{C}/{}^{12}\mathrm{C}$ ratio in a sample or standard material, respectively. Measurements are referenced against a standard carbon isotopic ratio, usually VPDB (Vienna Pee Dee Belemnite, see discussion below). Measurements of $\delta^{13}\mathrm{C}$ are commonly multiplied by 1000‰ for readability purposes. Species of a compound having relatively more of the heavier isotope may be termed enriched, whereas those that have relatively less may be described as depleted (Goldstein and Shaw, 2003; Brenninkmeijer 2009).

1.3 Isotope fractionations

Chemical (reaction caused), Physical (e.g. diffusion), and biological (e.g. photosynthesis), processes often act slightly differently on isotopologues, causing an enrichment or depletion (increase or decrease, resp.) in the isotope ratio of a species. The fractionation that results is known as an isotope effect. Generally the magnitude is closely tied to the mass difference between the isotopologues concerned and therefore is known as mass dependent. If the magnitude of observed fractionation does not follow mass dependency, the fractionation concerned falls under the category of mass independent fractionation (MIF).

1.3.1 Chemical isotope fractionation

Isotope fractionations that occur as a result of chemical reactions are known as chemical isotope effects. Isotopically lighter molecules usually react faster than isotopically heavier ones. In the case of carbon stable isotopes, this is because bonds in molecules containing solely ^{12}C atoms are weaker than those containing one or more ^{13}C atoms. This causes small deviations from the original $^{13}C/^{12}C$ ratio during chemical degradation (Goldstein and Shaw 2003). The ratio of the two reaction rate coefficients (*k,* with the isotope concerned denoted by subscript) of the respective isotopologues is known as a kinetic isotope effect (*KIE*) for a particular reaction. This is commonly expressed in one of several ways, and often expressed in per mille, again for readability:

$$KIE = \frac{k_{12}}{k_{13}} \tag{1.2}$$

$$\alpha = \frac{k_{13}}{k_{12}} \tag{1.3}$$

$$\varepsilon = \alpha - 1 \tag{1.4}$$

The latter is often known as an isotope fractionation. In lighter molecules an isotope substitution makes for a larger fractional mass difference and thus a larger isotope effect (Anderson et al., 2004).

Knowledge of the KIE or fractionation of relevant processes can provide a tool to improve the understanding of atmospheric processing of compounds (Rudolph and Czuba, 2000). As an example, the kinetic isotope effect inherent in the oxidation of various non-methane hydrocarbons with OH and other compounds causes an isotope enrichment that is clearly detectable and subsequently predictable in the atmosphere. These KIEs, as measured by e.g. Anderson et al. (2004) allows the calculation of the

change in isotope ratio given the passage of time. Also, the fractionation in the photolysis of chlorofluorocarbons causes an atmospheric enrichment over time that will likely be detectable in future measurements (see chapter 3).

1.3.2 Physical isotope fractionation

Similarly, physical processes can be responsible for fractionations in populations of species as well. Similar to intramolecular force changes within different isotopologues, intermolecular forces vary as well. By consequence, some physical properties, e.g. diffusive and phase change behavior may differ slightly. Measurements of the physical fractionations may be expressed similarly to chemical fractionations.

For example, the diffusive behavior of gases through unconsolidated snow (firn) is affected by the presence of isotopologues. Lighter species diffuse faster through the medium and therefore induce an isotopic gradient (Braunlich et al., 2001). This is relevant to the research for chapter 4, where firn air samples were analyzed for CFC δ^{13}C. Modeling of firn air properties had to be undertaken to determine the magnitude of this effect and to compensate for it in the analysis of the sample δ^{13}C data.

Another example exists in the water cycle, where water is evaporated from oceans and lakes, condensed in the atmosphere, and precipitated to the surface. Deuterium-containing water molecules have a slightly higher boiling point and thus an isotope fractionation occurs during evaporation and condensation. This is most clearly seen in measurements of precipitation δD, where strong isotope depletions are noted. Further, as the amount of evaporation and condensation varies per latitude because of temperature differences, precipitation in colder regions is more depleted than that in the tropics. This latitude dependence in precipitation δD resulting from the physical fractionation has been further noticed in molecular hydrogen emanating from biomass

burning, measured from wood samples collected from various regions around the globe (Röckmann et al., 2010).

1.3.3 Biological isotope fractionation

Similar to chemical processes, biological interactions can also change isotope ratios by preferentially taking up or releasing light or heavy isotopologues, As an example, the uptake of CO_2 by plants during the course of photosynthesis has been shown to discriminate between heavy and light isotopologues. Park and Epstein (1961) noted the preferential uptake of the light isotopologue of CO_2 by plants: the enzyme ribulose biphosphate carboxylase discriminates against $^{13}CO_2$. By consequence plant material is more depleted in $\delta^{13}C$ by nearly 20‰ than CO_2 in ambient air (O'Leary 1981). Respiration, on the other hand, returns depleted CO_2 to the atmosphere and causes an isotopic gradient in forest air with height (Farquhar et al.,1989).

In the realm of volatile organic compounds, a further example of a biological process that has an isotopic effect is the microbial degradation of methyl chloride. Keppler et al., 2005 reported that a kinetic isotope effect (KIE) of 47‰ exists for this sink, which has a best magnitude estimate of 180 Gg yr^{-1}, though much uncertainty remains. The large magnitude of this fractionation has a significant impact on the atmospheric budget of this compound (see also section 1.5).

1.4 Mass independent fractionation

The vast majority of isotope fractionations that have been detected thus far in processes are related to the differences in mass of isotopologues. However, there are a few exceptions, which are termed mass-independent fractionations. An example of this category is the isotope effect in the photolysis and reformation of ozone. The destruction of ozone by UV light (reaction R1.1) is often quickly followed by the recombination of O_2 and $O(^1D)$ to reform O_3. Both the photolysis and reformation of

ozone induce isotope enrichment as they proceed; however, the magnitude of the enrichment is nearly equal for ozone isotopologues containing ^{17}O and ^{18}O, contrary to expectations when considering the mass difference. This enrichment anomaly is also detected in species that interact with ozone, e.g. NO_2, which is formed from the reaction of NO with ozone (Brenninkmeijer et al., 2009).

1.5 The use of stable isotope ratios in atmospheric sciences

Beyond the use of isotope ratios in the determination of physical, chemical, and biological isotope effects in processes involving species, the most powerful and atmospherically relevant application lies in the establishment of atmospheric budget calculations, where all sources and sinks of compounds are described in their entirety. The atmospheric stable carbon isotope ratio of a compound may be expressed in general as the sum of its sources minus the sum of its sinks (Goldstein and Shaw 2003):

$$\delta_{\text{atmosphere}} = \sum_i \delta_i S_i - \sum_j \varepsilon_j L_j \qquad (1.5)$$

Where S_i is the magnitude and δ_i the isotope ratio of the source i, L_j the magnitude and ε_j the fractionation inherent in the sink j, By using this expression, with the help of extensive sampling (fingerprinting) of source and sink magnitudes and effects, a calculation can be made of what the atmospheric isotope ratio of a compound should be. If all sources and sinks and their effects are accounted for, this should match atmospheric measurements of the compound. This is called closing the budget, though fully doing so, and thereby completely eliminating uncertainties, is very difficult (Brenninkmeijer et al., 2009).

For example, Keppler et al. (2005) report the atmospheric budget of methyl chloride through this method; arriving to an atmospheric $\delta^{13}C$ value for this compound that

agrees well with concurrent measurements: (-36.2±0.3) ‰, after an exhaustive study of (anthropo- and biogenic) source and varying sink (aforementioned biological degradation, OH oxidation, photolysis and other) factors. The accounting of all the factors through the use of stable isotopes has been an ongoing concern for many other compounds (e.g. atmospheric molecular hydrogen, methane, nitrogen oxides, carbon monoxide and carbon dioxide), though much uncertainty exists for even the most abundant trace gases (Brenninkmeijer et al., 2009). Utilizing this understanding, measurement of isotope ratios as well as the establishment of kinetic isotope effects can be powerful tools to disentangle the relative contribution of different sources to the atmospheric burden of important atmospheric trace gases.

Another clear example of the usefulness of budget calculations lies in the $\delta^{13}C$ evolution of atmospheric CO_2. The atmospheric mixing ratio of this long-lived compound has increased dramatically since the industrial age, to nearly 395 ppm in the present day (NOAA 2012). However, the atmospheric $\delta^{13}C$ value has been continuously decreasing since approximately 1800, from a preindustrial value of -6.5 ‰ to less than -8.2 ‰ today (Francey et al., 1999; Scripps CO_2 2010). The change in the stable isotope value, combined with budget calculations, confirmed the role of the anthropogenic combustion of fossil fuel (by far the largest source) in the buildup of atmospheric carbon dioxide. The mean $\delta^{13}C$ value of CO_2 from this combustion lies around -27 ‰ (Goldstein and Shaw 2003); thus the addition of vast quantities of depleted CO_2 with this value will drive down the atmospheric $\delta^{13}C$ value as a whole.

In a further application of stable isotopes in atmospheric sciences, species in the atmosphere that are removed from the atmosphere in relatively short time periods can be used as tracers. For example, in the case of light non-methane hydrocarbons, the relatively short lifetime of these compounds in the atmosphere, from mere hours to

tens of days, gives the possibility of utilizing these as tracers. Through the isotopic hydrocarbon clock approach, a parameterization describing the change of the isotope ratio with time in a given removal reaction, this can constrain transport and aging in the atmosphere of these compounds (Rudolph et al., 1981; Rudolph et al., 2002; Goldstein and Shaw 2003; Redeker et al., 2007). An application of this principle is given in chapter 2.

1.6 Historical measurement of isotope ratios in volatile organic compounds

The development of instrumentation with the capability of measuring isotope ratios in specific compounds has been a relatively recent development. The coupled gas chromatography – (combustion interface) – isotope ratio mass spectrometer (IRMS), as pioneered by Matthews and Hayes (1978) for CO_2 and N_2 isotope work, substantially improved upon earlier techniques based on dual-inlet isotope ratio mass spectrometers by greatly reducing necessary sample size and eliminating the need to extract individual compounds from a sample, which is a difficult and time-consuming task. This breakthrough allowed significant research work into the stable isotopic ratios of carbon, nitrogen, oxygen and hydrogen containing compounds in the atmosphere.

For non-methane hydrocarbons and halocarbons appropriate instrument development is even more recent. Rudolph et al. (1997) developed the first instrument capable of compound specific stable carbon isotope ratio analysis measurements of multiple NMHCs. This instrument was initially used for observing carbon isotope ratios of emissions from biomass burning and transportation related sources, and urban environment atmospheric samples. The observance of the magnitude of the kinetic isotope effect in hydrocarbon reactions with OH and O_3 was also undertaken in

subsequent research with this instrument (Rudolph et al. 1997, Rudolph et al. 2002, Iannone et al. 2003, Anderson et al. 2004). Other applications of similar instruments that have been subsequently derived include measurements of NMHC $\delta^{13}C$ in urban, marine and coastal atmospheres and over the north Pacific and east Asia to evaluate atmospheric transport and airmass age (Tsunogai and Yoshida 1999, Saito et al. 2002, Nara et al. 2007, Saito et al. 2009); of NMHC from biomass burning (Czapiewski et al. 2002, Nara et al. 2006); with some extension, measurements of halocarbons and NMHC (Archbold et al. 2005, Redeker et al. 2007); specific measurement of methyl chloride from plants and its atmospheric budget (Bill et al., 2002; Harper et al. 2003; Keppler et al. 2005). However, despite these published works, there is still a relative paucity of reference material on non-methane hydrocarbon and halocarbon $\delta^{13}C$ values, not least when concerning isotope effects in their reactions and processes.

1.7 Instrumentation technical background

In order to contribute to this growing body of work, it was decided that the development of a leading-edge compound specific NMHC and halocarbon instrument should be undertaken in the Atmospheric Physics and Chemistry Group Laboratory at the University of Utrecht starting in 2006. The design and development of this instrument and its applications to date form the body of this thesis. In this section a brief overview of the underlying technologies is presented. The development of the instrument in its entirety including technical details is presented in chapter 2.

In order to arrive to isotope ratio results from a particular sample using the constant flow method of isotope analysis, several key steps have to occur. First the sample must be processed to remove unwanted compounds and concentrate it to volumes appropriate to measurement; then the compounds concerned must be separated from

each other in order to allow distinction between them; and finally the detector, the isotope mass spectrometer, must be applied with an appropriate calibration.

1.7.1 Sample processing

The first stage of an analysis system based on constant flow technologies is sample processing. The design of this part, often called the inlet and preconcentration stage, varies depending on the samples, compounds, and conditions. Most commonly however, cryogenic traps are employed using liquid nitrogen to fix and selectively release the compounds of interest and evacuate bulk gases that may be present in a sample. Chemical treatments or adsorbant processes may also be applied at this stage to remove e.g. water and CO_2 from the sample, which may interfere with compound seperation and detection.

The inlet and preconcentration stage should be constantly purged with ultra-pure gas, e.g. hydrogen or helium to preclude contamination. This purge gas is normally the same as that which is used as the mobile phase (carrier gas) in gas chromatography (see below). All flows should be regulated to ensure consistent transfer of the sample contents and deliver them smoothly to the next phase of analysis. A properly prepared sample preparation system has the characteristics of reliable operation and consistent sample delivery with minimal unwanted retention of compounds. This part of the measurement system may or may not be automated, but it is critical that operations undertaken by it are repeatable. Therefore it is preferential to automate the operation by the use of computer commanded hardware controllers of varying types.

The use of automated sample preparation is a major advance over previous techniques. Manual operation of preconcentration systems is a tedious affair, because it is very labor intensive and repeatability is more difficult to achieve through the possibility of human error. The use of hardware controllers and computer-driven

system management has therefore aided the development of instruments that are ever more precise.

1.7.2 Gas chromatography

Gas chromatography, the practice of separating compounds in a gas stream from each other with time through the use of selective adsorption and desorption has been in use since the middle of the last century. Its underlying principle is very simple: the sample to be analyzed, contained in a carrier gas (the mobile phase or carrier gas, commonly helium or hydrogen), is introduced at once to a chromatographic separation column. This contains a specific material, known as the stationary phase, which is appropriate for selectively retaining compounds that are introduced to it. The column is normally housed in an enclosure that can be heated, inducing the release (desorption) of compounds from the column; higher temperatures speed elution. A generalized diagram of a gas chromatograph is shown in fig. 1.1.

All being equal, compounds are released (eluted) from the end of the column in the order of their boiling points. For example, ethane, with a boiling point of 185 K, will elute before propane (T_{boil} = 231 K) from a column appropriate for separating hydrocarbons. However, compound polarity and composition can complicate elution timings, inducing departures from the above guideline. If the programmed heating rate of the column and the flow rate of the mobile phase remain identical between sample runs, the elution of a given compound from the column occurs at a predictable elapsed time (the retention time) from sample injection.

In common practice, the separation column is attached to a detector that measures the quantity of eluting compounds. The detector signal is used to determine amount of substance of compounds in the sample. There are several types of detector used for this purpose. The most common include the flame ionization detector, sensitive to e.g.

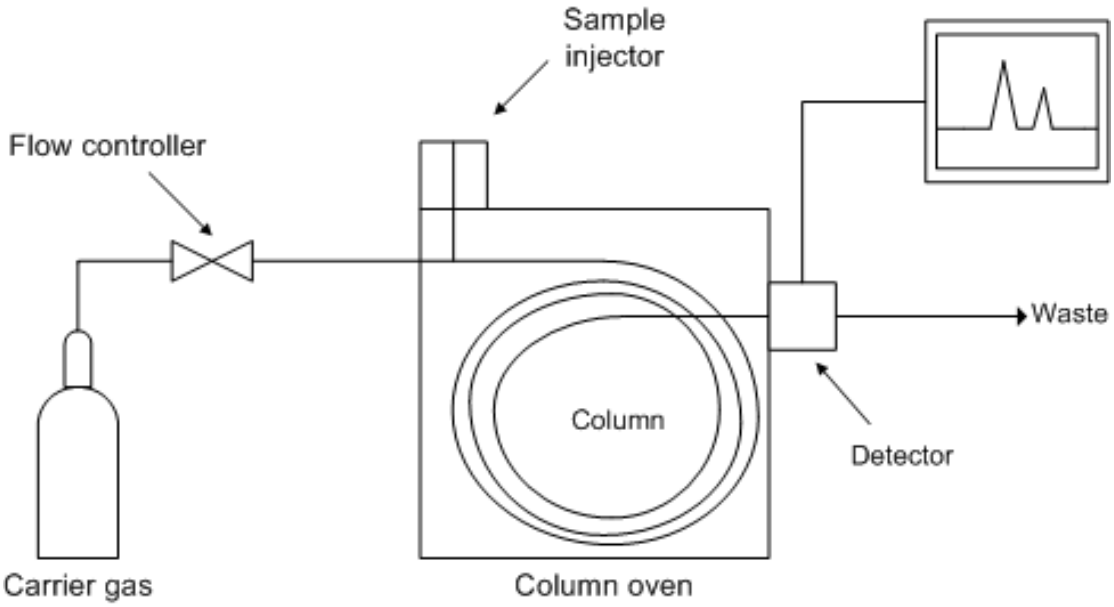

Figure 1.1. A generalized diagram of a gas chromatograph. Courtesy Wikimedia Commons.

carbon and hydrogen containing substances; the thermal conductivity detector, for verifying the purity of gases; the electron capture detector, sensitive to e.g. halogen containing compounds; or the mass spectrometer. A mass spectrometer has the capability of measuring the mass to charge ratio of ions and can in principle measure all species. There are mass filters based on electrical fields (e.g. ion trap, quadrupole type mass spectrometer) or spectrometers that separate species through electromagnetic deflection of the ions (e.g. magnetic sector field mass spectrometer). Each of these provides a signal intensity that can be plotted with time in the form of a chromatogram. An example of a chromatogram can be found in fig. 1.2, demonstrating the separation and detection of a gas mixture containing several compounds by a gas chromatograph. This figure shows the elution in series of the compounds contained in the mixture as sequential peaks with time. These peaks are integrated with time to establish the peak area, which is directly correlated to the quantity of compound injected. When combined with measurement of calibration

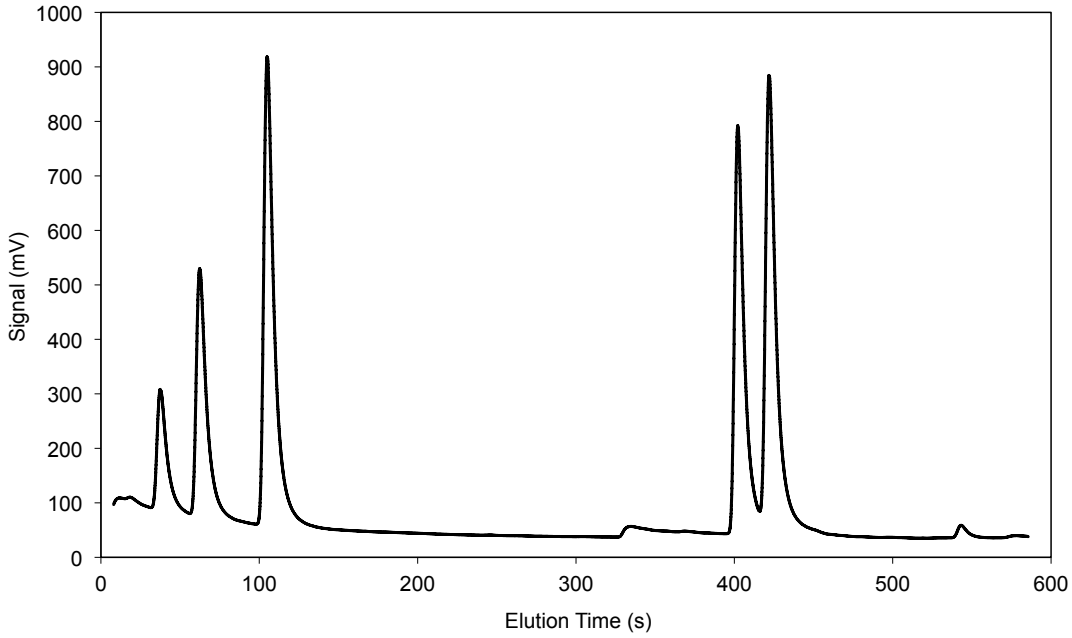

Figure 1.2. Example chromatogram from a mass spectrometer showing the sequential elution of compounds with time.

mixtures with predefined mixing ratios that establish the sensitivity of the measuring instrument, highly precise evaluations of sample mixing ratio can be obtained.

The use of calibration mixtures is vital for the accurate determination of mixing ratios. These gas mixtures may be purchased commercially or prepared per specification in the laboratory. Most commonly, in the case of volatile organic compounds, such a mixture contains one or more compounds of interest in a balance gas, for example pure nitrogen or high-quality synthetic air (78% nitrogen, 22% oxygen). The mixing ratios of the compounds are prepared to a high level of precision against a standard. The regular measurement of a calibration mixture establishes system stability in mixing ratio, and provides the aforementioned sensitivity scale to determine sample mixing ratios.

1.7.3 Combustion to analyzable species

Prior to isotope analysis through introduction to the isotope ratio mass spectrometer, species in samples must be properly prepared. Isotope ratio mass spectrometers as a rule operate on species that do not undergo fragmentation during the ionization process. Therefore, before introduction to the mass spectrometer, unless the compound to be measured for stable isotopes is already such a species (for example, $\delta^{13}C$ measurement of carbon dioxide or δD of atmospheric molecular hydrogen can be measured directly without such pretreatment), a catalytic oxidation (converting all carbon to CO_2) or reduction (converting all hydrogen to H_2) oven is used to obtain the species to be measured.

For the measurement of $\delta^{13}C$ of hydrocarbons, normally platinum, nickel oxide, copper oxide, or a combination of those materials is used in a ceramic oven at high temperature (>700 C) to oxidize hydrocarbons to CO_2 for measurement. Oxidation must be complete, for if it is not, fractionation can occur in the oxidation oven incurring erroneous results in isotope measurement.

For early isotope ratio measurement systems, this took place off-line, commonly with the oxidizing or reducing agent (and any required gases for the process) in a sealed container with the sample. This is heated to high temperatures for a time until the sample is fully converted to the analyzable species. The drawback of this technique is that components in gas mixtures cannot be analyzed separately, requiring these to be purified separately before combustion, a time consuming process. Development of the constant flow mass spectrometer coupled to a gas chromatography instrument in the 1980s allowed the use of inline combustion or reduction processes instead, paving the way for compound specific analysis in gas mixtures without this purification step.

However, any hydrocarbon oxidation process will produce water vapor. This is highly undesirable: ionization of water molecules produces free hydrogen ions which can then form HCO_2+ in the mass spectrometer, resulting in erroneous measurement of $\delta^{13}C$. To prevent this, a sulfonated tetrafluoroethylene polymer barrier such as Nafion is used in sequence after the oxidation oven. This barrier has the property of selectively allowing polar compounds such as water vapor to pass by diffusion given a concentration gradient, but preventing the passage of desired species. Typically the sample gas stream is inside a channel of this material with a dry gas stream outside, thus removing the water vapor. After these steps have been completed, the sample is ready for analysis by the isotope ratio mass spectrometer.

1.7.4 Isotope ratio mass spectrometry

A type of magnetic sector spectrometer is the isotope ratio mass spectrometer (IRMS), which is designed to measure the masses of only a few species very precisely. The basic design of the IRMS has in principle not changed since the 1950s, when it was first used in the analysis of the stable carbon isotope ratio of CO_2 (McKinney et al., 1950).

In its first practical incarnation as the dual inlet isotope ratio mass spectrometer, provided the possibility for very high precision measurements of ratios by repeatedly measuring a sample against a standard, and even now remains the benchmark technique for measurement precision (Goldstein and Shaw 2003). However, a major advance was accomplished with the development of the constant flow isotope mass spectrometer, which added a capability for accepting samples within continuous carrier gas streams (Barrie et al., 1984). This instrument has since become the standard detector for isotope measurement.

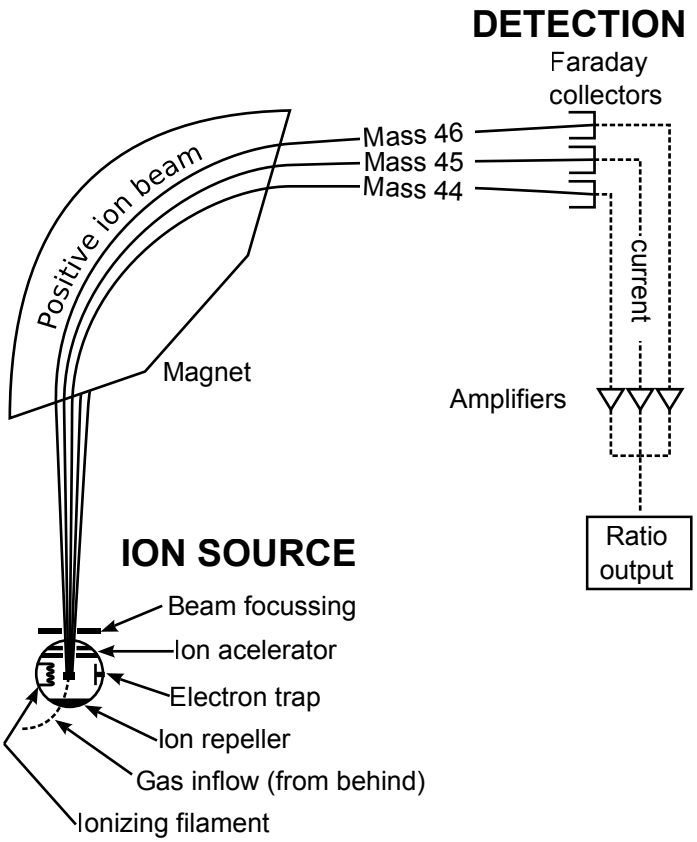

Figure 1.3. Diagram of an isotope mass spectrometer. Courtesy of the U.S. Geological Survey.

A diagram of the basic design can be found in fig. 1.3. The principle of operation is quite elegant: the separation of isotopologues of species by mass difference accomplished through the amount of deflection in a vacuum of ions in an electromagnetic field. This field is developed by a large and precisely calibrated electromagnet. Lighter isotopologues are deflected more by the electromagnetic field than heavier ones, thereby separating these in space.

Given appropriate tuning in magnetic field shape and intensity and ion acceleration voltage for the species desired, the ions are detected by a set of faraday cups, which register ion impact as electrical current. Coupled to amplifiers and high-precision resistors appropriate to the desired sensitivity of each channel, these produce

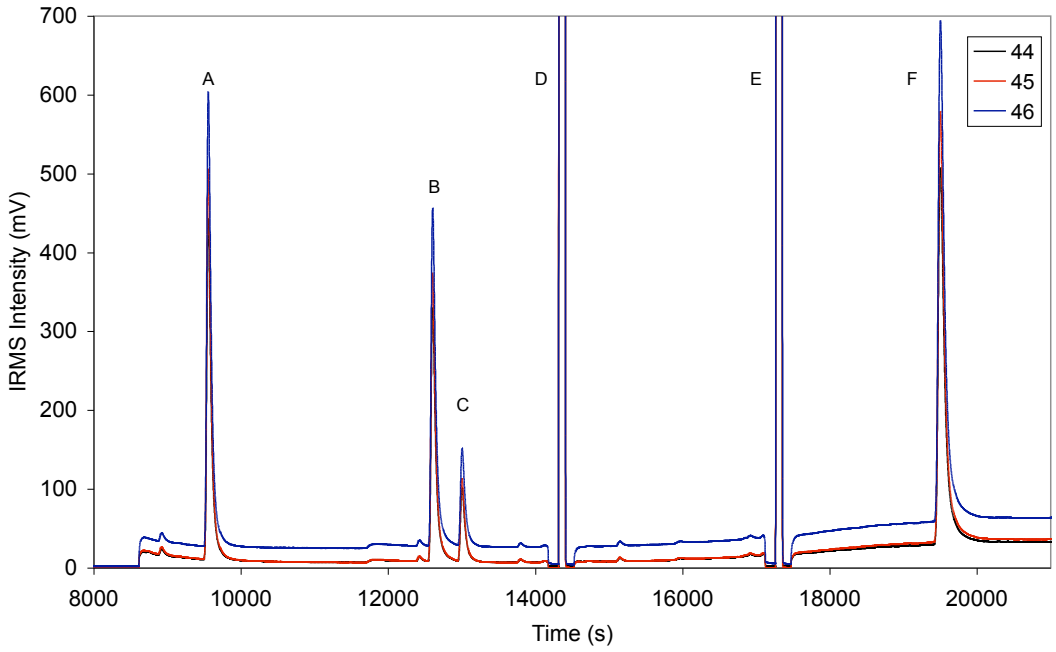

Figure 1.4. Chromatogram of isotope ratio mass spectrometer traces (m/z 44, 45, 46) for a 0.1 ml reference gas sample. Peak identity is as follows: A. ethane; B. propane; C. methyl chloride, D and E. CO_2 calibration; F. benzene.

measurable variations in voltage (or amperage) in each signal channel that can then be used for the evaluation of ratios.

An IRMS tuned for the measurement of $\delta^{13}C$ monitors 3 m/z (mass over charge) channels with 3 faraday cups: m/z 44, 45 and 46. An example of these signals as plotted with time is shown in fig. 1.4. These correspond to the molar masses of CO_2 and its principal stable isotopologues $^{12}C^{16}O^{16}O$, $^{13}C^{16}O^{16}O$ and $^{12}C^{18}O^{16}O$. By subtracting the background signal in each channel and integrating the signal with time per species peak gives the peak area per mass. Evaluation of mass ratios of the peak areas of 45/44 and 46/44 directly leads to isotope ratios $\delta^{13}C$ and $\delta^{18}O$, given a calibration. However, by assuming mass dependant fractionation processes and a corresponding abundance of the oxygen isotope ^{17}O in the m/z 45 and 46 signals, a small correction is applied to the $\delta^{13}C$ value to account for the isotopologues

$^{12}C^{17}O^{16}O$ and $^{13}C^{17}O^{16}O$, leading to a more accurate stable carbon isotope ratio measurement.

1.7.5 Stable isotope ratio calibration and reference strategies

For isotope ratio measurement, the calibration of an IRMS is generally accomplished through the use of several references that have been calibrated to an international standard. For daily use, at least two standards are used to evaluate instrument stability and linearity on the δ scale. The first is the *reference standard*, which is periodically injected directly to the mass spectrometer during the course of measurement. For $\delta^{13}C$ this is a small stream of CO_2, independently calibrated against an international standard (see below). This is intended to monitor the stability of the isotope mass spectrometer itself and is used for monitoring of the system stability. However, this cannot be used for a whole system calibration for two reasons, as the peak shape is square and thus not similar to that obtained from chromatography (see fig. 1.4, peaks D and E), and any fractionation effect inherent in the preconcentration system is completely omitted from evaluation.

Therefore, by the principle of equal treatment, a working standard is used, again independently calibrated against an international standard. This is processed in the same way as any sample introduced to the system, and therefore allows for evaluation of the system stability and linearity with peak area including any effects inherent in sample processing. Ideally, this calibration mixture contains all compounds of interest at similar mixing ratios to what may be expected in the measured samples. In situations where atmospheric mixing ratios are relatively high, e.g. carbon dioxide or methane, sample sizes are small and thus dried compressed ambient air that has been sampled at once in quantity and independently calibrated for its stable isotope ratio may be used in lieu of professionally prepared mixtures.

However, in the face of very low sample mixing ratios inherent in the measurement of atmospheric non-methane hydrocarbons (ppt level), this would necessitate very large volumes of calibration mixture, with associated storage issues and high cost. Therefore practicality dictates that mixtures with much higher mixing ratios than the samples to be measured be used in small volumes, focusing instead on the quantity of carbon injected. In such a situation it is sufficient to ensure that working standard compound peak areas are similar to those expected in the samples to be measured.

Further, the measurement of the working standard in varying volumes can serve to establish the isotope linearity of an instrument with peak area, and thus establish the minimum amount of substance that can be precisely analyzed. Below this threshold measurement errors increase, and the scale of the instrument may shift due to insufficient sensitivity.

Many international standards for stable isotope studies have existed throughout the years to attempt to establish an accepted scale upon which measurement intercomparisons may occur. Currently for $\delta^{13}C$, the universally accepted standard is Vienna Pee Dee Belemnite (VPDB), maintained by the International Atomic Energy Agency (IAEA). This is a laboratory-constructed standard that is based upon an exhausted previous standard from a sample of carbonate ($CaCO_3$) originating from a fossil excavated in North Carolina, USA. This fossil carbonate was chosen because of its unusually high ^{13}C content ($^{13}C/^{12}C = 0.0112372$), placing the vast majority of measured samples as more depleted ($\delta^{13}C < 0$ ‰) than the reference. VPDB also establishes a $\delta^{18}O$ ratio that is used for stable oxygen isotope studies. Other accepted international standards are Vienna Standard Mean Ocean Water (VSMOW, also maintained by IAEA) for both $\delta^{18}O$ and hydrogen stable isotope ($\delta^{2}H$) work, and the

stable isotope ratio of atmospheric nitrogen $\delta^{15}N$, which is identical throughout the atmosphere (Goldstein and Shaw 2003; Brenninkmeijer 2009).

With the exception of the latter, the defining reference materials are in short supply and cannot be widely distributed. To ease this, the IAEA develops and provides diverse reference standards with a defined δ value versus the standard. For example, certified CO_2 is available for laboratories to calibrate their reference gas or individual compounds that have been combusted to CO_2 for characterization, which can then be in turn used to calibrate working standards. Other laboratories may then depend on intercalibrations for their own work. As such, a laboratory calibration of a measuring instrument is built upon several intermediate steps, and rigorous tracking and documentation of each standard used and how this pertains to the reference assures the quality and validity of the final calibration.

In this way, the use of standards provides for the uniform comparison of results across laboratories and a common understanding of the isotope ratios of the compounds concerned.

1.8 Chapter overviews and key findings

1.8.1 Chapter 2

Analytical system for stable carbon isotope measurements of low molecular weight (C_2-C_6) hydrocarbons.

Chapter 2 (based on Zuiderweg et al. 2011) presents the setup, testing and initial results from the automated system for stable carbon isotope ratio measurements on C_2 to C_6 atmospheric hydrocarbons developed in the Atmospheric Physics and Chemistry Group laboratory at Utrecht University during 2006 to 2009. The main characteristic of this system is its flexibility, afforded by a sophisticated preconcentration setup that allows analysis of trace gases from air samples from diverse sources, volumes, and

compound mixing ratios by selectively removing the majority of undesired compounds in a sample efficiently.

In addition to several cryogenic traps to capture, remove bulk gases, and concentrate the samples introduced to the system, the key feature of the sample preparation is a chromatographic separation trap, which is used to separate CO_2 and methane from the compounds of interest, to prevent chromatographic interference. The output of the preconcentration system is passed to a chromatography column to separate the compounds from each other with time. The separated species subsequently are introduced to two different detectors: a quadrupole mass spectrometer for compound identification, and an isotope ratio mass spectrometer for determination of $\delta^{13}C$.

Testing and tuning of the instrument have established the following capabilities: (i) acceptance of diverse sample volumes from 50 mL to 300 L, (ii) accuracy levels of $\delta^{13}C$ in the range 0.3–0.8 ‰, (iii) detection limits of order 1.5–2.5 nanograms of carbon and excellent isotope linearity above these values, and (iv) 2-hour cycle times for frequent measurement. These capabilities compare favorably with other non-methane hydrocarbon stable carbon isotope ratio instruments worldwide.

The first application, in order to demonstrate the capabilities of the system, was the analysis of 21 ambient air samples taken during 48 h in August 2009 in Utrecht, the Netherlands, an urban location with many hydrocarbon sources present. These measurements were undertaken in a period of fine meteorological conditions, with calm or light winds and high temperatures with clear skies during the day.

Results obtained for a set of 10 hydrocarbon compounds show distinct diurnal patterns, e.g. buildup of mixing ratios during night due to loss of mixing and large isotope ratio variations in the reactive compounds due to atmospheric oxidative processes. All results, including source signatures, are generally in good agreement

with those from similar urban ambient air studies (e.g. Tsunogai and Yoshida, 1999; Rudolph et al., 2002; Goldstein and Shaw, 2003; Redeker et al., 2007).

1.8.2 Chapter 3

Stable carbon isotope fractionation in the UV photolysis of CFC-11 and CFC-12

Results of a set of experiments investigating the fractionation inherent in the photolysis of the chlorofluorocarbons CFC-11 and -12 are presented in chapter 3, which is based on Zuiderweg et al. (2012a). These compounds are the most abundant anthropogenic halocarbons in the atmosphere, and together account for approximately 55% of atmospheric chlorine loading, and have present-day mixing ratios of approximately 240 and 525 ppt respectively (Butler et al., 1999; WMO, 2010; AGAGE, 2011). These chlorofluorocarbons, which are used in refrigeration, as aerosol propellant and foam blowing, have exclusive industrial sources from use and leakage at the earth's surface. CFC-11 and -12 are long lasting and have atmospheric lifetimes of approximately 45 and 120 years, respectively, and have significant global warming potential as well (Forster et al., 2007).

The sinks of these compounds are located high in the stratosphere (19-34 km): Direct photolysis by UV-C ($\lambda < 220$nm) and reaction with $O(^1D)$. The former process is responsible for approximately 93 to 97% of the removal (Laube et al., 2010). These removal reactions are the trigger for the release of atmospheric chlorine radicals, which catalyze the destruction of stratospheric ozone, first proposed by Molina and Rowland (1974).

The discovery of a stable chlorine isotope ($\delta^{37}Cl$) gradient with height in CFC-12 from balloon samples and apparent fractionation (ε_{app}) published in Laube et al. (2010) led to the laboratory studies mentioned here to establish the stable carbon isotope fractionation in the dominant sink process at temperatures that are

stratospherically relevant. Using a powerful antimony lamp to produce 192-230 nm UV-C, a mixture of CFC-11 and -12 in oxygen-free nitrogen was photolyzed at temperatures from 203 to 288K, in half hour time intervals.

These samples were measured on the δ^{13}C instrument mentioned in chapter 2, for isotope ratios and mixing ratio. Isotope fractionations were calculated, ranging from (-23.8±0.9) to (-17.7±0.4) ‰ for CFC-11 and (-66.2±3.1) to (-51.0±2.9) ‰ for CFC-12 between 203 and 288 K. These are the first kinetic isotope fractionations measured for the photolysis of CFC to our knowledge. These large fractionations imply the existence of a strong δ^{13}C gradient with height (enrichment) in the stratosphere in these compounds. Also, the atmospheric reservoir of CFC-11 and -12 should continuously be enriching with time, and this should subsequently be evident in archives of atmospheric air.

1.8.3 Chapter 4

Extreme ^{13}C – depletion of CF_2Cl_2 in 2009 firn air samples from NEEM, Greenland

To that end, investigations of changes in δ^{13}C-CFC-12 with time in firn air samples collected in 2009 from the NEEM site in Greenland were conducted, the results of which are presented in chapter 4 (based on Zuiderweg et al., 2012b). Firn air, which is air trapped in the spaces in unconsolidated snow, is extracted through firn air sampling systems at depths up to the transition of snow to ice, which at the NEEM site was approximately 75m (Etheridge et al., 2009; Buizert et al., 2011). Very large volumes of air can be extracted from the firn; the samples that were measured in the investigation reported here were contained in high-pressure cylinders and had an effective volume of 600 liters (Etheridge et al., 2009).

Firn air has been used for the establishment of mixing ratio scenarios (historical trends) of diverse compounds when coupled with firn air modeling, which takes into account diffusive and gravitational effects in the firn. In fact, firn air measurements modeled in this way established that CFC-11 and -12 have no natural sources: none is detected in firn air prior to the beginning of the last century, which corresponds to the start of large scale use of the compound (Butler et al., 1999; McCulloch et al., 2003).

Of the 12 samples (each measured twice, non-sequentially, 35 L per sample) collected at the NEEM site, the upper 10 (to 69.4 m depth) have measurable peaks above the stability limit of the δ^{13}C instrument for CFC-12. The mixing ratio with depth series agrees well with that reported in Buizert et al. (2011, sampled from the same site but one year earlier), within measurement error. Raw δ^{13}C data indicates near constant -40‰ in the upper 60 m, which is comparable to present-day remote troposphere measurements, e.g. Bahlmann et al., 2011; see also Appendix A, CARIBIC aircraft flight 26 return measurements. However, the bottom two samples indicate a rapid depletion with depth to approximately -85 ‰. Firn air modeling similar to that used in Rommelaere et al. (1997) and Bräunlich et al. (2001) is subsequently employed to estimate the mean age of the deepest sample to be 43 ± 12 years old, but also calculates more extreme atmospheric depletion, to approximately -120 ‰ at that date. The model produces this solution due to its accounting for the diffusion of high mixing ratio enriched CFC-12 from above.

Using the best-reconstructed δ^{13}C scenario and CFC-12 production and release data from McCulloch et al. (2003) as input, a mass balance model is applied. This accounts for the fractionation in the atmospheric loss process as determined in Zuiderweg et al. (2012a), in order to retrieve a production and leakage δ^{13}C scenario, which suggests significant changes in stable carbon isotope ratios in order to force the

trend in the atmospheric reservoir. Technological industrial chemistry advances in the synthesis of CFCs and the feedstock of CFC production, CCl_4, which occurred in the middle of the 20th century could plausibly be responsible for this (Rossberg et al., 2003; Siegemund et al., 2003).

1.8.4 Chapter 5

Appendices

Appendix A: CARIBIC Flight 26 (Male, Maldives to Dusseldorf, Germany, August 17th, 2000) CFC-12 mixing ratio and $\delta^{13}C$ data are presented here as supporting material for Ch. 4. These data, measured by the instrument mentioned in Ch. 2, originate from cryogenically concentrated flight samples taken at 9.5 - 10.7 km altitude through use of the CARIBIC instrument container whole air sampler aboard a B767ER (Brenninkmeijer et al., 1996). Mean values measured were (532.7 ± 10 %) ppt and (-44.7 ± 0.65) ‰ vs. VPDB for mixing ratio and $\delta^{13}C$ respectively. As these samples were obtained from altitudes below the altitude region where CFCs are photolyzed and have mixing ratios comparable to those found at the surface, they may be considered to be representative of the well-mixed remote troposphere, and compare favorably with the few measurements that exist in that category (Laube et al., 2010, Bahlmann et al., 2011).

Appendix B: NEEM 2009 Firn air non-methane hydrocarbon data are presented here as a supplement to CFC-12 sample data from the same source discussed in ch. 4, the North Greenland Emian Ice Drilling (NEEM) site (77°25.898′ N, 51°06.448′ W, 2484m above sea level), collected as part of the summer 2009 firn air program (Etheridge et al., 2009). The mixing ratio and $\delta^{13}C$ variation with depth of the 7 compounds reported (acetylene, ethane, propane, isobutane, n-butane, hexane and benzene) have not been published until now. Measurement of these samples was

accomplished as in Ch. 4, with hydrocarbon calibration procedures as in Ch. 2. Notably, maxima of mixing ratio and minima of $\delta^{13}C$ are co-located for almost all compounds at near 70 meters depth. The combination of high mixing ratio and depleted $\delta^{13}C$ values implies large fresh emission (Rudolph and Czuba, 2001). Other published work involving NEEM 2008 samples indicates a carbon monoxide peak at this depth (firn modeling indicates 1975 for this peak) and subsequent reduction in mixing ratio to present day values. This is ascribed to changes in automobile use and technological advances (Wang et al., 2011). Whether the non-methane hydrocarbon features are truly coincident with this carbon monoxide peak and if these have the same cause are matters for future study.

References

Advanced Global Atmospheric Gases Experiment (AGAGE) data. Available online: http://agage.eas.gatech.edu/data.htm, 2011.

Anderson, R. S., Huang, L., Iannone, R., Thompson, A. E., and Rudolph, J.: Carbon kinetic isotope effects in the gas phase reactions of light alkanes and ethene with the OH radical at 296±4 K, *J. Phys. Chem. A*, **108**, 11537–11544, doi:10.1021/jp0472008, 2004.

Bahlmann, E., Weinberg, I., Seifert, R., Tubbesing, C., and Michaelis, W.: A high volume sampling system for isotope determination of volatile halocarbons and hydrocarbons, *Atmos. Meas. Tech.*, **4**, 2073-2086, doi:10.5194/amt-4-2073-2011, 2011.

Bräunlich, M., Aballain, O., Marik, T., Jöckel, P., Brenninkmeijer, C. A. M., Chappellaz, J., Barnola, J.-M., Mulvaney, R., and Sturges, W. T.: Changes in the global atmospheric methane budget over the last decades inferred from 13C and D isotopic analysis of Antarctic firn air, J. Geophys. Res., 106, 20,465–20,481, doi:10.1029/2001JD900190, 2001.

Brenninkmeijer, C. A. M., Crutzen, P. J., Fischer, H., Güsten, H., Hans, W., Heinrich, G., Heintzenberg, J., Hermann, M., Immelmann, T., Kersting, D., Maiss, M., Nolle, M., Pitscheider, A., Pohlkamp, H., Scharffe, D., Specht, K., and Wiedensohler, A.: CARIBIC—Civil Aircraft for Global Measurement of Trace Gases and Aerosols in the Tropopause Region. *J. Atmos. Oceanic Technol.*, **16**, 1373–1383, doi: 10.1175/1520-0426, 1999.

Brenninkmeijer, C. A. M.: Applications of stable isotope analysis to atmospheric trace gas budgets, *Eur. Phys. J. C*, **1**, 137–148, doi:10.1140/epjconf/e2009-00915-x, 2009.

Buizert, C., Martinerie, P., Petrenko, V. V., Severinghaus, J. P., Trudinger, C. M., Witrant, E., Rosen, J. L., Orsi, A. J., Rubino, M., Etheridge, D. M., Steele, L. P., Hogan, C., Laube, J. C., Sturges, W. T., Levchenko, V. A., Smith, A. M., Levin, I., Conway, T. J., Dlugokencky, E. J., Lang, P. M., Kawamura, K., Jenk, T. M., White, J. W. C., Sowers, T., Schwander, J. and Blunier, T.: Gas transport in firn: multiple-tracer characterisation and model intercomparison for NEEM, Northern Greenland, *Atmos. Chem. Phys. Discuss.,* **11**, 15975 - 16021, 2011

Butler, J. H., Battle, M., Bender, M. L., Monzka, S. A., Clarke, A. D., Saltzman, E. S., Sucher, C. M., Severinghaus, J. P., and Elkins, J. W.: A record of atmospheric halocarbons during the twentieth century from polar firn air. *Nature*, **399**, 749 - 755, 1999.

Conny, J. M. and Currie, L. A.: The isotopic characterization of methane, non-methane hydrocarbons and formadehyde in the troposphere, *J. Atmos. Environ*., **30**, 4, 621–638, 1996.

Czapiewski, K. V., Czuba, E., Huang, L., Ernst, D., Norman, A. L., Koppmann, R., and Rudolph, J.: Isotopic composition of non-methane hydrocarbons in emissions from biomass burning, *J. Atmos. Chem.,* **43**, 45–60, 2002.

Etheridge, D., Rubino, M., Courteaud, J., Patrenko, V., and Courville, Z.: *The NEEM 2009 firn air program: field report on sampling and analysis activities*. Available: http://neem.dk, 2009.

Farquhar, G.D., Ehleringer, J.R., and Hubrick, K.T.: Carbon isotope discrimination in photosynthesis, *Annu. Rev. Plant Physiol. Plant Mol. Biol.*, **40**, 503-537, 1989.

Forster, P., Ramaswamy, V., Artaxo, P., Berntsen, T., Betts, R., Fahey, D. W., Haywood, J., Lean, J., Lowe, D.C., Myhre, G., Nganga, J., Prinn, R., Raga, G., Schulz, M. and Van Dorland, R. Changes in Atmospheric Constituents and in

Radiative Forcing. *Climate Change 2007: The Physical Science Basis. Contribution of Working Group I to the Fourth Assessment Report of the Intergovernmental Panel on Climate Change* [Solomon, S., D. Qin, M. Manning, Z. Chen, M. Marquis, K.B. Averyt, M.Tignor and H.L. Miller (eds.)]. Cambridge University Press, Cambridge, United Kingdom and New York, NY, USA, 2007.

Francey, R. J., Allison, C.E., Etheridge, D.M., Trudinger, C.M., Enting, I.G., Leuenburger, M., Langenfelds, R.L., Michel, E. and Steele, L.P.:A 1000-year high precision record of $\delta^{13}C$ in atmospheric CO_2, *Tellus B*, **51(2)**, 170-193, doi:10.1034/j.1600-0889.1999.t01-1-00005.x, 1999.

Goldstein, A. H. and Galbally, I. E.: Known and unexplored organic constituents in the Earth's atmosphere, *Environ. Sci. Technol*., **41(5)**, 1514–1521, doi:10.1021/es072476p, 2007.

Goldstein, A. H. and Shaw, S. L.: Isotopes of volatile organic compounds: an emerging approach for studying atmospheric budgets and chemistry, *Chem. Rev.*, **103**, 5025–5048, 2003.

Guenther, A., Hewitt, C. N., Erickson, D., Fall, R., Geron, C., Graedel, T., Harley, P., Klinger, L., Lerdau, M., McKay, W. A., Pierce, T., Scholes, B., Steinbrecher, R., Tallamraju, R., Taylor, J., and Zimmerman, P.: A global-model of natural volatile organic-compound emissions, *J. Geophys. Res.-Atmos.*, **100**, 8873–8892, 1995.

Iannone, R., Anderson, R. S., Rudolph, J., Huang, L., and Ernst, D.: The carbon kinetic isotope effects of ozone-alkene reactions in the gasphase and the impact of ozone reactions on the stable carbon isotope ratios of alkenes in the atmosphere. *Geophys. Res. Lett.*, **30(13)**, 1684–1688, doi:10.1029/2003GL017221, 2003.

Keppler, F., Harper, D. B., Röckmann, T., Moore, R. M., and Hamilton, J. T. G.: New insight into the atmospheric chloromethane budget gained using stable carbon isotope ratios, *Atmos. Chem. Phys.*, **5**, 2403–2411, doi:10.5194/acp-5-2403-2005, 2005.

Laube, J. C., Kaiser, J., Sturges, W. T., Bönisch, H., and Engel, A.: Chlorine Isotope Fractionation in the Stratosphere. *Science*, **329(5996)**, 1167, DOI:10.1126/science.1191809, 2010.

Martinerie, P., Nourtier-Mazauric, E., Barnola, J.-M., Sturges, W. T., Worton, D. R., Atlas, E., Gohar, L. K., Shine, K. P., and Brasseur, G. P.: Long-lived halocarbon trends and budgets from atmospheric chemistry modelling constrained with measurements in polar firn. *Atmos. Chem. Phys.,* **9,** 3911-3934, doi:10.5194/acp-9-3911-2009, 2009.

Matthews, D. M. and Hayes, J. M.: Isotope-ratio-monitoring gas chromatography-mass spectrometry, *Anal. Chem*., **50**, 11, 1465–1473, 1978.

McCulloch, A., Midgley, P. M., and Ashford, P.: Releases of refrigerant gases (CFC-12, HCFC-22 and HFC-134a) to the atmosphere. *Atmos. Env.*, **37**, 7, 889-902, doi:10.1016/S1352-2310(02)00975-5, 2003.

McKinney, D. R.; McCrea, J. M.; Epstein, S.; Allen, H. A.; and Urey, H. C.: Improvements in Mass Spectrometers for the Measurement of Small Differences in Isotope Abundance Ratios. *Rev. Sci. Instrum.* **21**, 724-732, 1950.

Molina, M. J. and Rowland, F. S.: Stratospheric sink for chlorofluoromethanes: Chlorine atom catalyzed destruction of ozone. *Nature,* **249**, 810-814, 1974.

Nara, H., Toyoda, S., and Yoshida, N.: Measurements of stable carbon isotopic composition of ethane and propane over the Western North Pacific and Eastern Indian Ocean: a useful indicator of atmospheric transport process*, J. Atmos. Chem.,* **56**, 293–314, doi:10.1007/s10874-006-9057-3, 2007.

NOAA (Nationa Oceanic and Atmosperic Administration) *Mauna Loa CO_2 data*, Available: http://www.esrl.noaa.gov/gmd/ccgg/trends/co2_data_mlo.html, 2012.

O'Leary, M.H.: Carbon isotope fractionation in plants, *Phytochemistry*, **20(4)**, 553-567, 1981.

Park, R., and Epstein, S.: Carbon isotope fractionation during photosynthesis, *Plant Physiol.,* **36**, 133, 1961.

Redeker, K. R., Davis, S., and Kalin, R. M.: Isotope values of atmospheric halocarbons and hydrocarbons from Irish urban, rural, and marine locations, *J. Geophys. Res.*, **112**, D16307, doi:10.1029/2006JD007784, 2007.

Röckmann, T., Kaiser, J., Brenninkmeijer, C. A. M.: the isotopic fingerprint of the pre-industrial and the anthropogenic N_2O source. *Atmos. Chem. Phys.*, **3**, 315-323, 2003.

Röckmann, T., Gómez Álvarez, C. X., Walter, S., van der Veen, C., Wollny, A.G., Gunthe, S.S., Helas, G., Pöschl, U., Keppler, F., Greule, M., and Brand, W.A.: Isotopic composition of H_2 from wood burning: Dependency on combustion efficiency, moisture content, and δD of local precipitation, *J. Geophys., Res.,* **115**, D17308, doi:10.1029/2009JD013188, 2010.

Rommelaere, V., Arnaud, L., and Barnola, J.-M.: Reconstructing recent atmospheric trace gas concentrations from polar firn and bubbly ice data by inverse methods, *J. Geophys. Res.*, **102(D25)**, 30,069–30,083, doi:10.1029/97JD02653, 1997.

Rossberg, M., Lendle, W., Pfleiderer, G., Tögel, A., Dreher, E., Langer, E., Rassaerts, H., Kleinschmidt, P., Strack, P., Cook, R., Beck, U., Lipper, K., Torkelson, T. R., Löser, E., Beutel, K. K., and Mann, T.: Chlorinated Hydrocarbons. *Ullmann´s Encyclopedia of Industrial Chemistry*, 6th edition, Wiley-VCH, 2003.

Rudolph, J. and Czuba, E.: On the use of isotopic composition measurements of volatile organic compounds to determine the "photochemical age" of an air mass, *Geophys. Res. Lett.*, **27**, 23, 3865–3868, 2000.

Rudolph, J. and Ehhalt, D. H.: Measurements of C_2–C_5 hydrocarbons over the North Atlantic, *J. Geophys. Res*., **86**, C12, 11959–11964, 1981.

Rudolph, J., Lowe, D. C., Martin, R. J., and Clarkson, T. S.: A novel method for compound specific determination of ^{13}C in volatile organic compounds at ppt levels in ambient air, *Geophys. Res. Lett.,* **24(6)**, 659–662, 1997.

Rudolph, J., Czuba, E., Norman, A. L., Huang, L., and Ernst, D.: Stable carbon isotope composition of nonmethane hydrocarbons in emissions from transportation related sources and atmospheric observations in an urban atmosphere, *Atmos. Environ.*, **36**, 1173–1181, 2002.

Saito, T., Kawamura, K., Tsunogai, U., Chen, T., Matsueda, H., Nakatsuka, T., Gamo, T., Uematsu, M., and Huebert, B. J.: Photochemical histories of nonmethane hydrocarbons inferred from their stable carbon isotope ratio measurements over east Asia, *J. Geophys. Res.,* **114**, D11303, doi:10.1029/2008JD011388, 2009.

Saito, T., Tsunogai, U., Kawamura, K., Nakatsuka, T., and Yoshida, N.: Stable carbon isotopic compositions of light hydrocarbons over the Western North Pacific and implication for their photochemical ages, *J. Geophys. Res.,* **107(D4)**, 4040, doi:10.1029/2000JD000127, 2002.

Schwander, J., Barnola, J. M., Andrie, C., Leuenberger, M., Ludin, A., Raynaud, D., and Stauffer, B.: The age of the air in the firn and the ice at Summit, Greenland, *J. Geophys. Res.-Atmos.*, **98**, 2831–2838, 1993.

Scripps CO_2 (Scripps Institute of Oceanography CO_2 monitoring program): *Atmospheric $\delta^{13}CO_2$ data*, Available: http://scrippsco2.ucsd.edu/, 2010.

Seinfeld, J. H. and Pandis, S. N.: *Atmospheric Chemistry and Physics: from Air Pollution to Climate Change*, John Wiley and Sons, New York, 1326 pp., 1998.

Siegemund, G., Schwertfeger, W., Feiring, A., Smart, B., Behr, F., Vogel, H., and McKusick, B.: Organic Fluorine Compounds. *Ullmann´s Encyclopedia of Industrial Chemistry*, 6th edition, Wiley-VCH, 2003.

Tsunogai, U. and Yoshida, N.: Carbon isotopic compositions of C_2–C_5 hydrocarbons and methyl chloride in urban, coastal, and maritime atmospheres over the Western North Pacific, *J. Geophys. Res.,* **104**, D13, 16033–16039, 1999.

Wang, Z., Chappellaz, J., Martinerie, P., Park, K., Petrenko, V., Witrant, E., Blunier, T., Brenninkmeijer, C. A. M., and Mak, J. E.: The isotopic record of Northern Hemisphere atmospheric carbon monoxide since 1950, implications for the CO budget, *Atmos. Chem. Phys. Discuss.*, **11**, 30627-30663, doi:10.5194/acpd-11-30627-2011, 2011.

Warneck, P.: *Chemistry of the Natural Atmosphere.* Academic Press, Inc., San Diego, U.S.A., 1988.

World Meteorological Organization (WMO), *Global Ozone Research and Monitoring Project Report No. 52: Scientific Assesment of Ozone Depletion 2010*, available: http://ozone.unep.org, 2010.

Zuiderweg, A., Holzinger, R. and Röckmann, T.: Analytical system for stable carbon isotope measurements of low molecular weight (C_2-C_6) hydrocarbons. *Atmos. Meas. Tech.,* **4**, 1161-1175, DOI: 10.5194/amt-4-1161-2011, 2011.

Zuiderweg, A., Kaiser, J., Laube, J. C., Röckmann, T., and Holzinger, R.: Stable carbon isotope fractionation in the UV photolysis of CFC-11 and CFC-12. *Atmos. Chem. Phys.,* **12,** 4379-4385, doi:10.5194/acp-12-4379-2012, 2012a.

Zuiderweg, A., Holzinger, R., Martinerie, P., Schneider, R., Kaiser, J., Etheridge, D., Rubino, M., Courteaud, J., Petrenko, V., Courville, Z., and Röckmann, T.: Extreme ^{13}C – depletion of CF_2Cl_2 in 2009 firn air samples from NEEM, Greenland. Accepted for publication in *Atmos. Chem. Phys. Disc.*, 2012b.

Chapter 2: Analytical system for stable carbon isotope measurements of low molecular weight (C_2-C_6) hydrocarbons

A. Zuiderweg, R. Holzinger, and T. Röckmann

Published in Atmospheric Measurement Techniques, 4, 1161-1175, 2011.

Abstract

We present setup, testing and initial results from a new automated system for stable carbon isotope ratio measurements on C_2 to C_6 atmospheric hydrocarbons. The inlet system allows analysis of trace gases from air samples ranging from a few liters for urban samples and samples with high mixing ratios, to many tens of liters for samples from remote unpolluted regions with very low mixing ratios. The centerpiece of the sample preparation is the separation trap, which is used to separate CO_2 and methane from the compounds of interest. The main features of the system are (i) the capability to sample up to 300 liters of air, (ii) long term (since May 2009) operational $\delta^{13}C$ accuracy levels in the range 0.3 - 0.8 ‰ (1-σ), and (iii) detection limits of order 1.5 - 2.5 ngC (collected amount of substance) for all reported compounds.

The first application of this system was the analysis of 21 ambient air samples taken during 48 hours in August 2009 in Utrecht, the Netherlands. Results obtained are generally in good agreement with those from similar urban ambient air studies. Short sample intervals allowed by the design of the instrument help to illustrate the complex diurnal behavior of hydrocarbons in an urban environment, where diverse sources, dynamical processes, and chemical reactions are present.

2.1 Introduction

A significant amount of the total reactive carbon input (estimated as near 1150Tg y^{-1}, Guenther et al. 1995) to the atmosphere consists of non-methane hydrocarbons (NMHCs). These are emitted to the atmosphere through many processes, both natural as a product of vegetative growth, decay and natural combustion of plant material, and anthropogenic including biomass burning for energy or heating, fossil fuel combustion, and industrial processes. Non-methane hydrocarbons play important roles in atmospheric chemistry contributing to the production of tropospheric ozone and resultant photochemical pollution, the formation of aerosol particles, and the oxidative capacity of the atmosphere (Warneck 1988, Seinfeld & Pandis 1998, Goldstein and Galbally 2007).

Low molecular weight NMHC, consisting of compounds with 2 to 7 carbon atoms (C_2 to C_7), account for the vast majority of anthropogenic emissions to the troposphere (Middleton, 1995). Acetylene, ethylene, propyne, and propylene originate primarily from combustion processes such as fossil fuel combustion and biomass burning; alkanes mainly stem from natural gas leakage and petroleum product evaporation, with significant transportation sources as well; and aromatic compounds mainly from transportation sources and solvent evaporation (Goldstein and Shaw 2003, Redeker et al. 2007). Oxidative processes provide the atmospheric removal mechanism of NMHC compounds, mainly through reaction with OH, which is by far the dominant process (Conny and Currie 1996):

$$RH+OH \longrightarrow R+H_2O \qquad \text{(R2.1)}$$

Where R stands for any alkyl radical remaining after hydrogen abstraction from the hydrocarbon RH. Other removal mechanisms include NO_3, Cl, or O_3 (Warneck 1988, Seinfeld and Pandis 1998, Brenninkmeijer 2009).

The minor stable isotope of carbon, ^{13}C, has an average natural abundance of approximately 1.1%. Biological (e.g. photosynthesis), physical (e.g. diffusion) and chemical processes often act slightly differently on isotopologues and thus change the stable isotope ratio, which is expressed as

$$\delta^{13}C = \left[\frac{\left(\frac{[^{13}C]}{[^{12}C]} \right)_{sample}}{\left(\frac{[^{13}C]}{[^{12}C]} \right)_{standard}} - 1 \right] \quad (2.1)$$

where measurements are referenced against a standard carbon isotopic ratio, usually VPDB (Vienna Pee Dee Belemnite). Measurements of $\delta^{13}C$ are commonly multiplied by 1000‰ for readability purposes (Goldstein and Shaw, 2003, Brenninkmeijer 2009).

Isotopically lighter molecules usually react faster than isotopically heavier ones. In the case of hydrocarbons, this is because bonds in molecules containing solely ^{12}C atoms are weaker than those containing one or more ^{13}C atoms. This causes small deviations from the original $^{13}C/^{12}C$ ratio during chemical degradation. The ratio of the two rate coefficients of the different isotopologues is known as a kinetic isotope effect (KIE).

$$KIE = \frac{k_{12}}{k_{13}} \quad (2.2)$$

Knowledge of the KIE of relevant chemical reactions can provide a tool to improve the understanding of hydrocarbon atmospheric processing (Rudolph and Czuba, 2000).

Development of the coupled gas chromatography – (combustion interface) – isotope ratio mass spectrometer (IRMS), as pioneered by Matthews and Hayes (1978) for

CO_2 and N_2 isotope work, substantially improved upon earlier techniques based on dual-inlet isotope ratio mass spectrometers by greatly reducing necessary sample size and eliminating the need to extract individual compounds from a sample, which is a difficult and time-consuming task. This breakthrough allowed significant research work into the stable isotopic ratios of carbon, nitrogen, oxygen and hydrogen containing compounds in the atmosphere.

Development of instrumentation able to accomplish compound specific measurement of carbon isotope ratios of NMHC is somewhat newer (Rudolph et al. 1997, Goldstein and Shaw 2003, Brenninkmeijer 2009). Rudolph et al. (1997) developed the first instrument capable of compound specific stable carbon isotope ratio analysis measurements of multiple NMHCs. This instrument was initially used for observing carbon isotope ratios of emissions from biomass burning and transportation related sources, and urban environment atmospheric samples. The observance of the magnitude of the kinetic isotope effect in hydrocarbon reactions with OH and O_3 was also undertaken in subsequent research with this instrument (Rudolph et al. 1997, Rudolph et al. 2002, Iannone et al. 2003, Anderson et al. 2004).

The availability of such measurements allowed the subsequent development and application of the so-called isotopic hydrocarbon clock approach, which is expressed as follows (Rudolph and Czuba, 2000):

$$\delta_Z = t_{av} \cdot {}^{\mathrm{OH}}k_Z \cdot [\mathrm{OH}] \cdot {}^{\mathrm{OH}}KIE_Z + {}^{0}\delta_Z \qquad (2.3)$$

where δ_Z is the measured isotopic ratio of a compound Z, t_{av} the average age of the air mass, ${}^{OH}k_Z$ the rate of reaction of the compound with OH, $[OH]$ the concentration of OH, ${}^{OH}KIE_Z$ the KIE in the reaction of compound Z with OH, and ${}^{0}\delta_Z$ the source isotope ratio of compound Z; it may also be further extended by adding terms representing reactions with e.g O_3 or Cl. This approach can improve estimates of

compound age compared to previous efforts, which relied on ratios of mixing ratios of two compounds emitted at the same time (Rudolph and Czuba, 2000). In the case of light non-methane hydrocarbons, the relatively short lifetime of these compounds in the atmosphere, from mere hours to tens of days, gives the possibility of utilizing the isotopic hydrocarbon clock approach to constrain transport and aging in the atmosphere (Rudolph et al. 1981, Rudolph et al. 2002, Goldstein and Shaw 2003, Redeker et al. 2007).

Other applications of similar instruments that have been subsequently derived include measurements of NMHC $\delta^{13}C$ in urban, marine and costal atmospheres and over the north Pacific and east Asia to evaluate atmospheric transport and airmass age (Tsunogai and Yoshida 1999, Saito et al. 2002, Nara et al. 2007, Saito et al. 2009); of NMHC from biomass burning (Czapiewski et al. 2002, Nara et al. 2006); with some extension, measurements of halocarbons and NMHC (Archbold et al. 2005, Redeker et al. 2007); specific measurement of chloromethane from plants and its atmospheric budget (Bill et al., 2002; Harper et al. 2003; Keppler et al. 2005); and measurement of leaf emissions of acetaldehyde to investigate biochemical reaction pathways (Jardine et al. 2009). Such measurements can be powerful tools to disentangle the relative contribution of different sources to the atmospheric burden of important atmospheric trace gases.

Here we present a new instrument that is capable of high-precision measurements of NMHC stable carbon isotope ratios. It has the unique capacity of being able to process very high volume samples of up to 300 liters, such as those necessary for stable carbon isotope measurements of NMHC from very clean samples (e.g. stratospheric, firn air samples, or remote high volume air samples) and the flexibility

of accepting samples from many other sources. The system is constructed and tested to analyze $\delta^{13}C$ of non-methane hydrocarbons from C_2 to C_6, and methyl chloride.

2.2 Experimental

2.2.1 System description and procedure

2.2.1a The preconcentration system

The system (fig. 2.1) is largely based on well-established cryotrapping techniques and allows for stable isotope analysis of a variety of different samples. All cryotraps were operated at 77 K and cooled with liquid nitrogen. If not specified otherwise, electrical heating desorbed the trapped compounds. Helium was used as carrier gas to transfer the sample through the different components of the system. To allow the sampling of large volume samples, it is necessary to initially utilize large diameter cryotraps and progressively cryofocus to smaller volumes prior to GC injection. Cryogenic traps, when implemented properly, do not create isotopic fractionation (Archbold et al. 2005, Redeker et al. 2007). The following parts of the preconcentration system are described below: (i) the primary cryogenic sampling trap (referred to as SAMP trap); (ii) the separation trap to separate CO_2 from the NMHCs (referred to as SEP trap); (iii) the W-shaped cryogenic recovery trap (REC trap); and (iv) the final cryogenic focusing trap (FOC trap).

The SAMP trap is a 0.5 m x 4 mm ID stainless-steel tube filled with 100/120 mesh glass-bead packing material, capable of at least 100 standard mL min^{-1} (standard conditions are 0°C, 1 bar) flow rates without loss. Typically this trap is operated at a flow of 50 standard mL min^{-1}, maintained by a MKS thermal mass flow-controller. A dual-head rotary pump (KNF Neuberger GmbH, Germany) draws the sample through the trap, and provides removal of bulk gases (mainly N_2 and O_2).

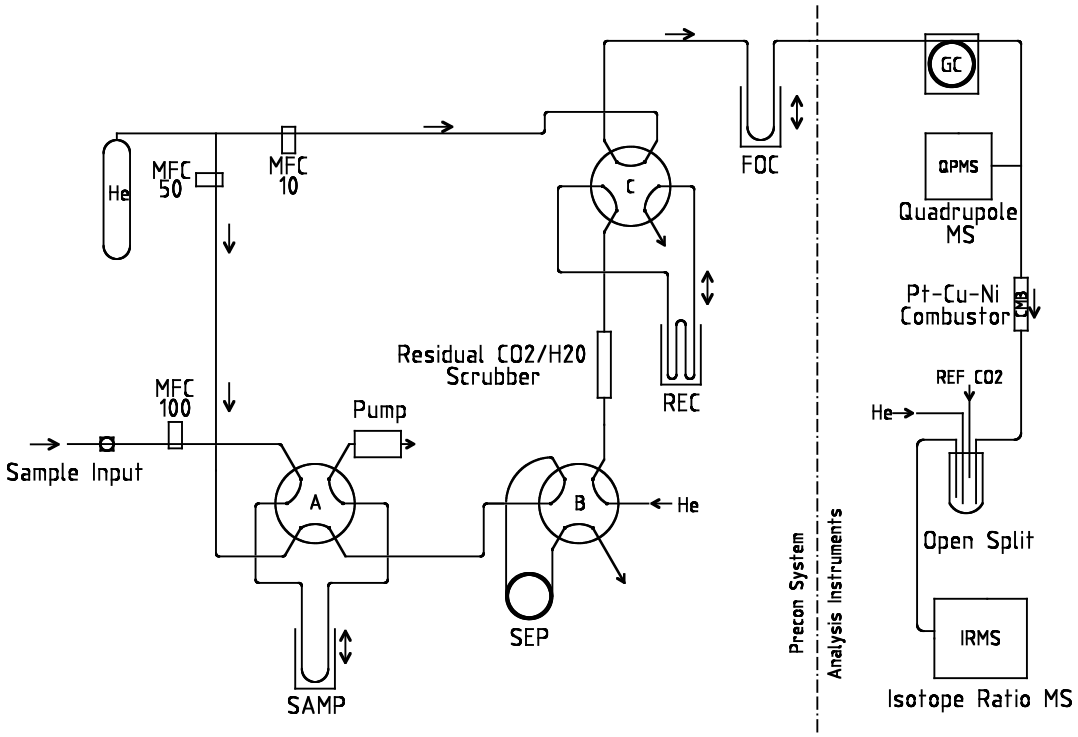

Figure 2.1. System diagram. A, B, C indicate Valco 6-port valves; SAMP, SEP, REC, and FOC indicate the primary sampling cryotrap, the separation trap, the recovery cryotrap, and the focusing cryotrap, respectively. Mass flow controller (MFC) maximum flow rates are indicated in units of mL min^{-1} (standard conditions).

Desorption of any sample on the trap is accomplished by heating it to 120ºC within 1 minute after extraction.

The most innovative design feature of the preconcentration system is the method of CO_2 removal. Whereas other systems (Rudolph et al. 1997, Tsunogai et al. 1999, Archbold et al. 2005) rely on chemical removal of any CO_2 employing Carbosorb, Ascarite II or other sodium hydroxide-on-silica beads, here a packed stainless steel GC-column (Supelco PoraPAK Q, 3 m x 4 mm ID, 100/120 mesh) acted as a trap for NMHCs and allowed unwanted CO_2 to pass. We designed the SEP trap as a non-chemical removal method to ensure effective separation for large samples, i.e. samples with a high CO_2 content. CO_2 must be removed before IRMS analysis can

occur, because the target compounds are oxidized to CO_2 for isotope analysis. In order to do so, the sample is injected on this trap at 70 mL min^{-1} with helium as the carrier gas. The system procedure developed as a result of SEP trap testing (see section 2.2.1b, below) reverses the flow through the column after 10 minutes (any CO_2 having been vented) to retrieve the compounds of interest from the column at a reduced helium flow rate (11.2 mL min^{-1}). During recovery, the column is heated to and kept at 120ºC over a period of 40 minutes.

Before the sample material is recovered on the REC trap, any small remnant CO_2 and any H_2O is removed in a small glass reactor containing Ascarite II and $Mg(ClO_4)_2$. The REC trap is a 0.7 m x 2.5 mm ID W-shaped stainless steel cryotrap containing 100/120 mesh glass beads. After the recovery time of 40 minutes, the REC trap is heated to 100ºC, thereby releasing the sample over the course of 5 minutes at 4.1mL min^{-1} to the FOC trap, a 0.5 m x 0.25 mm ID stainless steel-jacketed capillary cryotrap. Sample injection into the GC occurs by extracting and heating the FOC trap to a temperature of over 100ºC within 30s, at a flow rate of 2.1mL min^{-1}.

2.2.1b SEP trap verification and testing

Figure 2.2 displays a total ion abundance chromatogram demonstrating the separation properties of SEP trap under room temperature and aforementioned standard He flow rates of 70 mL min^{-1}, utilizing a 200 mL 50:50 CO_2/natural gas testing mix and a quadrupole mass spectrometer as a detector at the outlet of the SEP trap. Natural gas has a widely varying composition, but generally consists of methane (as bulk gas) and contains significant amounts of nitrogen, CO_2, and higher hydrocarbons such as ethane and propane (Škrbić and Zlatković 1983, Milton et al. 2010). The injected mixture of natural gas and CO_2 as chosen here represents a test of separation column performance of a very demanding sample introduced on the system, representing the

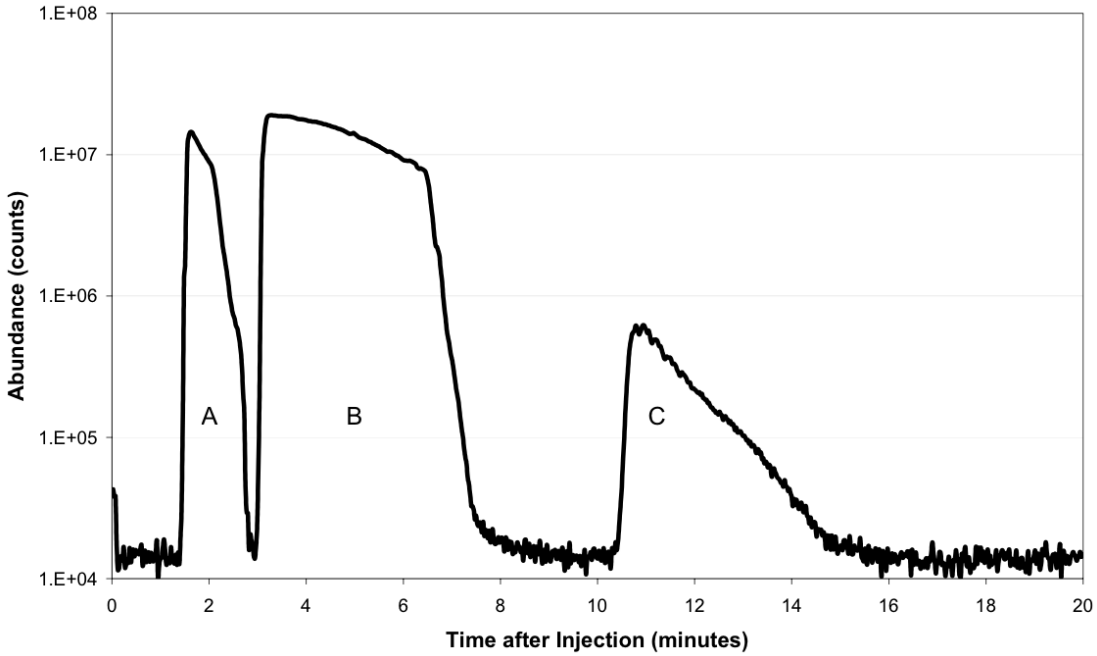

Figure 2.2. Performance of the separation trap. The identity of peaks A (methane and nitrogen), B (bulk carbon dioxide), and C (ethane and other hydrocarbons) was confirmed by individual mass signals of the quadrupole mass spectrometer.

CO_2 content of approximately 300 L of ambient air. Figure 2.2 shows that at 10 minutes after injection the bulk of methane, remnant nitrogen (peak A) and CO_2 (peak B), has eluted while ethane and other hydrocarbons (peak C) are still in the SEP trap. Therefore the system procedure has been set to reverse the flow through the column after 10 minutes to retrieve the compounds of interest, after venting all CO_2.

Further, we performed tests to confirm that the SEP trap has no significant effect on the $\delta^{13}C$ measurements of the selected hydrocarbons. The tests consisted of 10 measurements of calibration gas (working standard gas, AiR Inc., described further in section 2.2.1c) in two configurations: (i) with the system in standard configuration but the SEP trap short-cut (removed), and (ii) with the system in standard configuration, respectively. Table 2.1 shows that the means and standard deviations are nearly

Table 2.1. Mean and standard deviation in $\delta^{13}C$ (‰) SEP trap evaluation data.

Compound	No SEP trap[a] mean $\delta^{13}C$	No SEP trap[a] σ $\delta^{13}C$	Standard config.[b] mean $\delta^{13}C$	Standard config.[b] σ $\delta^{13}C$
Ethane	-28.4	0.33	-28.6	0.27
Propane	-34.6	0.49	-34.3	0.49
Methyl Chloride	-46.4	0.69	-48.8	0.72
Benzene	-27.4	0.36	-27.5	0.39

[a] SEP trap removed from system, n=10

[b] Standard configuration, SEP trap installed, n=10

identical for the hydrocarbons. However, there is a consistent shift (-2 ‰) for methyl chloride, for which a correction is neccessary. A similar effect was noted in Archbold et al. (2005), for chemical removal and adsorbance traps. The cause of this shift is as yet unexplained.

2.2.1c GC separation, combustion and detection

Gas chromatographic separation is done on a 52.5 m x 0.25 mm Varian PoraPLOT Q GC column in a HP 5890 GC. The column is maintained at 40 ºC for 10 minutes, thereafter being heated at a rate of 12 ºC min^{-1} to 240 ºC. This temperature is maintained for 35 minutes, giving a total run time of 65 minutes. When not in use, the GC oven is maintained at 150 ºC. Helium is used as the carrier gas and a constant flow of 2.1 mL min^{-1} is maintained by a mass flow controller (MKS).

The effluent from the GC column is roughly split 1:1 between a quadrupole mass spectrometer (HP5970) for identification of the compounds, and the remainder sent to a ThermoFinnigan $Delta^{+}$ XP IRMS by way of a platinum-copper-nickel ceramic combustor (maintained at 900 ºC and restored daily with O_2), a nafion drier, and an open-split interface (Röckmann et al., 2003). The actual flow into the IRMS is approximately 0.5 mL min^{-1}. IRMS $\delta^{13}C$ drift is monitored through direct injection of

CO_2 via the open-split as a working standard. The stable carbon isotope ratio of this CO_2 has been calibrated as (-34.0 ± 0.1) ‰ vs. VPDB by Rijksuniversiteit Groningen, The Netherlands. Mixing ratios are calculated from the IRMS m/z 44 peak area measurements of each peak in the chromatogram, relative to peak areas from the working standard gas at accuracy levels of ±10 % (see below). Mixing ratios of compounds not contained in the regularly measured working standard gas were estimated by extrapolation based on the number of carbon atoms in the molecules of the species in question and can therefore contain a larger systematic error (±30 %). $\delta^{13}C$ values are calculated from the individual ion signals of the IRMS, integrated per trace (m/z 44, 45, 46; automatic peak detection under normal operation, manual evaluation if necessary), and mathematically corrected for ^{17}O through the ISODAT isotope ratio analysis package, utilizing the correction from Santrock et al. (1985).

The sample chromatograms shown in Fig. 2.3 show the IRMS intensity traces at m/z 44 of two gas standards and an ambient air sample; and a 44/45 ratio trace for that ambient air sample, respectively, thus demonstrating the separation performance of the GC-IRMS system.

2.2.1d Ambient air sampling unit

As an addition to the basic system described above, a high-flow sampling unit (diagram Fig. 2.4) was developed allowing ambient air sampling at rates of up to 1 L min^{-1}. The unit is set up as an auxiliary 2-stage cryogenic trapping system consisting of a large diameter stainless steel water trap (0.25 m x 2.1 cm ID) and a stainless steel U-trap (0.5 m x 1.0 cm ID) filled with glass beads (80/100 mesh). The water trap is constructed of 2.54 cm tubular stainless steel with large diameter Swagelok fittings and 0.32 cm (ID) stainless steel lines. The internal volume of this trap (approximately

Figure 2.3. Example chromatograms (IRMS, m/z 44 signal) of the working gas standard (green trace), the second calibration gas standard (blue trace), and an ambient air sample (black trace), respectively. Peak identification of the ambient sample is based on retention time and the mass spectrum obtained with the quadrupole mass spectrometer. Additionally, the ambient air sample 44/45 ratio trace is provided (red trace) to demonstrate peak separation.

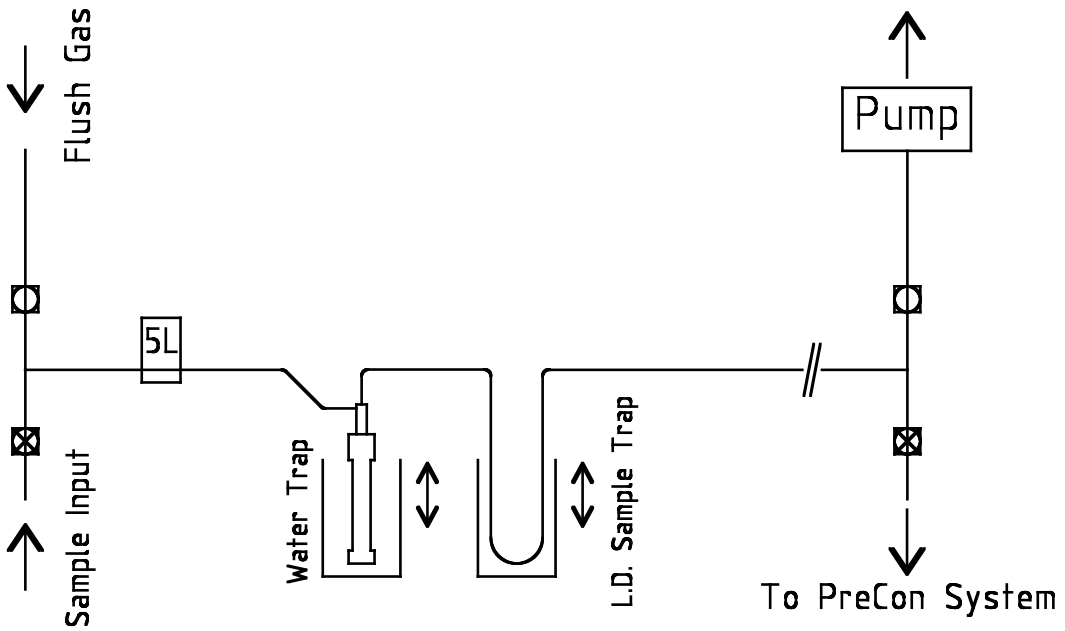

Figure 2.4. Ambient air sampling unit. The water trap and the sample trap are large diameter cryogenic stainless steel traps. Flush gas may be He, N_2 or synthetic air. Flows are regulated by a 5L min^{-1} mass flow controller (MKS instruments). After extraction, the contents of the sample trap are flushed to the preconcentration system (Fig. 2.1).

100 mL) is large enough to freeze out water vapor from very large and humid air samples.

Sampling proceeds as follows: both traps are immersed in liquid nitrogen while flush gas (ultra pure synthetic air or nitrogen) is drawn through the system at 50 mL min^{-1} by a dual head high-flow rotary pump downstream of the traps. The use of a pump keeps pressure inside the traps low at all times to prevent the condensation of oxygen. Once both traps are at temperature (approximately 2 minutes), the synthetic air supply is closed, the ambient sample line valve is opened, flow rates are increased to 0.5-1 L min^{-1} and sampling begins. Following the sampling of the desired volume, the flow rate is reduced to 50 mL min^{-1}, the sampling valve is closed, and the flush gas is reintroduced. Subsequently the pump valve is closed and the valve to the

preconcentration system is opened and the traps are extracted from the liquid nitrogen in turn: first the water trap is removed and left to warm in laboratory ambient air for 5 minutes to reduce pressure effects from rapid warm up of such a large volume. Then it is inserted in a warm water bath at 40 ºC to release adsorbed volatiles, while retaining water in liquid form at the bottom of the trap. The liberated volatiles are transferred to the large diameter U trap over 5 minutes. This trap is then extracted from the liquid nitrogen and allowed to warm in ambient laboratory air over 5 minutes, and is subsequently heated out under a 500 ºC air stream for 5 minutes to transfer all sampled compounds to the preconcentration system.

2.2.1e Automatization

With the exception of the ambient air sampling unit, the system has fully automatic operation. Pneumatic lifters are used to move the traps in or out the Dewar vessels filled with liquid nitrogen. The traps, flow controllers, and valves are operated electronically via a process/time table. Autonomous operation is limited to about 10 hours by the supply of liquid nitrogen in the Dewar vessels.

2.2.2 Performance and stability

For calibration, a 9-compound reference gas (Apel-Riemer, AiR Environmental, Inc.) is used as the primary working standard. Of the compounds in this gas, 4 are monitored in test and calibration runs at the start and end of each measuring day, and during night (automated), namely ethane (206 ppb), propane (103 ppb), methyl chloride (103 ppb) and benzene (103 ppb). Calibration runs with the standard were done with varying volumes, either 50, 100, or 200 mL, to ensure a range of peak areas similar to results in sample measurements and to test for non-linearity effects. Calibation runs using 100mL of this gas were most commonly done. Usage of low volume high concentration calibration gas as compared to a high volume dilution of

the same was found to have no effect in calibration results, similar to previous research (e.g. Archbold et al. 2005, Redeker et al. 2007), further verifying trap performance.

The $\delta^{13}C$ values of propane, methyl chloride, and benzene in the working standard were established utilizing the method described in Fisseha et al. (2009), at the Forschungszentrum Jülich, Germany, to be (-34.8 ± 0.4), (-48.7 ± 0.4), and (-28.1 ± 0.3) ‰ vs. VPDB, respectively. These calibration results agree (±0.3 to ±0.8 ‰, depending on compound) with all measurements of these compounds obtained by our system when calibrated against the aforementioned injected CO_2, and taking into account the shift in methyl chloride. Unfortunately, no independent measurement of ethane was achieved by the Jülich group. However, calibration results of the other tested gases and the reference CO_2 give high confidence that our estimate of (-28.6 ± 0.4) ‰ vs. VPDB is valid for ethane.

If the peak area of a given eluted compound was maintained above 0.5 Vs, the IRMS measured $\delta^{13}C$ values showed no dependency on the sample size. Below this value peak integration can yield inaccurate results and therefore a signal of 0.5 Vs was considered the limit of detection.

Figure 2.5a and b show time series of $\delta^{13}C$ (‰) and system sensitivity to illustrate the long-term stability of the system in the current configuration (since May 2009). The sensitivity was typically in the range 0.2 - 0.32 Vs ngC^{-1}. Some variability is evident from Figure 2.5b and can be attributed to the internal variability of the filament emission in the IRMS. This variation is taken into account by referencing against the aforementioned gas standard. Repeatability of mixing ratio measurements is evaluated to be less than ±5 % for all compounds. Together with the specified accuracy of ±5 % for the gas standard this defines the overall error of ±10 % for

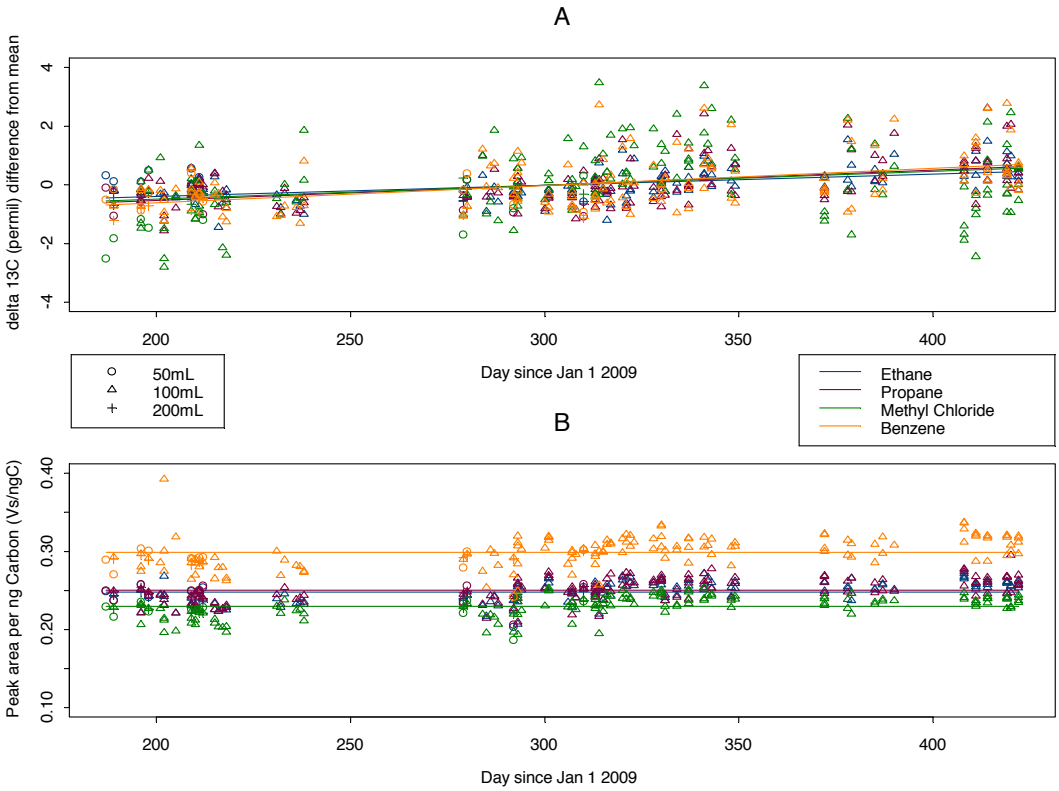

Figure 2.5. Time-stability of the system. Panels A and B show the difference from mean of $\delta^{13}C$ (‰, panel A); and sensitivity (Vs ngC^{-1}, panel B) of the 4 tested compounds in the working gas standard, respectively. Data of various injection volumes (50, 100, and 200mL) are plotted. The lines in panel A represent linear fits; the horizontal lines in panel B do not represent any trend but are plotted to make the long term variability more visible.

measured mixing ratios. The detection limit in terms of collected amount of carbon is calculated to be 1.5-2.5 ngC, based on the limit of 0.5 Vs for the IRMS signal and the observed sensitivity range. Figure 2.5a illustrates also a drift of $\delta^{13}C$ in the system over the selected period. In order to correct for drift in $\delta^{13}C$, detrending is accomplished by observing weekly averages as compared to long-term calibration measurement means.

To evaluate the overall precision a series of Gaussian-fitted histograms of detrended $\delta^{13}C$ for the compounds measured in the standard gas are provided in figures 2.6a-d,

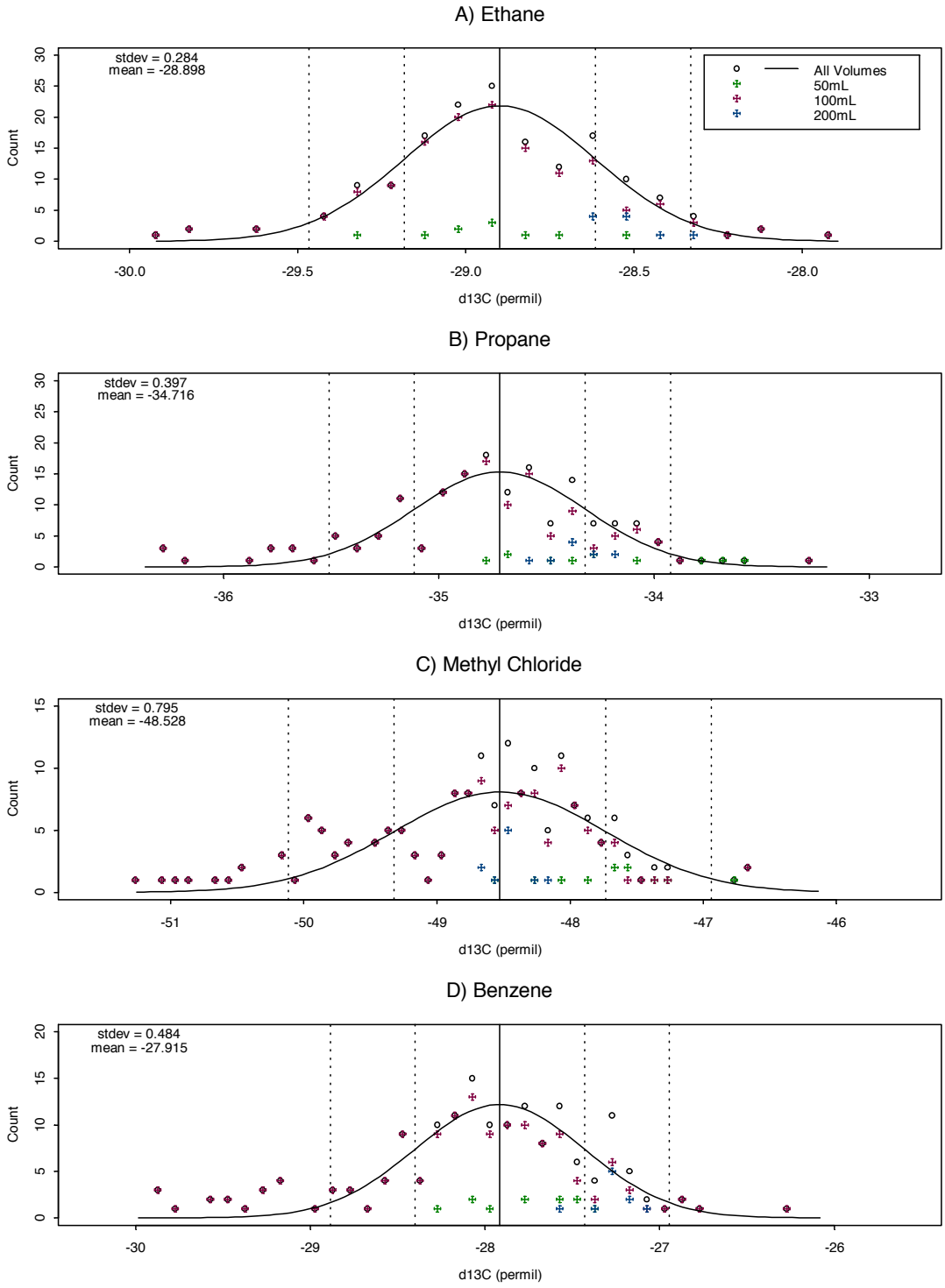

Figure 2.6. Histograms of detrended $\delta^{13}C$ (‰) data, together with Gaussian fit for the Apel-Riemer (AiR) multicompound NMHC calibration gas, including measurements of various volumes (50, 100, 200 mL) for peak area ranges comparable to measurements. Dashed lines indicate 1 and 2 σ intervals.

with a bin size of 0.1 ‰, outliers greater than 3σ rejected. For ethane, propane and benzene the 1-σ error was below 0.5 ‰ for all volumes tested. For methyl chloride, the standard deviation is ~0.8 ‰ for all tested volumes. These values are based on the entire dataset. The same analysis based on sub-samples including only the 50, 100, or 200 mL measurements yield very similar results. For example, for ethane, the mean $\delta^{13}C$ is -28.9, -28.9, -28.6 and -28.9 ‰, for 50, 100, 200 mL data, and all data, respectively; the corresponding standard deviations are 0.308, 0.296, 0.205, and 0.284 ‰. These values show that the sample volume does not influence the measurements. For other tested compounds, behavior is similar.

The reproducibility for other compounds was tested by introducing another standard gas, containing 20 to 50 ppb of acetylene, ethylene, propylene and C_4 and C_5 saturated hydrocarbons (also see Fig. 2.3). The results of stability evaluations of these compounds are broadly similar to those of the primary working standard. Table 2.2 summarizes $\delta^{13}C$ and sensitivity means and 1-σ errors of all tested compounds.

2.3 First results

To demonstrate capabilities of this instrument, we present the results of a 48-hour measurement campaign of selected non-methane hydrocarbons undertaken over 4-6 August 2009. Samples were taken from an ambient air inlet located ~20m above ground level at 52º05´14" N, 5º09´57" E. The sampling location is within 500 m of a traffic highway, and is located outside our laboratory on the Utrecht University campus, in a semi-urban environment. Thus, an abundance of local sources, dominated by traffic emissions, can be expected for hydrocarbons. Atmospheric conditions at the time of the campaign were characterized by warm stable summer weather. During this period, high surface pressure was located above the North Sea. The sample days were similar meteorologically, with clear skies, light winds, and

Table 2.2. Means and 1-σ standard deviations of $\delta^{13}C$ (‰) and IRMS Sensitivity (Vs ngC^{-1}) for compounds in regularly used calibration gases.

Compound	$\delta^{13}C$ mean ± σ (‰)	Sensitivity mean ± σ (Vs ngC^{-1})
	Primary NMHC working standard[a]	
Ethane	-28.898 ± 0.284	0.249 ± 0.0053
Propane	-34.716 ± 0.397	0.254 ± 0.0063
MeCl	-48.528 ± 0.795	0.231 ± 0.0058
Benzene	-27.915 ± 0.484	0.302 ± 0.0083
	Other tested compounds[b]	
Acetylene	-40.922 ± 0.441	0.241 ± 0.0062
Ethylene	-36.307 ± 0.716	0.239 ± 0.010
Propylene	-32.955 ± 0.658	0.258 ± 0.010
Isobutane	-32.209 ± 0.542	0.271 ± 0.0097
Butane	-35.658 ± 0.476	0.273 ± 0.0083
Isopentane	-34.927 ± 0.308	0.33 ± 0.0095

[a] 9-month detrended long-term accuracy levels

[b] n=20, over period of 1 month

high temperatures near 30 ºC. At night, temperatures decreased to near 20 ºC and the winds became near calm.

The samples were taken and processed in situ using the aforementioned ambient sampling unit, with 20 L samples (sampling rate 0.5 L min^{-1}) taken at approximately 2-hour intervals (excepting necessary calibration runs of the instrument) and processed immediately. The short time interval between samples afforded by the instrument design allowed detailed insight into diurnal evolution of NMHC $\delta^{13}C$; more so than the majority of previous urban stable carbon isotope studies. The 20 L sample size was chosen to ensure IRMS peak areas of >0.5 Vs for the all hydrocarbons of interest.

2.3.1 Mixing Ratio

Broadly, mixing ratios are in line with what may be expected for an urban environment (e.g. Seinfeld and Pandis, 1998), although for some compounds, especially the alkanes, quite high mixing ratios of several ppb were measured. The

mixing ratios (Fig. 2.7A-J and Table 2.3) show a clear diurnal cycle, which corresponds very well to patterns of urban activity. The unsaturated compounds (acetylene, ethylene, and propylene) exhibit a peak in the morning hours, minimum values in the afternoon, and elevated values at night. Such diurnal cycles agree well with traffic patterns and the development of the boundary layer mixing height. Morning vehicular traffic is intense; heavy congestion on local highways is common in the periods from 07:00 to 09:00 (all times in Central European Summer Time). The afternoon-evening (16:00 to 18:00) peak of traffic, though generally less intense than that of the morning but still notable, is not clearly observed in the data. This is attributed to increased mixing in the afternoon due to the breakup of the nighttime boundary layer, as compared to the morning hours.

Ethane also displays a clear diurnal cycle, but in contrast to the above compounds has peaks in mixing ratio during the night and early morning, far earlier than other compounds. The prevailing meteorological conditions of (near) calm winds during night suppressed mixing and allowed the buildup of continuously emitted gasses. Presuming that the main urban source of ethane is leakage of natural gas, local leakage could cause such an increase of mixing ratio. The daytime decrease may be similarly ascribed to the increase in mixing and dilution.

Isopentane, hexane, and benzene show profiles similar to the unsaturated hydrocarbons mentioned above. The change in mixing during daytime and nighttime can help to explain the afternoon decrease and nighttime buildup in mixing ratio of all alkanes measured, with the exception of n-pentane (Fig. 2.7h), which exhibits larger daytime than night-time mixing ratios. This implies a different, non-local source that dominates the mixing ratios for this compound.

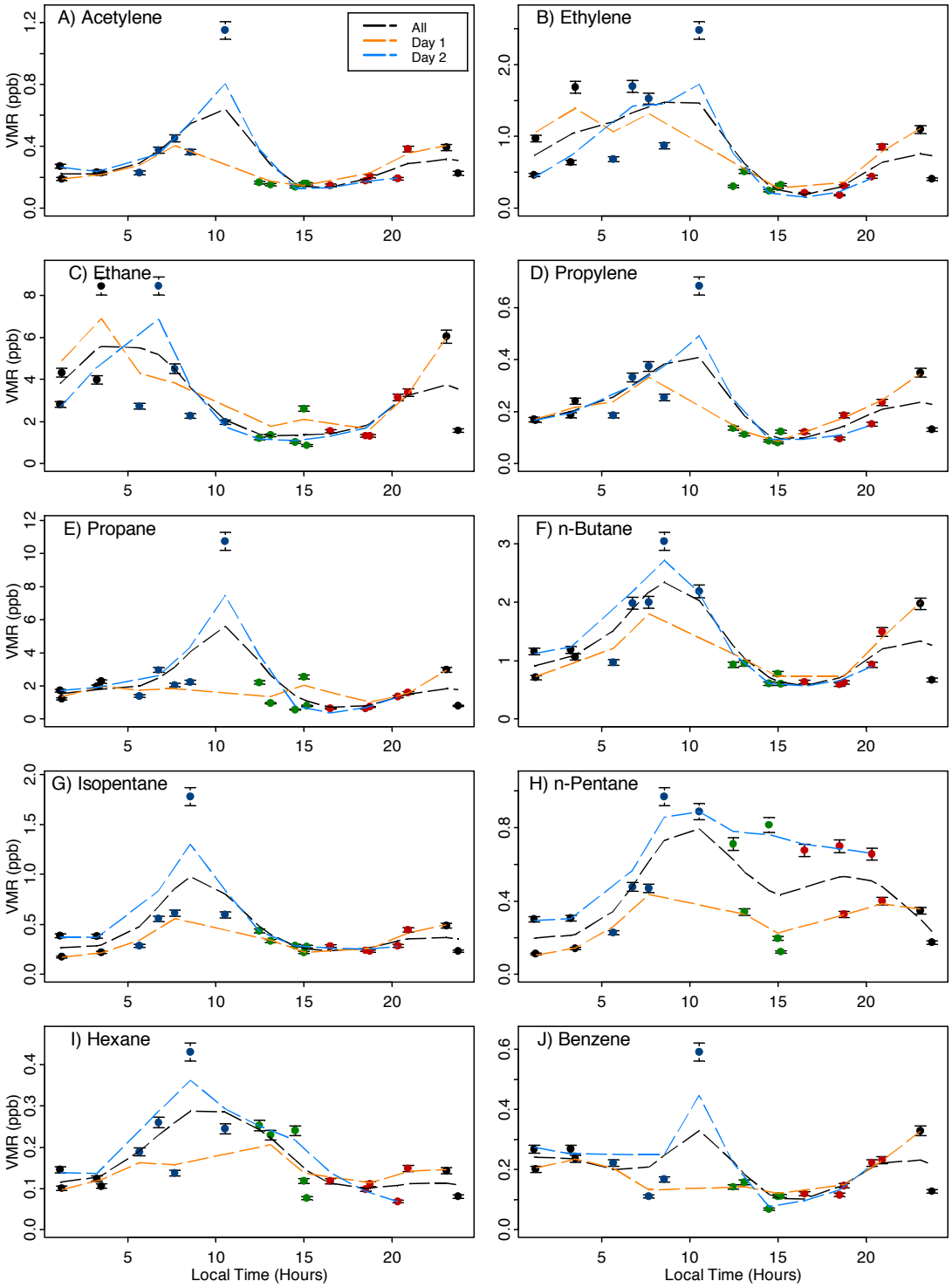

Figure 2.7. Mixing ratios (ppb) versus time over 48-hour (4-6 August 2009) period, overlapped on one diurnal cycle. Error bars indicate the 10% accuracy levels. Period means in table 2.3. Colors indicate time periods: P1 (black): 21:00 – 05:00; P2 (blue): 05:00 – 11:00; P3 (green): 11:00 – 15: 30; P4 (red): 15:30 – 21:00; these correspond to time period colors in figs. 8 and 9. Period codes correspond to those in tables 2.3, 2.4 and 2.5. Dashed lines are running averages.

Table 2.3. Mean mixing ratio and sample standard deviation, 48-h measurements, 4 to 6 August 2009.

Compound	Mean VMR all (ppb)	σ (ppb)	Mean VMR P1[a] (ppb)	σ (ppb)	Mean VMR P2 (ppb)	σ (ppb)	Mean VMR P3 (ppb)	σ (ppb)	Mean VMR P4 (ppb)	σ (ppb)
Acetylene	0.29	0.22	0.26	0.07	0.51	0.36	0.15	0.01	0.22	0.09
Ethylene	0.77	0.62	0.88	0.48	1.45	0.71	0.33	0.10	0.40	0.27
Ethane	3.09	2.23	4.52	2.43	3.98	2.68	1.41	0.69	2.14	1.03
Propylene	0.21	0.14	0.21	0.08	0.36	0.19	0.11	0.02	0.16	0.05
Propane	2.02	2.14	1.83	0.77	3.87	3.88	1.41	0.90	0.99	0.45
n-Butane	1.19	0.67	1.13	0.47	2.03	0.74	0.77	0.17	0.85	0.38
Isopentane	0.42	0.34	0.31	0.12	0.76	0.58	0.31	0.08	0.30	0.09
n-Pentane	0.45	0.27	0.23	0.10	0.61	0.31	0.43	0.30	0.55	0.17
Hexane	0.16	0.09	0.12	0.03	0.25	0.11	0.18	0.08	0.11	0.03
Benzene	0.20	0.11	0.24	0.07	0.27	0.21	0.12	0.03	0.17	0.06

[a] Period codes are the same as those defined in Fig. 2.7.

Supporting evidence for a distinct and non-local source can be found in the stable isotope measurements of this compound, of which discussion follows.

2.3.2 Stable carbon isotope composition

Figures 2.8a-j show $\delta^{13}C$ measurements over the sampling period. In general, $\delta^{13}C$ averages over the 48-hour period (Table 2.4) agree well with published values from studies of urban air.

Acetylene has a large daily variation (maximum of 5 ‰ and minimum of -15 ‰), but its mean over the entire period is -9.1 ‰, which falls well in the urban range of (-8 ± 4) ‰ as reported in Goldstein and Shaw, (2003). The maximum observed in acetylene is more enriched than previous measurements reported in urban environments, but is within the range of daytime summer values reported from rural/marine environments (Redeker et al., 2007).

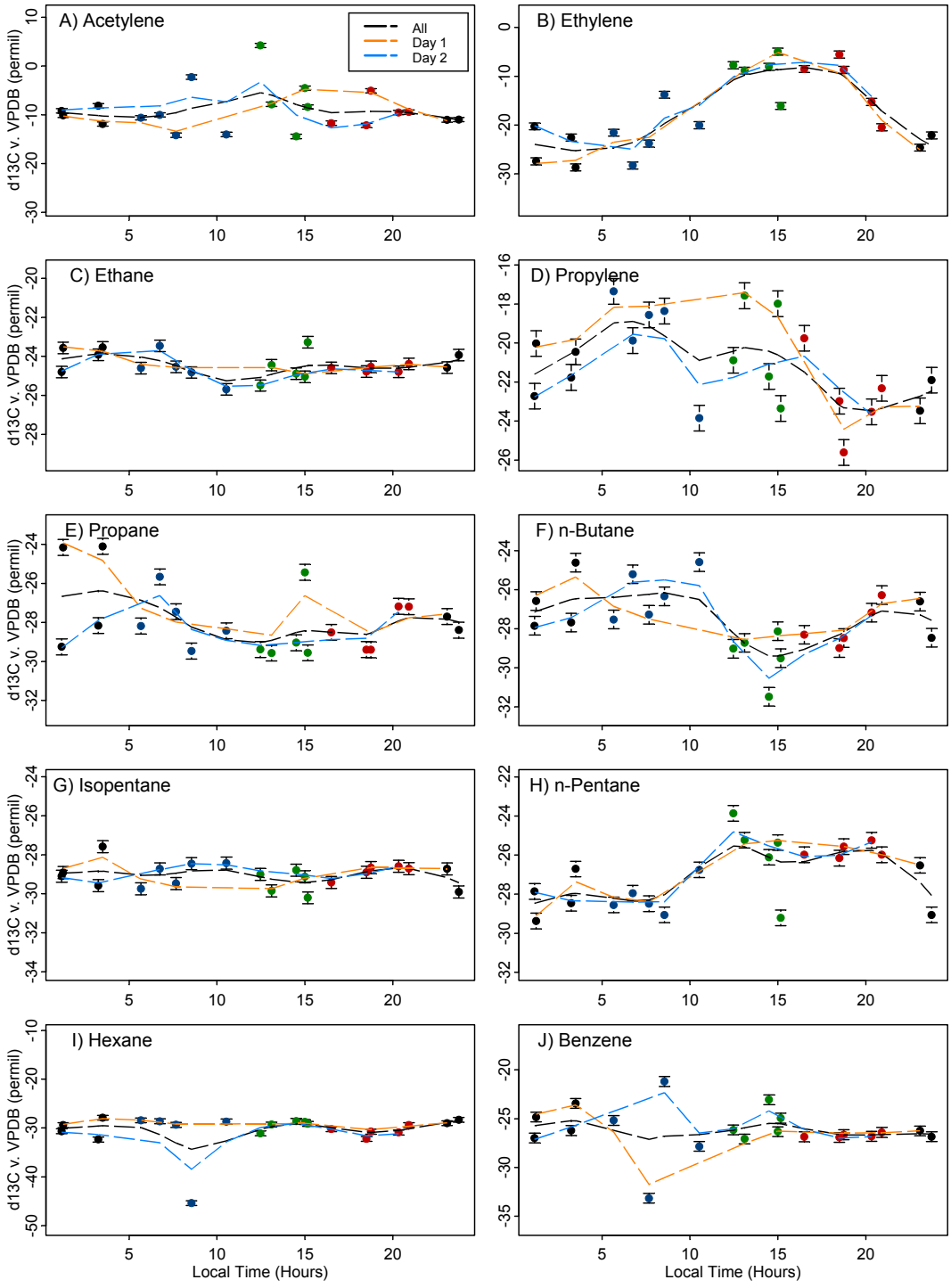

Figure 2.8. Compound $\delta^{13}C$ (‰ vs. VPDB) vs. time (hours) over 48-hour (4-6 August 2009) period, overlapped. Error bars indicate 1-σ ranges. Period means and standard deviations in table 2.4. Colors of points denote the time periods, which are defined in fig. 2.7.

Table 2.4. Mean $\delta^{13}C$ (‰) vs. VPDB and sample standard deviation, 48-h measurements, 4 to 6 August 2009.

Compound	Mean $\delta^{13}C$ (‰) all	σ (‰)	Mean $\delta^{13}C$ P1 [a] (‰)	σ (‰)	Mean $\delta^{13}C$ P2 (‰)	σ (‰)	Mean $\delta^{13}C$ P3 (‰)	σ (‰)	Mean $\delta^{13}C$ P4 (‰)	σ (‰)
Acetylene	-9.1	4.4	-10.2	1.4	-10.2	4.8	-6.2	6.8	-9.6	2.8
Ethylene	-17.0	7.9	-23.3	3.2	-21.5	5.3	-9.1	4.2	-11.7	6.1
Ethane	-24.5	0.6	-24.1	0.5	-24.6	0.8	-24.6	0.8	-24.6	0.17
Propylene	-21.1	2.3	-21.7	1.3	-19.6	2.5	-20.3	2.5	-22.8	2.1
Propane	-27.9	1.7	-27.0	2.3	-27.8	1.4	-28.6	1.7	-28.3	1.1
n-Butane	-27.6	1.7	-27.0	1.4	-26.2	1.3	-29.3	1.3	-27.8	1.1
Isopentane	-29.0	0.6	-29.0	0.8	-29.0	0.6	-29.4	0.6	-28.9	0.3
n-Pentane	-27.0	1.6	-28.0	1.2	-28.2	0.9	-26.0	2.0	-25.8	0.4
Hexane	-30.4	3.7	-28.6	1.7	-32.1	7.4	-29.4	1.0	-30.7	1.0
Benzene	-26.2	2.3	-25.9	1.4	-26.8	5.1	-25.5	1.6	-26.7	0.2

[a] Periods are the same as in Table 2.3.

Ethylene, which shows a very well defined diurnal cycle with minima near -30 ‰ in the early morning hours and maxima near -5 ‰ during the afternoon (24 h mean -17 ‰), agrees with expected mean values for C_2 to C_5 alkenes (-22±8 ‰, Goldstein and Shaw, 2003). The large diurnal variation, can be expected for such a reactive compound with a high *KIE* (18.6 ‰, Anderson et al., 2004). Strong fractionation occurs during summer daylight hours when OH levels are considerably high. Utilizing the isotopic clock parameterization (equation 2.3, Rudolph and Czuba 2000) provides additional support for this: assuming that the nighttime $\delta^{13}C$ value (mean -27‰) and daytime value (mean -10‰) represent the unoxidized ($^0\delta_{C2H4}$) and oxidized (δ_{C2H4}) isotope ratios of ethylene, respectively, a value for $^{OH}KIE_{C2H4}$ of 18.6 ‰ and $^{OH}k_{C2H4} = 7.9x10^{-12}$ cm^3 s^{-1} (at 296K, Atkinson et al. 2006), it is calculated that [OH] required for causing this fractionation is $3.6x10^6$ molecules cm^{-3} for a 9 hour atmospheric processing time. This OH concentration is well within the range for summer tropospheric conditions (e.g., Lu and Khalil, 1991).

The ethane stable isotope ratios we measured are in general more enriched than higher alkanes. This is due to its differing source from natural gas, the ethane in

which is known to be relatively enriched. The mean $\delta^{13}C$ of ethane was measured to be (-24.5 ± 0.6) ‰ for the entire period. Tsunogai et al. 1999 reported values between -28 to -22 ‰ in urban and marine locations. There is almost no diurnal variation in our measurements (with the exception of a slight depletion during the period of highest mixing ratio values, in the morning), which is also reasonable to expect for the most stable and longest-lived non-methane hydrocarbon.

The $\delta^{13}C$ of the C_3 to C_6 alkanes (with the exception of n-butane and n-pentane, see below) show little (clearly apparent) diurnal variation and mean values of -27 to -30 ‰ during all periods. Previously reported measurements indicated (-27 ± 2.5) ‰ (Rudolph et al. 2002, Goldstein and Shaw 2003). The presence of a single very depleted point (-45 ‰) in measurements of hexane is notable, but this outlier may be due to an unidentified experimental problem. Apart from this point, standard deviations for these compounds also correspond well to previous results. Benzene also fits well to previous measurements despite some apparent high morning variability: mean (-26.2 ± 2.3) ‰, compared to literature values of (-27 ± 2) ‰ (Goldstein and Shaw 2003).

2.3.3 Source Signatures

A common tool for atmospheric isotope research to decipher sources is the Keeling plot analysis, which was first developed for the analysis of stable carbon isotopes of carbon dioxide (Keeling 1958). This involves correlating $\delta^{13}C$ against the inverse of the mixing ratio, and linearly fitting the result. The y-intercept of this fit then indicates the isotopic composition of the contaminating source that mixes into background air. This procedure is based on a few assumptions, most importantly: 1.) there should be only one source and a stable reservoir into which it is being diluted; and 2.) the $\delta^{13}C$ and inverse mixing ratio should be well-correlated; lest the values

calculated become unclear and unreliable (Keeling 1958). In our dataset, the Keeling plot analysis works well for ethylene, n-butane, and n-pentane (Figs. 2.9a-c). The isotope source signatures determined this way are given in Table 2.5. Other measured compounds are not included because of small isotopic variation or low correlation, indicating that the above conditions are violated.

For ethylene the source signatures (~-27 ‰) derived from this analysis agree well with engine emission measurements (Rudolph et al. 2002 and Goldstein and Shaw 2003). The positive slopes of the Keeling fits are in line with the interpretation of the diurnal variation of the VMR and $\delta^{13}C$ (see discussion above).

The interpretation for n-butane and n-pentane is more complicated because their lifetimes are longer. As a result their mixing ratios are controlled by transport and mixing of different sources. The source signatures of n-butane during periods 3 and 4 (-25.4 and -24.5 ‰, respectively) suggest that emissions from fossil fuel combustion (-27 ± 2.5 ‰, Goldstein and Shaw 2003) are the dominant local source. However, the reversed slope may indicate that background concentrations of n-butane originate mainly from other sources.

In n-pentane there is a strong departure in source signature values in table 2.5 period 3: here a strongly correlated source signature of -23.9 ‰ occurs, as compared to more depleted values at other times. This would lend support to the speculation that there is a distinct isotopically different emission occurring at this time as discussed above for the mixing ratios.

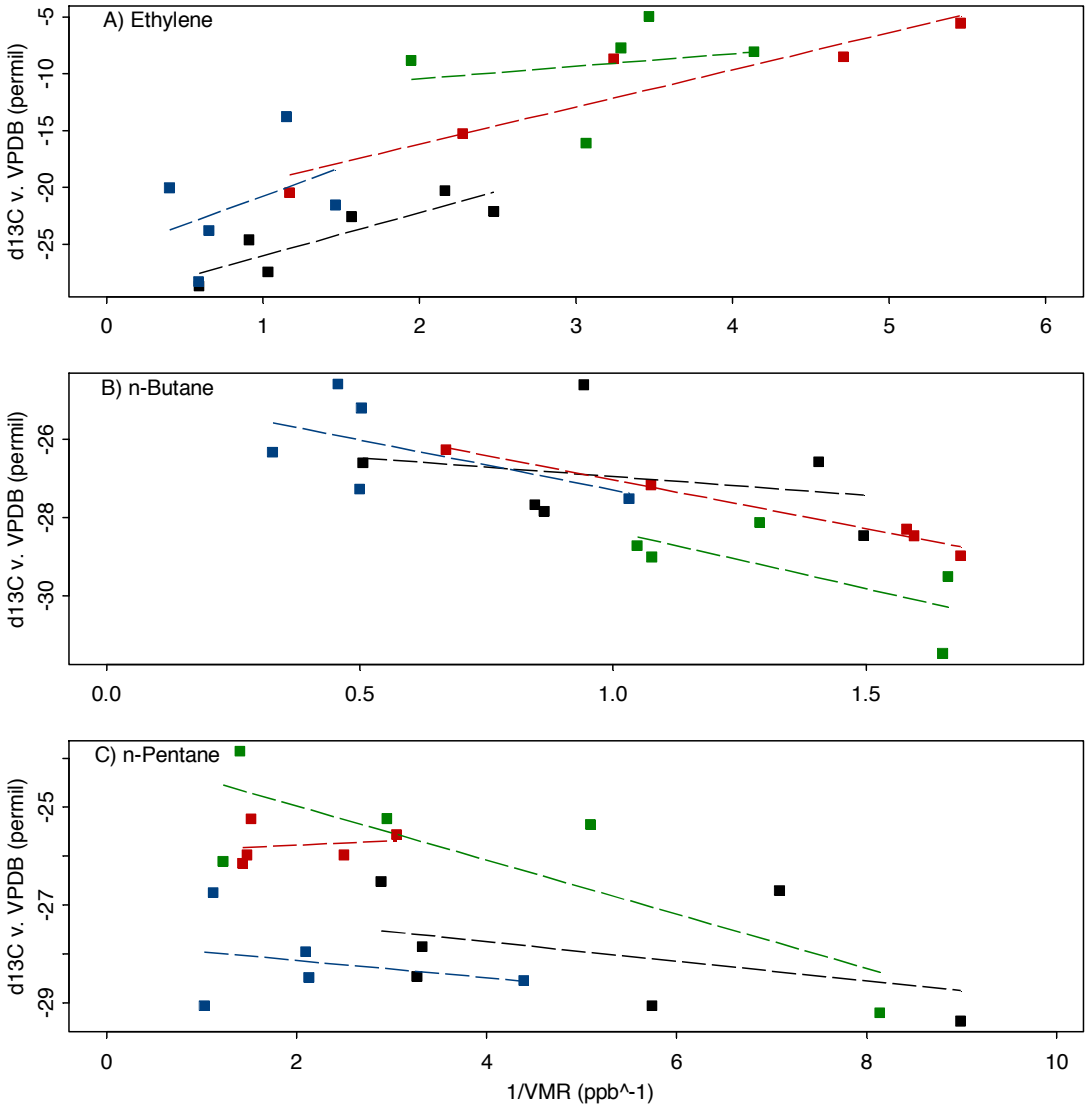

Figure 2.9. Ethylene, n-butane, and n-pentane $\delta^{13}C$ (‰ vs. VPDB) plotted versus inverse mixing ratio (ppb^{-1}) over the 48-hour (4-6 August 2009) period, with linear fits to points of each time period. Derived values for isotope source signatures are given in table 2.5. Colors indicate periods as indicated in fig. 2.7.

Table 2.5. Source signature (SS, in ‰ vs. VPDB) and r^2 from fits in Fig. 2.9, 48-h measurements, 4 to 6 August 2009.

Compound	SS All (‰)	R^2 All	SS P1 [a] (‰)	R^2 P1	SS P2 (‰)	R^2 P2	SS P3 (‰)	R^2 P3	SS P4 (‰)	R^2 P4
Ethylene	-26.8	0.68	-29.8	0.76	-25.7	0.17	-12.6	0.04	-22.7	0.89
n-Butane	-24.7	0.52	-26	0.07	-24.7	0.29	-25.4	0.47	-24.5	0.98
n-Pentane	-25.9	0.22	-27	0.17	-27.8	0.08	-23.9	0.65	-26	0.03

[a] Periods are the same as in Table 2.3.

2.4 Conclusions

We have presented a NMHC stable carbon isotope analysis system capable of high-resolution measurements of many compounds from a large variety of sample sources with small measurement errors (1 ‰ vs. VPDB or less). In particular, the capability to process high volume atmospheric allows examination of samples with large quantities of bulk gases and CO_2, without loss of any compounds of interest, and with a short processing time as well. As the first results demonstrate, $\delta^{13}C$ values measured during a 48-hour ambient air measurement campaign agree well with previous research, while highlighting the complex diurnal behavior of hydrocarbons in an urban environment. This on the one hand demonstrates reliable operation of the system and on the other opens the doorway to exciting future measurements.

Acknowledgements

We would like to thank Henk Jansen, of Rijksuniversiteit Groningen, The Netherlands, for calibration of the CO_2 reference standard; and Iulia Gensch, of Forschungscentrum Jülich, Germany, for calibration of the NMHC working standard.

References

Anderson, R. S., Huang, L., Iannone, R., Thompson, A. E., and Rudolph, J.: Carbon kinetic isotope effects in the gas phase reactions of light alkanes and ethene with the OH radical at 296±4 K, *J. Phys. Chem. A*, **108**, 11537–11544, doi:10.1021/jp0472008, 2004.

Archbold, M. E., Redeker, K. R., Davis, S., Elliot, T., and Kalin, R. M.: A method for carbon stable isotope analysis of methyl halides and chlorofluorocarbons at pptv concentrations, *Rapid Commun. Mass Sp.*, **19**, 337–340, doi:10.1002/rcm.17, 2005.

Atkinson, R., Baulch, D. L., Cox, R. A., Crowley, J. N., Hampson, R. F., Hynes, R. G., Jenkin, M. E., Rossi, M. J., Troe, J., and IUPAC Subcommittee: Evaluated kinetic and photochemical data for atmospheric chemistry: Volume II – gas phase reactions of organic species, *Atmos. Chem. Phys.*, **6**, 3625–4055, doi:10.5194/acp-6-3625-2006, 2006.

Bill, M., Rhew, R. C., Weiss, R. F., and Goldstein, A. H.: Carbon isotope ratios of methyl bromide and methyl chloride emitted from a coastal salt marsh, *Geophys. Res. Lett.*, **29**, 4, 4 pp., doi:10.1029/2001GL012946, 2002.

Brenninkmeijer, C. A. M.: Applications of stable isotope analysis to atmospheric trace gas budgets, *Eur. Phys. J. C*, **1**, 137–148, doi:10.1140/epjconf/e2009-00915-x, 2009.

Conny, J. M. and Currie, L. A.: The isotopic characterization of methane, non-methane hydrocarbons and formadehyde in the troposphere, *J. Atmos. Environ.*, **30**, 4, 621–638, 1996.

Czapiewski, K. V., Czuba, E., Huang, L., Ernst, D., Norman, A. L., Koppmann, R., and Rudolph, J.: Isotopic composition of non-methane hydrocarbons in emissions from biomass burning, *J. Atmos. Chem.,* **43**, 45–60, 2002.

Fisseha, R., Spahn, H., Wegener, R., Hohaus, T., Brasse, G., Wissel, H., Tillmann, R., Wahner, A., Koppmann, R., and Kiendler-Scharr, A.: Stable carbon isotope composition of secondary organic aerosol from *β*-pinene oxidation, *J. Geophys. Res*., **114**, D02304, doi:10.1029/2008JD011326, 2009.

Goldstein, A. H. and Galbally, I. E.: Known and unexplored organic constituents in the Earth's atmosphere, *Environ. Sci. Technol*., **41(5)**, 1514–1521, doi:10.1021/es072476p, 2007.

Goldstein, A. H. and Shaw, S. L.: Isotopes of volatile organic compounds: an emerging approach for studying atmospheric budgets and chemistry, *Chem. Rev.,* **103**, 5025–5048, 2003.

Guenther, A., Hewitt, C. N., Erickson, D., Fall, R., Geron, C., Graedel, T., Harley, P., Klinger, L., Lerdau, M., McKay, W. A., Pierce, T., Scholes, B., Steinbrecher, R., Tallamraju, R., Taylor, J., and Zimmerman, P.: A global-model of natural volatile organic-compound emissions, *J. Geophys. Res.-Atmos.*, **100**, 8873–8892, 1995.

Harper, D. B., Hamilton, J. T. G., Ducrocq, V., Kennedy, J. T., Downey, A., and Kalin, R. M.: The distinctive isotopic signature of plant-derived chloromethane: possible application in constraining the atmospheric chloromethane budget, *Chemosphere*, **52**, 433–436, doi:10.1016/S0045-6535(03)00206-6, 2003.

Iannone, R., Anderson, R. S., Rudolph, J., Huang, L., and Ernst, D.: The carbon kinetic isotope effects of ozone-alkene reactions in the gasphase and the impact of ozone reactions on the stable carbon isotope ratios of alkenes in the atmosphere. *Geophys. Res. Lett.*, **30(13)**, 1684–1688, doi:10.1029/2003GL017221, 2003.

Jardine, K. J., Karl, T., Lerdau, M., Harley, P., Guenther, A., Mak, J. E.: Carbon isotope analysis of acetaldehyde emitted from leaves following mechanical stress and

anoxia, *Plant Biology*, **11(4)**, 591–597, doi: 10.1111/j.1438-8677.2008.00155.x, 2009.

Keeling, C. D.: The concentration and isotopic abundances of atmospheric carbon dioxide in rural areas, *Geochim. Cosmochim. Acta*, **13**, 322–334, 1958.

Keppler, F., Harper, D. B., Röckmann, T., Moore, R. M., and Hamilton, J. T. G.: New insight into the atmospheric chloromethane budget gained using stable carbon isotope ratios, *Atmos. Chem. Phys.*, **5**, 2403–2411, doi:10.5194/acp-5-2403-2005, 2005.

Lu, Y. and Khalil, M. A. K.: Tropospheric OH: model calculations of spatial, temporal, and secular variations, *Chemosphere,* **23**, 397–444, 1991.

Matthews, D. M. and Hayes, J. M.: Isotope-ratio-monitoring gas chromatography-mass spectrometry, *Anal. Chem*., **50**, 11, 1465–1473, 1978.

Middleton, P.: Sources of air pollutants, in: *In Composition, Chemistry, and Climate of the Atmosphere*, edited by: Singh, H. B., John Wiley & Sons Inc., New York, 88-119, 1995.

Milton, M. J. T., Harris, P. M., Brown, A. S., and Cowper, C. J.: Normalization of natural gas composition data measured by gas chromatography, *Meas. Sci. Technol.,* **20**, 025101, doi:10.1088/0957-0233/20/2/025101, 2010.

Nara, H., Nakagawa, F., and Yoshida, N.: Development of two-dimensional gas chromatography/ isotope ratio mass spectrometry for the stable carbon isotopic analysis of C_2–C_5 non methane hydrocarbons emitted from biomass burning, *Rapid Commun. Mass Sp.*, **20**, 241–247, doi:10.1002/rcm.2302, 2006.

Nara, H., Toyoda, S., and Yoshida, N.: Measurements of stable carbon isotopic composition of ethane and propane over the Western North Pacific and Eastern Indian Ocean: a useful indicator of atmospheric transport process*, J. Atmos. Chem.,* **56**, 293–314, doi:10.1007/s10874-006-9057-3, 2007.

Redeker, K. R., Davis, S., and Kalin, R. M.: Isotope values of atmospheric halocarbons and hydrocarbons from Irish urban, rural, and marine locations, *J. Geophys. Res.,* **112**, D16307, doi:10.1029/2006JD007784, 2007.

Röckmann, T., Kaiser, J., Brenninkmeijer, C. A. M. and Brand, W. A.: Gas-chromatography, isotope-ratio mass spectrometry method for high-precision position-dependent ^{15}N and ^{18}O measurements of atmospheric nitrous oxide, *Rapid Commun. Mass Spectrom.* **17**, 1897-1908, 2003.

Rudolph, J. and Czuba, E.: On the use of isotopic composition measurements of volatile organic compounds to determine the "photochemical age" of an air mass, *Geophys. Res. Lett.*, **27**, 23, 3865–3868, 2000.

Rudolph, J. and Ehhalt, D. H.: Measurements of C_2–C_5 hydrocarbons over the North Atlantic, *J. Geophys. Res*., **86**, C12, 11959–11964, 1981.

Rudolph, J., Lowe, D. C., Martin, R. J., and Clarkson, T. S.: A novel method for compound specific determination of ^{13}C in volatile organic compounds at ppt levels in ambient air, *Geophys. Res. Lett.,* **24(6)**, 659–662, 1997.

Rudolph, J., Czuba, E., Norman, A. L., Huang, L., and Ernst, D.: Stable carbon isotope composition of nonmethane hydrocarbons in emissions from transportation related sources and atmospheric observations in an urban atmosphere, *Atmos. Environ.*, **36**, 1173–1181, 2002.

Saito, T., Kawamura, K., Tsunogai, U., Chen, T., Matsueda, H., Nakatsuka, T., Gamo, T., Uematsu, M., and Huebert, B. J.: Photochemical histories of nonmethane hydrocarbons inferred from their stable carbon isotope ratio measurements over east Asia, *J. Geophys. Res.,* **114**, D11303, doi:10.1029/2008JD011388, 2009.

Saito, T., Tsunogai, U., Kawamura, K., Nakatsuka, T., and Yoshida, N.: Stable carbon isotopic compositions of light hydrocarbons over the Western North Pacific

and implication for their photochemical ages, *J. Geophys. Res.,* **107(D4)**, 4040, doi:10.1029/2000JD000127, 2002.

Santrock, J., Studley, S. A., and Hayes, J. M.: Isotopic analyses based on the mass spectra of carbon dioxide, *Anal. Chem.,* **57,** 7, 1444–1448, doi:10.1021/ac00284a060, 1985.

Seinfeld, J. H. and Pandis, S. N.: *Atmospheric Chemistry and Physics: from Air Pollution to Climate Change*, John Wiley and Sons, New York, 1326 pp., 1998.

Skrbic, B. D. and Zlatkovic, M. J.: Simple method for the rapid analysis of natural gas by gas chromatography, *Chromatographia*, **17(1),** 44–46, 1983.

Tsunogai, U. and Yoshida, N.: Carbon isotopic compositions of C_2–C_5 hydrocarbons and methyl chloride in urban, coastal, and maritime atmospheres over theWestern North Pacific, *J. Geophys. Res.,* **104**, D13, 16033–16039, 1999.

Warneck, P.: *Chemistry of the Natural Atmosphere*, Academic Press, San Diego, CA, 757 pp., 1988.

Chapter 3: Stable carbon isotope fractionation in the UV photolysis of CFC-11 and CFC-12

A. Zuiderweg, J. Kaiser, J. C. Laube, T. Röckmann, and R. Holzinger

Published in Atmospheric Chemistry and Physics, 12, 4379-4385, 2012.

Abstract

The chlorofluorocarbons CFC-11 ($CFCl_3$) and CFC-12 (CF_2Cl_2) are stable atmospheric compounds that are produced at the earth's surface, but removed only at high altitudes in the stratosphere by photolytic reactions. Their removal liberates atomic chlorine that then catalytically destroys stratospheric ozone. For such long-lived compounds, isotope effects in the stratospheric removal reactions have a large effect on their global isotope budgets. We have demonstrated a photolytic isotope fractionation for stable carbon isotopes of CFC-11 and CFC-12 in laboratory experiments using broadband UV-C (190-230 nm) light. $^{13}C/^{12}C$ isotope fractionations (ε) range from (-23.8±0.9) to (-17.7±0.4) ‰ for CFC-11 and (-66.2±3.1) to (-51.0±2.9) ‰ for CFC-12 between 203 and 288 K, a temperature range relevant to conditions in the troposphere and stratosphere. These results suggest that CFCs should become strongly enriched in ^{13}C with decreasing mixing ratio in the stratosphere, similar to what has been recently observed for CFC chlorine isotopes. In conjunction with the strong variations in CFC emissions before and after the Montréal Protocol, the stratospheric enrichments should also lead to a significant temporal increase in the ^{13}C content of the CFCs at the surface over the past decades, which should be recorded in atmospheric air archives such as firn air.

3.1 Introduction

The chlorofluorocarbons CFC-11 ($CFCl_3$) and CFC-12 (CF_2Cl_2) are the most abundant anthropogenic halocarbons in the atmosphere. Before their production was banned under the Montréal Protocol and its amendments, the usage of these compounds as refrigerants, cleansers, aerosol propellants and foam-blowing agents worldwide resulted in significant atmospheric loading; at their peaks in 1990 and 2003, respectively, mean mixing ratios in the troposphere were approximately 260 ppt (ppt = pmole $mole^{-1}$ = 10^{-12} mole $mole^{-1}$) for CFC-11 and 550 ppt for CFC-12 (Forster et al., 2007; AGAGE 2010). Due to the buildup of these and other anthropogenic halocarbons, total organic chlorine levels in the troposphere increased from approximately 600 ppt in 1900 to nearly 3350 ppt in 2008. CFC-11 and CFC-12 account for approximately 55% of the total, outweighing contributions by natural compounds such as methyl chloride, HCl and naturally emitted molecular chlorine (Butler et al., 1999; WMO 2010).

Chlorofluorocarbons such as CFC-11 and CFC-12 are produced by anthropogenic processes at the earth's surface, but have their only significant sinks in the stratosphere, at altitudes where UV-C radiation ($\lambda < 220$nm) is sufficiently abundant to dissociate the C-Cl bond: Eq. (R3.1). A minor sink (approximately 3-7 %) is due to Cl abstraction by $O(^1D)$, which is produced from the photolysis of ozone in the stratosphere: Eq. (R3.2) (Seinfeld and Pandis, 1998; Laube et al., 2010a).

$$CF_mCl_{4-m} + h\nu \xrightarrow{\lambda<220\ \text{nm}} CF_mCl_{3-m} + Cl\cdot \qquad \text{(R3.1)}$$

$$CF_mCl_{4-m} + O(^1D) \longrightarrow CF_mCl_{3-m} + ClO \qquad \text{(R3.2)}$$

These reactions cause the initial release of chlorine to begin the now well-known catalytic decomposition of ozone first proposed by Molina and Rowland (1974).

In addition, CFC-11 and CFC-12 have a significant global warming potential (4,750 and 10,900 times that of CO_2 per kg, respectively, over a 100 year time horizon), resulting together in an atmospheric radiative forcing of approximately 0.233 W/m^2 in 2005 and thus contributing to anthropogenic climate change (Massie and Goldman, 1992; Forster et al., 2007).

Since the implementation of the Montréal Protocol in 1987, the mixing ratios of CFC-11 and CFC-12 in the troposphere have decreased from their peak values to 240 ppt and 530 ppt, respectively, as sources have decreased in strength and the stratospheric sink has become dominant (Engel et al., 1998; Forster et al., 2007; AGAGE 2010). However, due to the long atmospheric lifetimes of these compounds (45 and 100 years for CFC-11 and CFC-12, respectively, WMO 2010), it is expected that atmospheric effects caused by the presence of these CFCs will persist for decades to centuries (Engel et al., 1998; Forster et al., 2007).

The stable isotope composition of species in the atmosphere can be altered by chemical reactions due to differences in chemical bond strengths ascribed to isotopic substitution, causing fractionation between the different isotopologues of a given molecule (Brenninkmeijer et al., 2003). Isotope values are conveniently expressed in δ notation, in the case of ^{13}C:

$$\delta^{13}\mathrm{C} = \frac{^{13}R_{\mathrm{sample}}}{^{13}R_{\mathrm{standard}}} - 1 \qquad (3.1)$$

where ^{13}R is the ^{13}C/^{12}C ratio in a sample or standard material, respectively. The internationally accepted reference material for ^{13}C is Vienna Pee Dee Belemnite (VPDB), and the δ value is commonly multiplied by 1000 ‰ to express it in per mille (‰) for readability. Assuming a Rayleigh-type fractionation, the isotope fractionation

ε relates the change in δ value and mixing ratio during a photolysis reaction as follows:

$$\ln\left(\frac{\delta^{13}\mathrm{C}+1}{\delta^{13}\mathrm{C}_0+1}\right) = \varepsilon \ln(F) \qquad (3.2)$$

where $\delta^{13}C_0$ and $\delta^{13}C$ are the stable carbon isotope ratios of the compound before and after photolysis, respectively, and F is the fraction remaining after photolysis. ε is also commonly expressed in ‰.

CFC-11 and CFC-12 have similar atmospheric cycles as N_2O, which is also long-lived (120 years lifetime) and has mainly surface sources and stratospheric sinks. In the case of N_2O, laboratory experiments, field measurements and modelling studies have shown strong heavy isotope enrichments in the stratosphere, which have an important effect on the isotopic composition in the troposphere (e.g. Rahn and Wahlen, 1997; Röckmann et al., 2001; Kaiser et al., 2003 and 2006; Blake et al., 2003; von Hessberg et al., 2004; Morgan et al., 2004). For CFC-12, recent measurements of the stable chlorine isotope ratio ($^{37}Cl/^{35}Cl$) of stratospheric CFC-12 have shown strong ^{37}Cl enrichments. Associated with the well-established decrease in mixing ratio above the tropopause, a progressive increase in the $^{37}Cl/^{35}Cl$ ratio by up to 27 ‰ relative to tropospheric air was observed over 14 – 34 km altitude, with an apparent isotope fractionation of ε_{app} = (–12.1 ± 1.7) ‰ (Laube et al., 2010a).

In this study we report a carbon ($^{13}C/^{12}C$) isotope fractionation (ε) in CFC-11 and CFC-12 during laboratory broadband UV-C (190-230 nm) photolysis at atmospherically relevant temperatures.

3.2 Method

Photolysis experiments were carried out in March 2011 with a mixture of CFC-11 and CFC-12 in nitrogen, utilizing a photolysis setup at the University of East Anglia in Norwich, UK. The gas mixture used in the experiments was prepared using a custom dilution system with sample loops of 2.5 and 0.1 mL (Laube et al., 2010b). This system is built into a HP5890 GC oven and is maintained at 353 K to ensure that compounds are in the gas phase when they are diluted. It uses a Valco 6-port valve for switching sample loops, Nupro valves for controlling input and extraction of compounds, a scroll pump for evacuation, and oxygen-free nitrogen (BOC Gases Inc.) for dilution.

Using this system, 5 μmol CFC-11 and 0.2 μmol of CFC-12 were mixed in turn with nitrogen into a single 3 L canister at 300 kPa total pressure, which yielded mixing ratios of 13 ppm for CFC-11 and 530 ppb for CFC-12, both with an error of ± 10%. These high mixing ratios were chosen in order to provide adequate material for analysis, while keeping sample volumes small. The use of oxygen-free nitrogen in the mixture excludes the O(^1D) reaction described in Eq. (R2) from taking place in the reaction chamber. The gas amount of the prepared mixture was sufficient for all experiments.

Figure 3.1 shows a diagram of the photolysis setup. The quartz-glass reactor, which has a volume of 125 mL (total system volume including lines is approximately 160 mL), is temperature controlled through an ethanol regulator and cooler. Pressures in the reactor system are measured through an array of pirani, piezo and CMR pressure sensors; evacuation of the entire system is facilitated through a scroll pump. Photolysis of the CFC mixture is induced by a water-cooled 1 kW antimony (hereafter Sb) lamp (mfr. Heraeus, Hanau, Germany) with a broadband emission

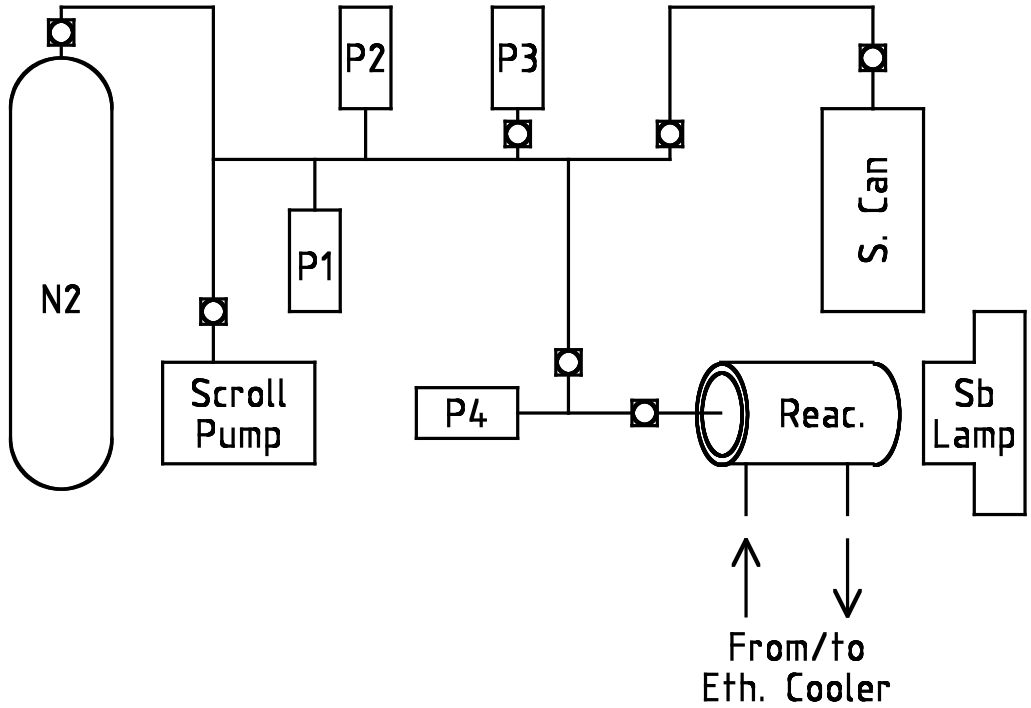

Figure 3.1. Diagram of the photolysis setup at the School of Enviromental Sciences at the University of East Anglia. P1 – P4 indicate pressure sensors, S. Can the sample canister. During filling of the reactor, the source canister containing the unphotolyzed CFC-mixture is installed in place of the sample canister.

spectrum covering the range 190 to 230 nm, which is ideal for inducing photolysis in CFCs. A spectrum of the Sb lamp emission and solar flux at 20 and 30 km for the relevant wavelengths and the absorption spectra of CFC-11 and -12 are shown in fig. 3.2. The normalized product of the absorption spectra with Sb lamp and 30 km flux (folded spectra) is shown in fig. 3.3. This lamp has previously been used for photolysis experiments with N_2O (Röckmann et al., 2000 and 2001; Kaiser et al., 2002 and 2003).

The gas mixture, at pressures near 100 kPa, was irradiated with UV light with exposure times varying from 0 to 3 hours while the reactor was kept at various

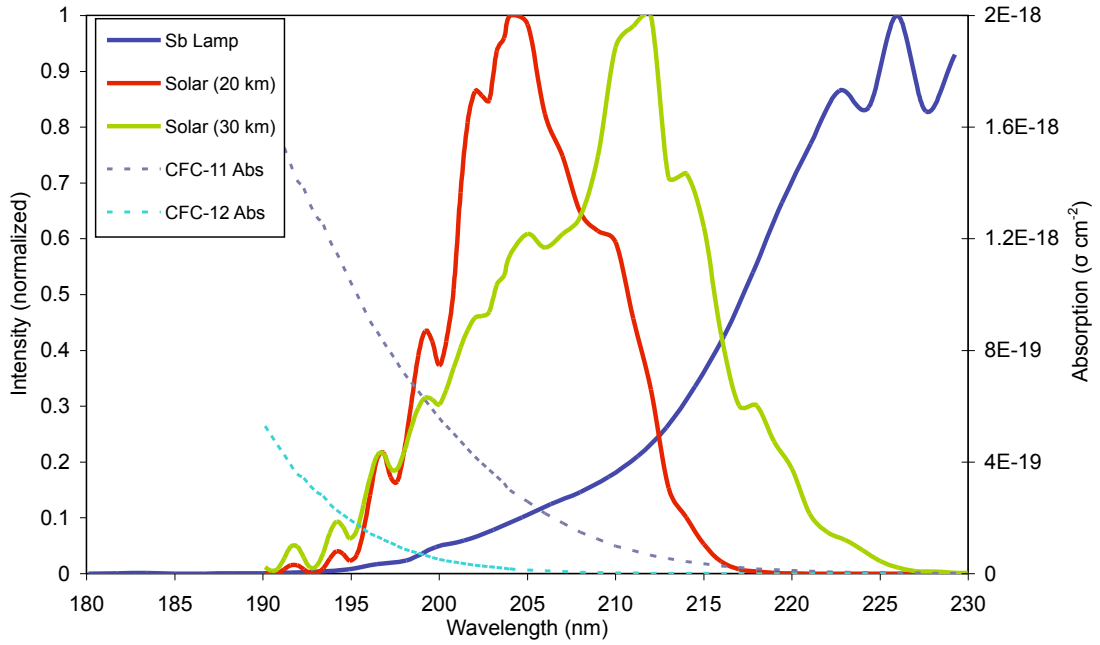

Figure 3.2. Normalized UV-C intensity of the Sb lamp and actinic UV-C (Minschwaner et al., 1993) in the altitude range where CFC photolysis takes place (19-34km), and absorption spectra for CFC-11 and -12 in the relevant wavelength range.

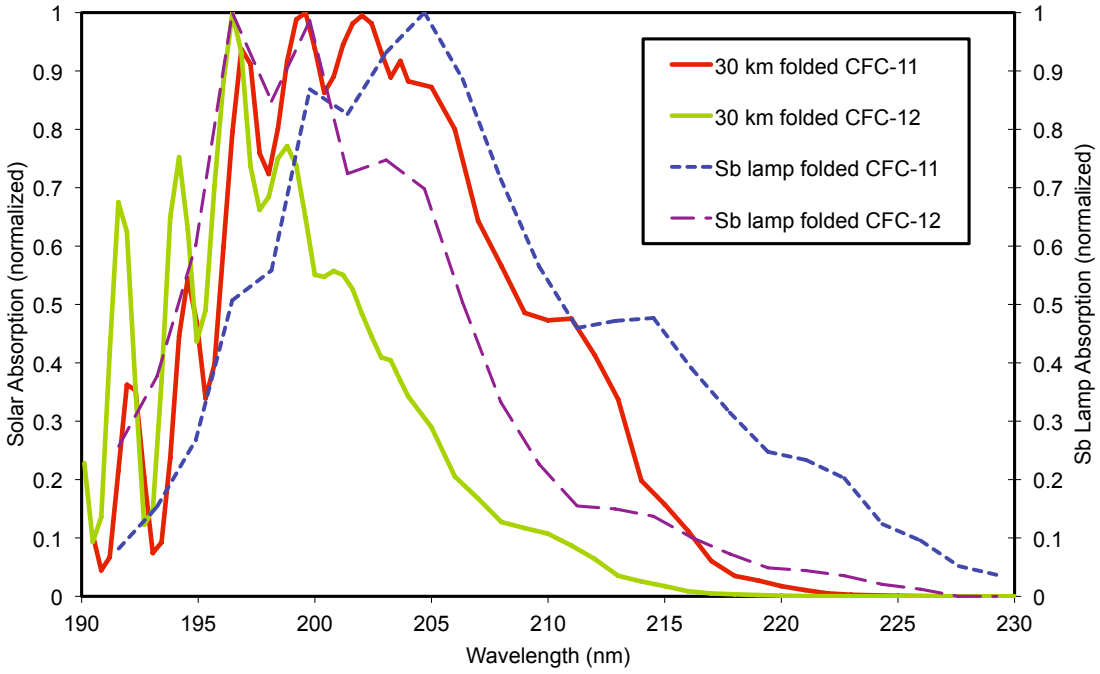

Figure 3.3. Product (folded spectra) of CFC-11 and -12 absorption spectra and solar and Sb lamp spectra, normalized.

temperatures (203, 233, and 288 K): at 203 and 233 K the exposure times were 0-3 hours with 0.5 hour intervals (7 samples each), and at 288 K the exposure times were 0, 1.5, and 3 hours. This gave a total of 17 samples.

After each experiment, the content of the reactor was expanded into a 1.75 L evacuated stainless steel canister. These were subsequently topped up to 200 kPa pressure with oxygen-free nitrogen, to provide adequate volumes and mixing ratios for the analysis system.

The sample canisters were measured in April 2011 in the isotope laboratory of the Institute for Marine and Atmospheric Research Utrecht (IMAU) of Utrecht University (The Netherlands) for mixing ratio and $\delta^{13}C$ using the system described in Zuiderweg et al. (2011). This instrument was originally designed for the measurement of stable carbon isotope ratios of non-methane hydrocarbons. It features a novel method of removing unwanted compounds (e.g. CO_2 and CH_4) by use of a 3 m × 6.35 mm packed Porapak Q pre-column, where compounds to be excluded from analysis are separated from the compounds of interest gas chromatographically. Separation of compounds is accomplished by using a 52.5 m × 0.25 mm Poraplot Q column, the effluent of which is split to 1) a HP 5970 quadrupole MS and 2) a Thermo Finnigan Delta Plus XL isotope ratio mass spectrometer by way of a Pt-Cu-Ni combustor and open split. Peak integration is accomplished through the ISODAT software package. $\delta^{13}C$ results from this instrument are reported relative to the international Vienna Pee Dee Belemnite standard (VPDB) in per mil (‰). Details of calibration procedures are elaborated in Zuiderweg et al. (2011).

This system was tested for measurement capability of C_1 chlorofluorocarbons with a PraxAir Inc. calibration mixture containing 150 ± 8 ppb of both CFC-11 and CFC-12, among other compounds. Testing results with various volumes showed that the

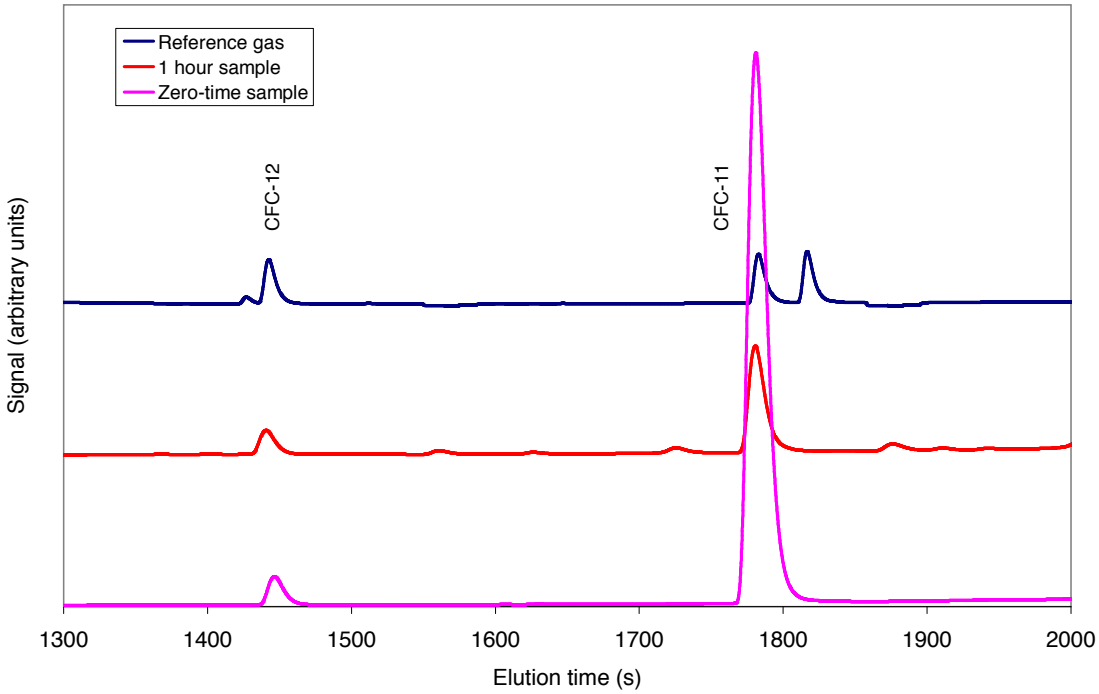

Figure 3.4. Example chromatogram from instrument of the Praxair calibration mixture (0.1 L), 1 hour exposure sample at 233 K (1 L), and zero-time exposure sample at 233 K (1 L) respectively, demonstrating separation performance.

isotopic results were volume independent and stable for CFC measurement, with $\delta^{13}C$ repeatability (1σ, n = 30) of 0.9 and 0.7 ‰ for CFC-11 and CFC-12, respectively, above peak areas of 0.5 Vs (2 ng C equivalent), and mixing ratio measurement precision of ±5 %. Sensitivity of the instrument is approximately 0.25 Vs/(ng C) (Zuiderweg et al., 2011). A sample chromatogram demonstrating compound separation can be found in fig. 3.4. Daily calibration of the instrument was accomplished by measuring the above standard before the start and after the finish of that day´s measurement series. Blank measurements showed no remnant CFC or interfering peaks.

To ensure that peak areas for the samples exposed longest were still above the specified threshold limit of 0.5 Vs, each analysis consumed 1 L (100 kPa, 295 K) of

analyte, which allowed for 2 measurements of each of the sample canisters, under normal circumstances.

The theoretical zero photolysis time mixing ratios used for calculating F (the unphotolysed fraction remaining) were established by calculating the number of moles of each CFC in the reactor prior to exposure given a particular reactor temperature. Subsequently, the number of moles of each CFC in the reactor post-exposure was back-calculated from the VMR measurements of each can. All calculations took into account pressure gauge offsets.

3.3 Results and discussion

The photolysis rate coefficient J is given by:

$$J = -\frac{\ln(F)}{t} \tag{3.3}$$

and the isotope fractionation ε is given by Eq. (3.2). Therefore, we have plotted the natural logarithm of fraction remaining, ln(F), against photolysis time (Fig. 3.5A & 3.5B) and ln(δ^{13}C +1) against ln(F) (Fig. 3.5C & 3.5D) respectively for both compounds at all three temperatures, in order to obtain J and ε through the slope of linear fits to the data. A summary of least-squares fit parameters for the photolysis rate coefficient and isotope fractionation is given in Table 3.1. For CFC-11, a neighbouring peak interferes in samples with ln(F) < -3. This interference disturbs the peak integration, leads to incorrect δ^{13}C values, and consequently affects ε obtained from the plotted data. The samples affected and thus rejected have exposure times above 2 hours, at 233 and 288 K.

Figures 3.5A & 3.5B show the photolysis behavior of CFC-11 and CFC-12 with exposure time. As expected, the Sb-lamp is very effective in photolyzing CFC-11 and -12, with 95% and 33% photolysis of the respective compounds achieved at

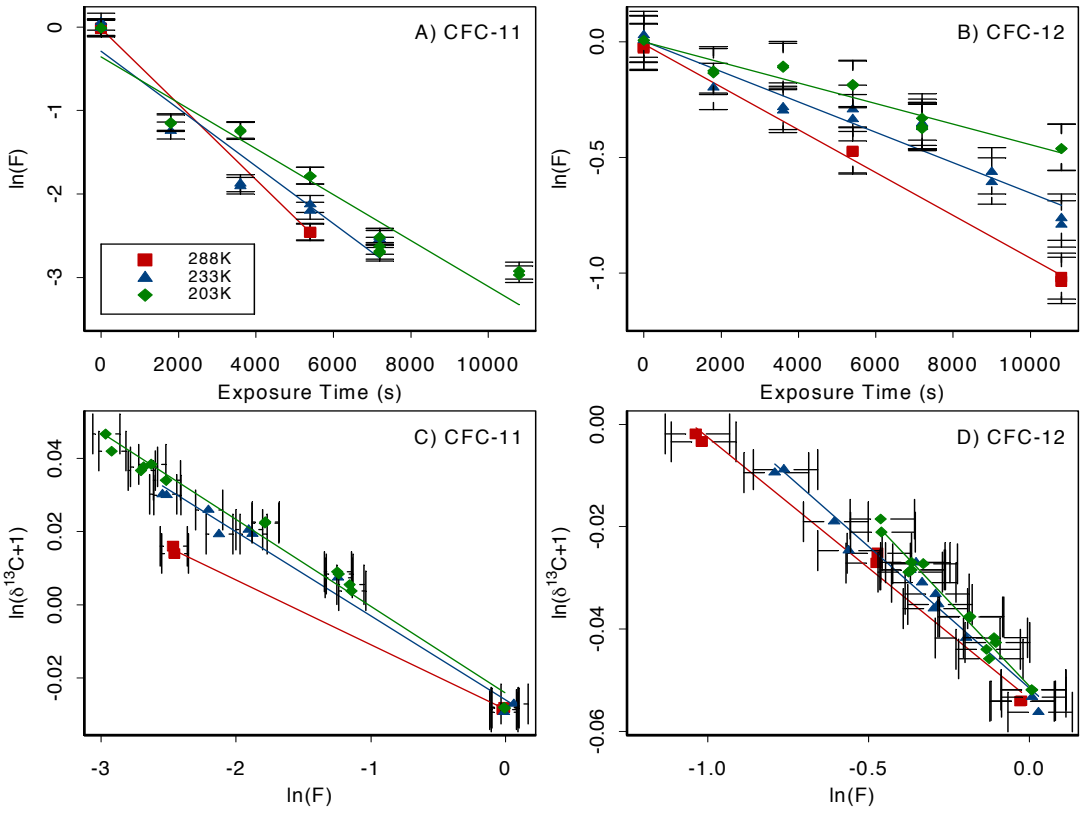

Figure 3.5. Plots of ln (F) vs. exposure time in seconds (panels A and B) and ln(δ^{13}C+1) vs. ln (F) (panels C and D) for samples at different exposures and temperatures for CFC-11 and -12 with least-squares fits to obtain J and ε. The instrument used has ±10% uncertainty for mixing ratio measurement, and its δ^{13}C (1σ) error is 0.9 and 0.7‰ for CFC-11 and -12 respectively. Summary of J and ε values from fits in Table 3.1.

exposures of 3 hours at the coldest reactor temperature of 203K. At higher temperatures, photolysis occurs faster and thus compound destruction is more complete for a given exposure time. This is in good agreement with absorption cross sections measured at the respective temperatures (Atkinson et al., 2005 and 2008). Photolysis rates measured range from 2.8×10^{-4} to 4.5×10^{-4} s^{-1} for CFC-11 and 4.4×10^{-5} to 9.3×10^{-5} s^{-1} for CFC-12 at 203 and 288K respectively. However, there are slight deviations in the linear relationship. These are not the result of the error of the measuring instrument as repeat measurements are very close. Rather, these are

Table 3.1. Summary of photolysis rates and isotope fractionations from fits in Fig. 3.5.

	CFC-11			CFC-12		
Temp (K)	203	233	288	203	233	288
J (s^{-1})	$2.8x10^{-4}$	$3.4x10^{-4}$	$4.5x10^{-4}$	$4.4x10^{-5}$	$6.6x10^{-5}$	$9.3x10^{-5}$
ε (‰)	-23.8±0.9	-23.0±1.1	-17.7±0.4	-66.2±3.1	-55.3±3.0	-51.0±2.9
ε fit r^2	0.992	0.992	0.999	0.993	0.984	0.993

ascribed to possible moisture condensation on the reactor (despite ventilation) reducing light intensity, variations in reactor-lamp alignment, or lamp intensity variation. Alignment variations can occur in the photolysis setup as the reactor must be occasionally dismounted to remove accumulated bubbles in the reactor cooling fluid. Additionally, although no discernable lamp intensity instability was reported in previous research with this same lamp (Röckmann et al., 2000 and 2001; Kaiser et al., 2002 and 2003), it is possible that such instability has developed over time.

However, the aforementioned nonlinearity in the data in Figs. 3.5A and 3.5B does not impact the validity of these results for the calculation of ε as the data plotted in Rayleigh fractionation plots (Figs. 3.5C & 3.5D) are very well correlated, with least-square r^2 values above 0.98. This result suggests that any lamp intensity variations that alter the amount of photolysis that takes place in the reactor during at a given elapsed photolysis time does not affect the fractionation inherent in the photolysis reaction. At all temperatures, isotope fractionations are far larger for CFC-12 than for CFC-11. The strongest fractionations are observed at 203 K, (-66.2 ± 3.1) ‰ for CFC-12 and (-23.8 ± 0.9) ‰ for CFC-11. The magnitudes of the isotope fractionations become larger (i.e. ε becomes more negative) towards lower temperatures, similar to the situation with N_2O (Kaiser et al. 2002). It is interesting to note that the CFC-12 fractionations are similar in magnitude to the fractionation in

the reaction CH_4 + Cl (Saueressig et al., 1995) or the reaction CH_3Cl + OH (Gola et al., 2005).

In the stratosphere, CFC-11 photodissociates faster than CFC-12 and its atmospheric lifetime is shorter by approximately a factor of 2 (Forster et al., 2007). In our experiments, the photolysis rate of CFC-11 is also faster, but by a factor of 5. The difference can be explained by the fact that the lamp spectrum and the solar actinic flux at altitudes where CFC photolysis occur (19-34 km, Laube et al., 2010a) do not match (see fig. 3.2 and 3.3). Integrating the product of the intensity (both Sb-lamp and 30 km solar) and absorption spectra, we calculate that the difference between the CFC-11 and -12 photolysis rates is approximately 1.7 times greater in the reactor than in the atmosphere, explaining a large part of the observed discrepancy.

This mismatch in UV-C wavelengths may also impact calculated fractionations as these have been shown to be wavelength dependent in laboratory N_2O photolysis experiments. On the other hand, laboratory fractionations obtained with this same lamp are considered to be in good agreement with stratospherically observed fractionations, excepting the impact of dynamic processes, which reduce the magnitude of the fractionation by about half (Röckmann et al., 2001; Kaiser et al., 2006; Laube et al., 2010a). Ascertaining the scale of wavelength dependence is beyond the scope of this study and is a viable point of examination for future experiments.

In addition, interaction of CFC-11 and -12 with photolysis products and photolysis product recombination cannot be excluded in our experiments and could potentially be an issue. However, Rebbert and Ausloos (1975) note that any remnant complex molecules (e.g. CF_2 or CF_2Cl) are unreactive to their parent molecules. Additionally, chlorine abstraction from an intact halocarbon molecule due to interaction with

radical chlorine is a very slow process due to the bond energies involved (Alapi et al., 2007). Recombination of chlorine with CFC radicals from photolysis to reform CFCs, on the other hand, is a real possibility. The rate of recombination is dependent on the mixing ratios of the CFC radicals and chlorine. Initial products of photolysis are radicals, which rapidly react with impurities either on the wall of the reactor or in the gas phase. The box model used to evaluate this took into account the photolysis rates of Cl_2 and CFC compounds and the recombination of the radicals with Cl_2:

$$CF_2Cl_2 + h\nu \longrightarrow CF_2Cl + Cl \quad \text{(R3.3)}$$

$$Cl_2 + h\nu \longrightarrow Cl + Cl \quad \text{(R3.4)}$$

$$Cl + Cl + M \longrightarrow Cl_2 + M \quad \text{(R3.5)}$$

$$CF_2Cl + Cl_2 \longrightarrow CF_2Cl_2 + Cl \quad \text{(R3.6)}$$

$$CF_2Cl + X \longrightarrow products \quad \text{(R3.7)}$$

$$Cl + X \longrightarrow products \quad \text{(R3.8)}$$

Reactions 3.5-3.8 have been assumed to occur at fast rates of 3 x 10^{-11} cm^3 s^{-1}, and photolysis rates (R3.3, R3.4) have been calculated by folding the absorption cross section of Cl_2 and CF_2Cl_2 with the lamp spectrum, respectively. Results indicate that recombination is below 5 % if impurities (X) have an equivalent above 0.4 ppb in the gas phase. Given the rather high concentrations of CFCs and the large surface/volume ratio of the reactor, we think that it is a conservative assumption that impurities exceeded this threshold. Therefore we think that recombination likely does not represent an issue to our results. However, we have to acknowledge that we cannot rule out possible recombination for 100 %. Further, any isotope effect in recombination is impossible to assess at this point as there is no data on the fractionations inherent in these reactions to our knowledge. Future experiments

should be performed with well-defined levels of gases that can scavenge the produced radicals to definitively preclude any recombination.

Assuming the observed fractionations hold true in nature, these imply that there should be a strong vertical gradient in $\delta^{13}C$ in the stratosphere for both CFC-11 and CFC-12, similar to the ones found for $\delta^{15}N$-, $\delta^{18}O$-N_2O (Röckmann et al., 2001), $\delta^{37}Cl$ (Laube et al., 2010a) or $\delta^{13}CH_4$ (Röckmann et al., 2011). The fractionations found here are very large and in particular stratospheric (photolytically aged) CFC-12 would then be expected to be exceptionally enriched in ^{13}C.

For example, sample calculations using the measured fractionations at 203 and 233 K and a stratospheric profile of CFC-12 mixing ratio from Laube et al., 2010a would indicate $\delta^{13}C$ potential enrichments in excess of 60‰ compared to tropospheric values at 34 km altitude if the fractionations are applicable to the stratosphere. However, these are likely to be less due to the effect of atmospheric mixing, which causes apparent (observed) fractionation in the atmosphere ε_{app} to be approximately half of the intrinsic (laboratory measured) fractionation. Unphotolyzed CFC is continuously brought into the stratosphere and mixed with CFC that has been photolyzed previously, changing the isotope ratio of the whole and suppressing the inherent fractionation (Röckmann et al., 2001; Kaiser et al., 2006; Laube et al., 2010a).

Similar to the situation for other long-lived trace gases, the fractionations in the removal reactions affect the tropospheric isotope budgets. This is because stratospherically processed air is transported down to the troposphere again after partial removal and corresponding isotope enrichment of the CFCs. In addition, a particular atmospheric signal is expected after the introduction of the Montreal protocol. As the emissions from sources have decreased significantly since 1990

(Forster et al., 2007), the isotope effect in the stratospheric removal reactions should be continuously enriching the entire tropospheric reservoir. This should continue for the coming decades as atmospheric CFC levels are decreasing and should also be observable in atmospheric air archives or polar firn air and eventually in ice cores, similar as to what has been ascertained in firn air for N_2O nitrogen and oxygen stable isotopes (Röckmann et al., 2003).

3.4 Conclusion

A set of stable carbon isotopic fractionations in the UV-C (190-230 nm) photolysis reactions for CFC-11 and CFC-12 has been demonstrated. Strong isotope enrichments are associated with UV photolysis at environmentally relevant temperatures. The fractionations increase from (-17.7 ± 0.4) ‰ and (-51.0 ± 2.9) ‰ at 288K to (-23.8 ± 0.9) ‰ and (-66.2 ± 3.1) ‰ at 203K for the respective compounds. These fractionations imply that strong heavy isotope enrichments should be found in the stratosphere. Expected effects are isotope gradients with CFC removal (e.g. vertical and polewards) in the stratosphere (as have already been ascertained for chlorine isotopes through balloon samples), and a change of the stable carbon isotopic ratio of these compounds in the atmosphere over time.

References

Advanced Global Atmospheric Gases Experiment (AGAGE) data. Available online: http://agage.eas.gatech.edu/data.htm, 2010.

Alapi, T., van Craeyenest, K., van Langenhoeve, H., Dewulf, J., and Dombi, A.: Direct VUV photolysis of chlorinated methanes and their mixtures in a nitrogen stream. *Chemosphere,* **66**, 139-144, 2007.

Atkinson, R., Baulch, D.L., Cox, R.A., Crowley, J.N., Hampson, Jr., R.F., Kerr, J.A., Rossi, M.J., and Troe, J.: *Summary of evaluated kinetic and photochemical data for atmospheric chemistry*, Available online: http://www.iupac-kinetic.ch.cam.ac.uk/summary/IUPACsumm_web_latest.pdf, 2005.

Atkinson, R., Baulch, D.L., Cox, R.A., Crowley, J.N., Hampson, Jr., R.F., Hynes, R.G., Jenkin, M.E., Rossi, M.J., Troe, J., and Wallington, T.J.: Evaluated kinetic and photochemical data for atmospheric chemistry: Volume IV - gas phase reactions of organic halogen species, *Atmos. Chem. Phys.,* **8**, 4141-4496, 2008.

Brenninkmeijer, C. A. M., Janssen, C., Kaiser, J., Röckmann, T., Rhee, T. S., and Assonov, S. S.: Isotope effects in the chemistry of atmospheric trace gases, *Chem. Rev.*, **103**, 5125-5162, 2003.

Blake, G. A., Liang, M. C., Morgan, C. G., and Yung, Y. L.: A Born-Oppenheimer photolysis model of N_2O fractionation, Geophys. Res. Lett., **30**, 1656, doi:10.1029/2003GL016932, 2003.

Butler, J. H., Battle, M., Bender, M. L., Monzka, S. A., Clarke, A. D., Saltzman, E. S., Sucher, C. M., Severinghaus, J. P., and Elkins J. W.: A record of atmospheric halocarbons during the twentieth century from polar firn air. *Nature*, **399**, 749 – 755, 1999.

Engel, A., Schmidt, U., and McKenna, D.: Stratospheric trends of CFC-12 over the past two decades: recent observational evidence of declining growth rates, *Geophys. Res. Lett*., **25**, 3319-3322, 1998.

Forster, P., Ramaswamy, V., Artaxo, P., Berntsen, T., Betts, R., Fahey, D. W., Haywood, J., Lean, J., Lowe, D. C., Myhre, G., Nganga, J., Prinn, R., Raga, G., Schulz, M., and Van Dorland, R.: Changes in Atmospheric Constituents and in Radiative Forcing. *Climate Change 2007: The Physical Science Basis. Contribution of Working Group I to the Fourth Assessment Report of the Intergovernmental Panel on Climate Change* [Solomon, S., D. Qin, M. Manning, Z. Chen, M. Marquis, K.B. Averyt, M.Tignor and H.L. Miller (eds.)]. Cambridge University Press, Cambridge, United Kingdom and New York, NY, USA, 2007.

Gola, A. A., D'Anna, B., Feilberg, K. L., Sellevåg, S. R., Bache-Andreassen, L., and Nielsen, C. J.: Kinetic isotope effects in the gas phase reactions of OH and Cl with CH_3Cl, CD_3Cl, and $^{13}CH_3Cl$. *Atmos. Chem. Phys.,* **5**, 2395-2402, 2005.

Kaiser, J., Röckmann, T., and Brenninkmeijer, C. A. M.: Temperature dependence of isotope fractionation in N_2O photolysis, *Phys. Chem. Chem. Phys.*, **4**, 4420-4430; 4410.1039/b204837j, 2002.

Kaiser, J., Röckmann, T., Brenninkmeijer, C. A. M., and Crutzen, P. J.: Wavelength dependence of isotope fractionation in N_2O photolysis, *Atmos. Chem. Phys.*, **3**, 303-313, 2003.

Kaiser, J., Engel, A., Borchers, R., and Röckmann, T.: Probing stratospheric transport and chemistry with new balloon and aircraft observations of the meridional and vertical N_2O isotope distribution, *Atmos. Chem. Phys.*, **6**, 3535-3556, 2006.

Laube, J. C., Kaiser, J., Sturges, W. T., Bönisch, H., and Engel, A.: Chlorine Isotope Fractionation in the Stratosphere. *Science*, **329(5996)**, 1167, DOI:10.1126/science.1191809, 2010a.

Laube, J. C., Martinerie, P., Witrant, E., Blunier, T., Schwander, J., Brenninkmeijer, C. A. M., Schuck, T. J., Bolder, M., Röckmann, T., van der Veen, C., Bonisch, H., Engel, A., Mills, G. P., Newland, M. J., Oram, D. E., Reeves, C. E., and Sturges, W. T.: Accelerating growth of HFC-227ea (1,1,1,2,3,3,3-heptafluoropropane) in the atmosphere, *Atmos. Chem. Phys.*, **10**, 5903-5910, 2010b.

Massie, S. T., and Goldman, A.: Absorption parameters of very dense molecular spectra for the HITRAN compilation. *J. Quant. Spectrosc. Radiat. Transfer*, **48(516),** 713-719, 1992.

Minschwaner, K., Salawitch, R. J., and McElroy, M. B.: Absorption of solar radiation by O_2: Implications for O_3 and lifetimes of N_2O, $CFCl_3$, and CF_2Cl_2, *J. Geophys. Res.*, **98 (D6)**, 10 543–10 561, 1993.

Morgan, C. G., Allen, M., Liang, M. C., Shia, R. L., Blake, G. A., and Yung, Y. L.: Isotopic fractionation of nitrous oxide in the stratosphere: Comparison between model and observations. *J. Geophys. Res.*,**109**, D04305, doi:10.1029/2003JD003402, 2004.

Rahn, T., and Wahlen, M.: Stable isotope enrichment in stratospheric nitrous oxide, *Science*, **278**, 1776-1778, 1997.

Rebbert, R. E. and Ausloos, P. J.: Photodecomposition of $CFCl_3$ and CF_2Cl_2. *J. Photochem.,* **4 (5-6)** 419-434, 1975.

Röckmann, T., Brenninkmeijer, C. A. M., Wollenhaupt, M., Crowley, J. N., and Crutzen, P. J.: Measurement of the isotopic fractionation of $^{15}N^{14}N^{16}O$, $^{14}N^{15}N^{16}O$ and $^{14}N^{14}N^{18}O$ in the UV photolysis of nitrous oxide, *Geophys. Res. Lett.,* **27**, 1399-1402, 2000.

Röckmann, T., Kaiser, J., Brenninkmeijer, C. A. M., Crowley, J. N., Borchers, R., Brand, W. A., and Crutzen, P. J.: Isotopic enrichment of nitrous oxide ($^{15}N^{14}NO$, $^{14}N^{15}NO$, $^{14}N^{14}N^{18}O$) in the stratosphere and in the laboratory, *J. Geophys. Res.*, **106**, 10,403-10410, 2001.

Röckmann, T., Kaiser, J., Brenninkmeijer, C. A. M.: the isotopic fingerprint of the pre-industrial and the anthropogenic N_2O source. *Atmos. Chem. Phys.*, **3**, 315-323, 2003.

Seinfeld, J. H. and Pandis, S. N. *Atmospheric Chemistry and Physics: from Air Pollution to Climate Change*, John Wiley and Sons, New York, 1326 pp., 1998.

Röckmann, T., Brass, M., Borchers, R., and Engel, A.: The Isotopic Composition of Methane in the Stratosphere: High-Altitude Balloon Sample Measurements, *Atmos. Chem. Phys. Discuss.,* **11**, 12039–12102, 2011.

Saueressig, G., Bergamaschi, P., Crowley, J. N., Fischer, H., and Harris, G. W.: Carbon kinetic isotope effect in the reaction of CH_4 with Cl atoms. *Geophys. Res. Lett.* **22 (10),** 1225-1228, 1995.

von Hessberg, P., Kaiser, J., Enghoff, M. B., McLinden, C. A., Sorensen, S. L., Yung, Y. L., and C. E Miller: Isotopic fractionation of stratospheric nitrous oxide, *Science*, **278**, 1778-1780, 1997.

World Meteorological Organization (WMO): Global Ozone Research and Monitoring Project Report No. 52: Scientific Assesment of Ozone Depletion 2010, Available: http://ozone.unep.org, 2010.

Zuiderweg, A., Holzinger, R., and Röckmann, T.: Analytical system for stable carbon isotope measurements of low molecular weight (C_2-C_6) hydrocarbons. *Atmos. Meas. Tech.,* **4**, 1161-1175, DOI: 10.5194/amt-4-1161-2011, 2011

Chapter 4: Extreme ^{13}C depletion of CCl_2F_2 in firn air samples from NEEM, Greenland

A. Zuiderweg, R. Holzinger, P. Martinerie, R. Schneider, J. Kaiser, E. Witrant, D. Etheridge, M. Rubino, V. Petrenko, T. Blunier, and T. Röckmann

Accepted for publication in Atmospheric Chemistry and Physics Discussions, July 16th, 2012.

Abstract

A series of 12 high volume air samples collected from the S2 firn core during the North Greenland Eemian Ice Drilling (NEEM) 2009 campaign have been measured for mixing ratio and stable carbon isotope composition of the chlorofluorocarbon CFC-12 (CCl_2F_2). While the mixing ratio measurements compare favorably to other firn air studies, the isotope results show extreme ^{13}C depletion at the deepest measurable depth (65 m), to values lower than $\delta^{13}C$ = -80 ‰ vs. VPDB (the international stable carbon isotope scale), compared to present day surface tropospheric measurements near -40 ‰. Firn air modeling was used to interpret these measurements. Reconstructed atmospheric time series indicate even larger depletions (to -120 ‰) near 1950 AD, with subsequent rapid enrichment of the atmospheric reservoir of the compound to the present day value. Mass-balance calculations show that this change must have been caused by a large change in the isotopic composition of anthropogenic CFC-12 emissions, probably due to technological changes in the CFC production process over the last 80 years. Propagating the mass-balance calculations into the future demonstrates that as emissions decrease to zero, isotopic

fractionation by the stratospheric sinks will lead to continued ^{13}C enrichment in atmospheric CFC-12.

4.1 Introduction

Before it was banned under the Montréal protocol and subsequent amendments, the use of chlorofluorocarbon-12 (CFC-12, CCl_2F_2) as a refrigerant and aerosol propellant worldwide has resulted in significant atmospheric loading; at its peak in 2003, the mean mixing ratio of this compound in the troposphere was approximately 550 ppt (ppt = parts per trillion = pmol mol^{-1}), making it the most abundant anthropogenic halocarbon compound in the atmosphere (McCulloch et al., 2003; Forster et al., 2007). Due to the buildup of this and other anthropogenic halocarbons, total chlorine loading in the troposphere has increased from approximately 600 ppt (1900) to nearly 3350 ppt (2008) (Forster et al., 2007; WMO 2010).

Trends in CFCs have been directly observed since the 1970s, when regular observations of atmospheric halocarbon compounds started (e.g. ALE, GAGE and AGAGE projects (AGAGE, 2011)). The atmospheric mixing ratio history of CFC-12 prior to this period has been reconstructed through the measurement of firn air samples combined with firn air modeling and emissions estimates (Butler et al., 1999; Sturrock et al., 2002; McCulloch et al., 2003; Martinerie et al., 2009; Buizert et al., 2011). Firn air is extracted from compacted snow to depths above bubble close off and analyzed on-site, or captured in sample vessels for later analysis. The large volumes of air contained in compacted snow allow for the extraction of tens to hundreds of liters of ancient air (Schwander et al., 1993).

Interpretation of the measured data must be paired with firn air modeling, which takes into account the physics of trace gas transport in firn and allows the reconstruction of atmospheric histories of the compounds concerned (Trudinger et al., 1997; Buizert et

al., 2011; Witrant et al., 2011). Analysis of firn air combined with firn air modeling proved that there is no natural source of CFC-12, as no trace of this compound was found in samples from Antarctica and Greenland corresponding to dates before 1930, when large-scale use began (Butler et al., 1999; McCulloch et al., 2003; Martinerie et al., 2009).

CFC-12 is a very stable compound and has its only sink in the middle and upper stratosphere, where ultraviolet radiation is energetic enough to break the C-Cl bond (reaction R4.1). A minor sink (3-7%) exists through Cl abstraction by $O(^1D)$, which is produced from the photolysis of ozone in the stratosphere (reaction R4.2; Seinfeld and Pandis 1998, Laube et al., 2010a).

$$CF_mCl_{4-m} + h\nu \xrightarrow{\lambda<220\ nm} CF_mCl_{3-m} + Cl\cdot \qquad \text{(R4.1)}$$

$$CF_mCl_{4-m} + O(^1D) \longrightarrow CF_mCl_{3-m} + ClO \qquad \text{(R4.2)}$$

These reactions provide the initial release of chlorine, which begins the now well-known catalytic decomposition of ozone first proposed by Molina and Rowland (1974). The fact that CFC-12 can only be removed in the stratosphere leads to a long atmospheric lifetime of approximately 100 years (Forster et al., 2007). Due to this long lifetime, the mixing ratio of CFC-12 has decreased in the atmosphere only slowly after the Montréal protocol came into effect, to approximately 530 ppt in 2010 (AGAGE 2011).

Whereas the mixing ratio of CFC-12 has been well established by many studies, few studies of the stable isotope ratio of this compound have been completed. Stable isotope ratio studies can give insight into the budget of a compound, i.e. its sources and sinks (Goldstein and Shaw, 2003). The stable isotope composition of quantities of compounds can be altered by the mixing of molecules with differing isotope ratios, or

through chemical reactions due to differences in chemical bond strengths ascribed to isotopic substitution. These cause fractionation between the different isotopologues of a given molecule (e.g. Brenninkmeijer et al., 2003). Isotope values are conveniently expressed in δ notation, in the case of ^{13}C:

$$\delta^{13}\mathrm{C} = \frac{^{13}R_{\mathrm{Sample}}}{^{13}R_{\mathrm{Standard}}} - 1 \qquad (4.1)$$

where ^{13}R is the $^{13}C/^{12}C$ ratio in a sample or standard material. The internationally accepted reference material for $^{13}C/^{12}C$ ratios is Vienna Pee Dee Belemnite (VPDB). The δ value is expressed in per mil (parts per thousand = ‰) for readability.

Zuiderweg et al. (2012) recently reported an unusually strong ^{13}C fractionation associated with the photolytic destruction of CFC-12 under stratospherically relevant conditions. Fractionation constants (defined as $\varepsilon = {}^{13}J/{}^{12}J$, the ratio of the photolysis rate constants of the heavy and light isotopologues and similarly expressed in per mil) in the range -50 ‰ to -70 ‰ were determined in laboratory photolysis experiments at temperatures between 288 K and 203 K. Such a strong isotope effect in the removal process should result in a continuous enrichment of the atmospheric reservoir now that production and emissions have largely ceased (Zuiderweg et al., 2012). Air trapped in polar firn is a valuable tool to investigate whether this isotope signal is present.

Applications of stable isotope ratio studies of atmospheric compounds in firn air are diverse. $\delta^{15}N(N_2)$ and $\delta^{18}O(O_2)$ can be used for constraining ice core trapped air age (Schwander et al., 1993; Bender et al., 1994; Severinghaus et al., 2010). For methane (CH_4), carbon dioxide (CO_2), carbon monoxide (CO), and nitrous oxide (N_2O), historical isotope scenarios have been derived to explore trends in emissions (Trudinger et al., 1997; Etheridge et al., 1998; Francey et al., 1999; Bräunlich et al.,

2001; Sowers et al., 2001; Röckmann et al., 2003; Monteil et al., 2011; Wang et al., 2011; Sapart et al., 2012, manuscript in preparation). However, to date, no isotope ratio history has been reconstructed for CFC compounds, though $\delta^{13}C$ CFC measurements in urban and rural air do exist (Archbold et al., 2005; Redeker et al., 2007; Mead et al., 2008; and Bahlmann et al., 2011). Here we present the first measurements and interpretation of a combined depth profile of CCl_2F_2 mixing ratio and isotopic composition from the firn air campaign at the North Greenland Eemian Ice Drilling (NEEM) site (77° 25′ 54.93′′ N, 51° 03′ 19.89′′ W, 2484 m above sea level), collected as part of the summer 2009 NEEM firn air program.

4.2 Method

4.2.1 Firn Sampling

A series of 12 large volume firn air samples were obtained from the S2 firn borehole at the NEEM site to a depth of 73.6 m. Here, a firn air sampling device (FASD) constructed of a 3 m long rubber bladder, with sample lines passing through it, was lowered to the bottom of a borehole. The FASD was expanded with air to provide an airtight seal to the walls of the borehole, and air was extracted through the sampling lines from below the FASD. Once on-site CO_2 mixing ratio measurement confirmed that the seal of the FASD to the borehole wall was leak tight and surface air had been pumped away, air is extracted from the firn in large quantities. After sampling at each depth was completed air pressure in the firn layer was allowed to re-equilibrate to prevent surface air contamination of the firn. Following this, the FASD was deflated, extracted, and the hole was bored to the next depth to be sampled. The sampling continued downward until a depth was reached where firn porosity decreases to an extent that air can no longer be extracted from the firn using this method, due to

compression from the weight of the firn above it. Further details of the sampling methods used are described by Etheridge et al. (2009).

The large air samples used for the analysis presented here were dried, and then compressed to 120 bar pressure into 5 L Luxfer aluminium cylinders using a three-stage oil free piston compressor (Mak and Brenninkmeijer 1994).

4.2.2 Analytical Procedure

The CFC-12 of each of the sample cylinders was measured twice, non-sequentially and on different days to detect instrument drift, for mixing ratio and $\delta^{13}C$ at the stable isotope laboratory of the Institute for Marine and Atmospheric Research Utrecht (IMAU). The isotope measurement system used is described by Zuiderweg et al. (2011). This instrument was originally designed for the measurements of stable carbon isotope ratios of non-methane hydrocarbons, and features a novel method of removing unwanted compounds that would otherwise interfere with analysis (e.g. CO_2 and CH_4) by use of a 3 m x 6.35 mm Porapak Q column. Subsequent peak separation of compounds prior to mass spectrometry is accomplished by using a 52.5 m x 0.25 mm Poraplot Q column, the effluent of which is split to 1) a HP 5970 quadrupole MS for compound identification and 2) a Thermo Finnigan Delta+ XL IRMS instrument by way of a Pt-Cu-Ni combustor (for combustion to CO_2) and open split. The scale of this instrument was established by the use of two reference gases: a multicompound nonmethane hydrocarbon gas as a working standard, and a CO_2 direct reference. These were independently calibrated to VPDB by external laboratories and were consistent with each other. Further information about these calibration procedures can be found in Zuiderweg et al. (2011; 2012).

In this work, the system was extended for ^{13}C measurements of monocarbon chlorofluorocarbons. Reproducibility of the system was established with a PraxAir

Inc. calibration mixture containing approximately 150 ppb ± 5 % CFC-12 among other compounds. The mean $\delta^{13}C$ of CFC-12 in this gas was established as -41.6 ‰ vs. VPDB. Testing results with various sample volumes showed that the instrument was volume independent and stable for CFC measurement, with nominal $\delta^{13}C$ instrument repeatability (1σ, 34 experiments) of 0.65‰ for CFC-12 above integrated peak areas of 0.5 Volt-seconds (Vs), corresponding to a carbon mass of 2 ng. The instrument is linear with peak area above this threshold (Fig. 4.1). Mixing ratio measurement precision is ±5 %. Sensitivity of the instrument per mass carbon is approximately 0.25 Vs/ng (Zuiderweg et al., 2012). This instrument behavior for CFC-12 is consistent in terms of stability (in $\delta^{13}C$ and mixing ratio), linearity, and sensitivity levels with other measured compounds as reported in Zuiderweg et al. (2011). Routine calibration of the instrument was accomplished by measuring the above standard before the start and after the finish of the daily measurement series. Blank measurements showed no remnant CFC or interfering peaks.

4.2.3 Data integration

Calculation (through peak integration) of all $\delta^{13}C$ data presented here was accomplished via raw data processing using a custom made MATLAB code as described in Bock et al., 2010 and Schmitt et al., 2011. For all firn samples, CFC-12 peaks suffer from peak interference with the preceding methyl chloride peak (shoulder overlap), prohibiting baseline-separated signals. The MATLAB routine extrapolates the peak tail of methyl chloride via an exponentially decaying function to distinguish the two gas species. This technique is not possible with the standard ISODAT software used for isotope ratio measurements. Figure 4.2 illustrates the background removal in chromatograms of two samples (30.2 m and 69.4 m depth, upper and lower traces, respectively). Peaks are integrated with time between the

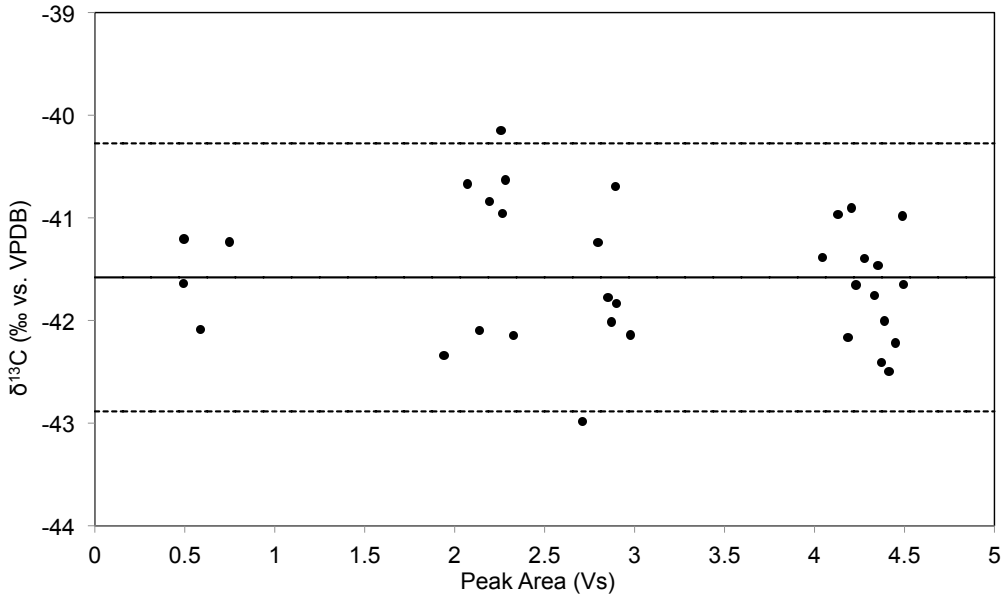

Figure 4.1. Plot of $\delta^{13}C$ (CFC-12, vs. VPDB) against peak area shows sample size linearity of isotope ratio measurements of the calibration mixture (34 samples). Horizontal lines indicate mean (solid) and instrument ±2 σ (dashed).

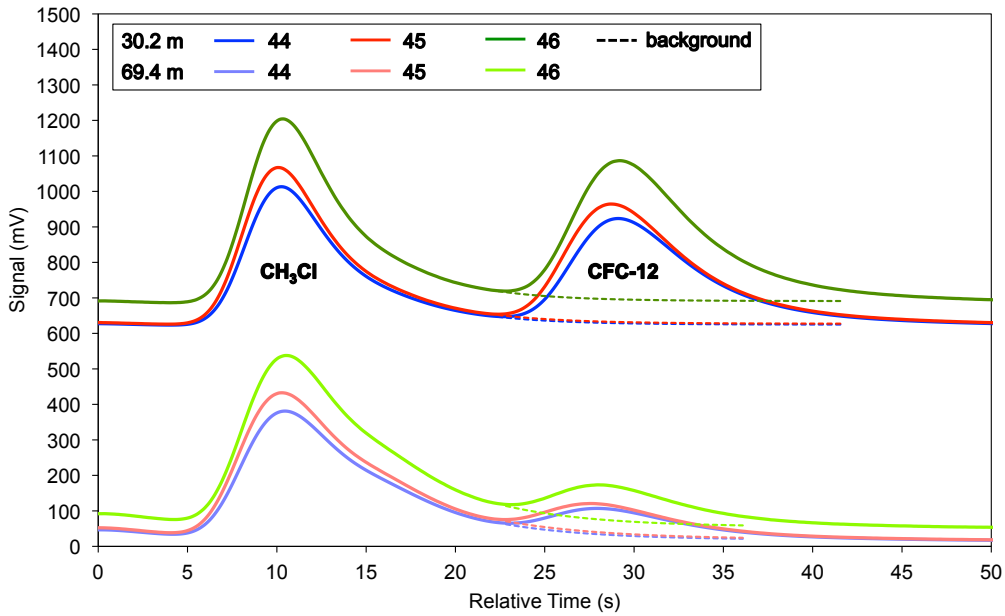

Figure 4.2. Chromatograms of CH_3Cl and CFC-12 m/z 44, 45, and 46 signals (mV) from 30.2 m (upper traces) and 69.4 m (lower traces) depth samples, showing sloping background calculation (dashed). Traces have been aligned through a +10 s time shift to the 30.2 m sample; additionally, the 30.2 m traces have been offset by 600 mV for presentation purposes.

exponentially decaying background and the CFC-12 peak. Beside this shoulder overlap, all CFC-12 peaks are free of artifacts and interfering peaks. As all firn samples are treated identically, relative differences reflect the true atmospheric trend combined with firn effects.

4.3 Results and discussion

4.3.1 NEEM firn dataset

Duplicate measurements of vertical profiles of CFC-12 mixing ratio and $\delta^{13}C$ in the firn air column and their arithmetic mean with 98% confidence intervals are shown in Figs. 4.3 and 4.4, respectively. All data are summarized in Table 4.1. Mixing ratio results from our instrument show the expected decrease with depth, from present values near 550 ppt in the top part of the firn to approximately 14 ppt at 71.9 m depth; at and below this depth CFC-12 peak areas were far below the limit of 0.5 Vs required for isotope measurements: at 71.9 m by at least factor of 10 less; at 73.6 m the CFC-12 peak was entirely absent.

In general, both sets of mixing ratio measurements are close together, and the series as a whole agree well (within instrument and calibration error of 10 %) with NEEM 2008 campaign CFC-12 firn air data from Buizert et al. (2011).

The $\delta^{13}C$ profile (Fig. 4.4) down to 63 m is relatively stable at approximately -40 to -45 ‰, reflecting recent atmospheric values (see also Fig. 4.5). These values are somewhat more depleted in ^{13}C than mean values reported from Belfast, Northern Ireland (-37.0 ± 1.3) ‰ and (-37.2 ± 3.9) ‰ (Archbold et al., 2005 and Redeker et al., 2007); and (-37.9 ± 1.1) ‰ in Hamburg, Germany (Bahlmann et al., 2011). However, these values were measured at urban locations where local emissions may have had an impact, as standard deviations are large. By contrast, Bahlmann et al. (2011) report (-41.2 ± 0.2) ‰ from a set of 3 samples obtained on the North Sea Coast on the Island

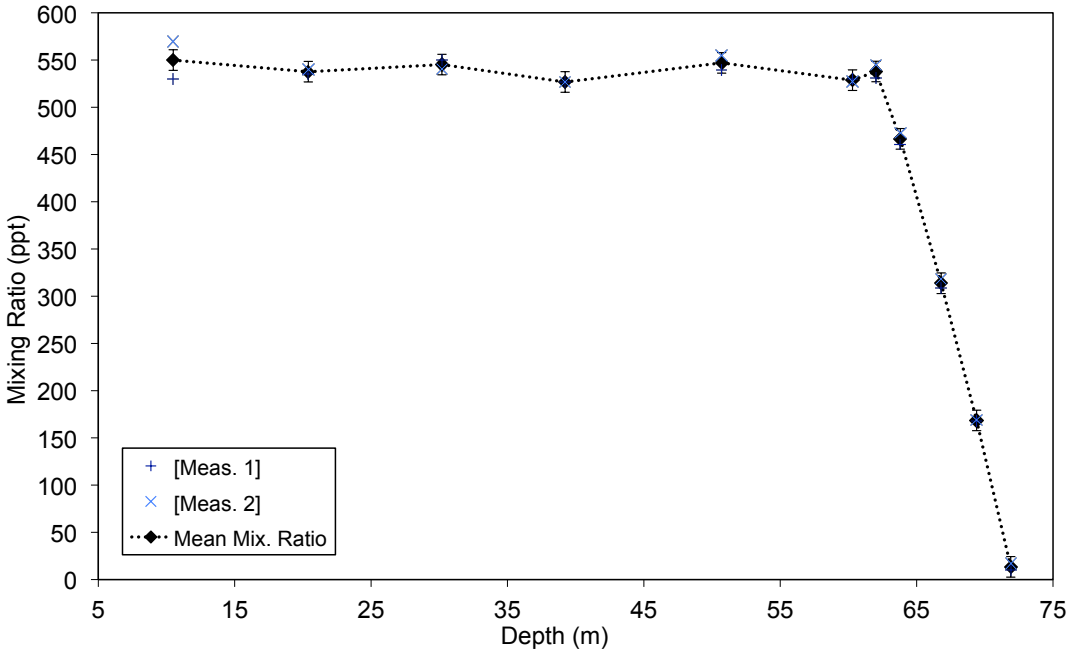

Figure 4.3. Vertical profiles of CFC-12 mixing ratios (ppt) from firn air extracted from the S2 hole, NEEM, Greenland, for independent measurements 1 and 2, and mean values. Error bars represent 98% confidence intervals with respect to the mean. All data summarized in table 4.1.

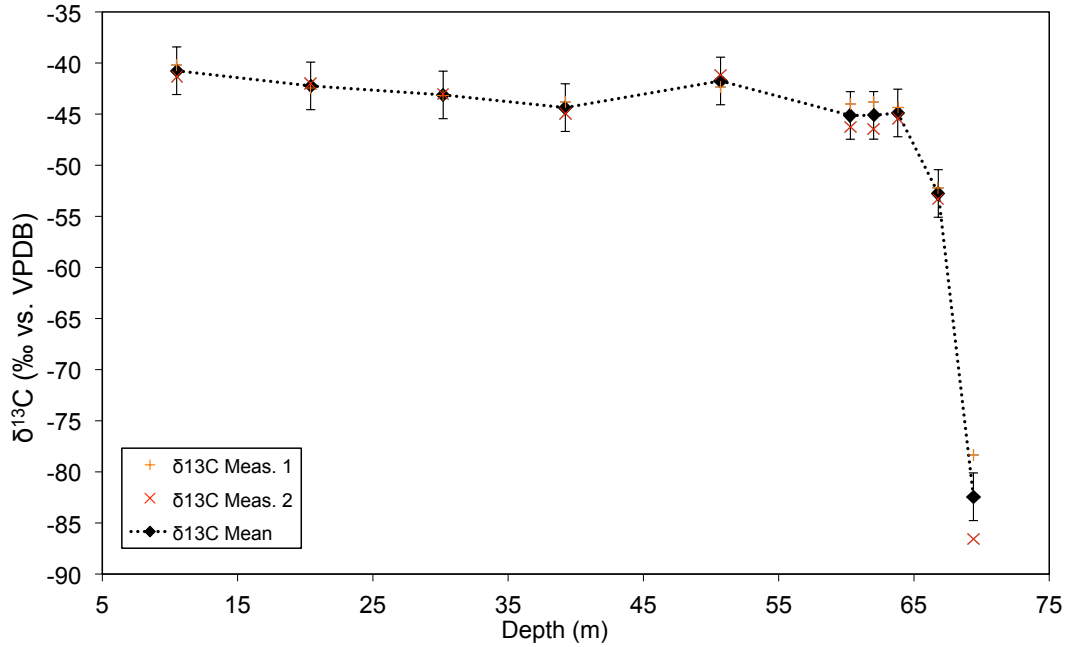

Figure 4.4. Vertical profiles of $\delta^{13}C$ (CFC-12) (‰, vs VPDB) from firn air at S2 drill site, NEEM, Greenland, for independent measurements 1 and 2 and mean values. Error bars represent 98% confidence intervals with respect to the mean. All data summarized in table 4.1.

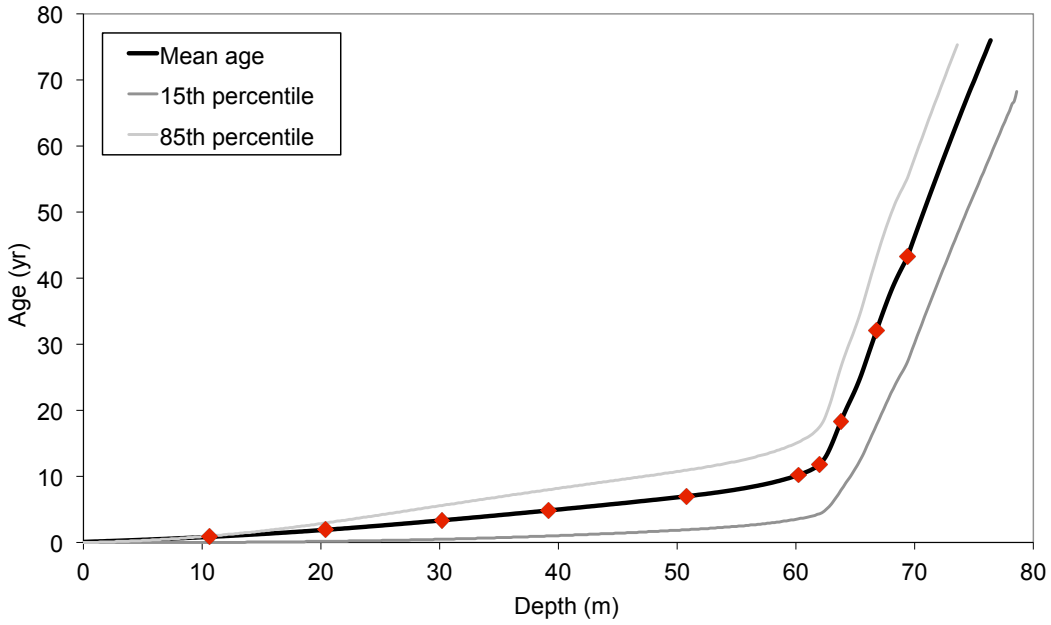

Figure 4.5. Age (prior to 2009) distribution in the firn air column as a function of depth from the forward model. Red diamonds indicate sampling depths for reference.

of Sylt, Germany. Also, CARIBIC project flight 26 measurements (Male, Maldives, to Düsseldorf, Germany, August 17th, 2000; Zuiderweg, 2012) give (-44.7 ± 0.6) ‰. These aircraft samples were collected from the temperate to tropical upper troposphere region (9-11 km), well below the altitude where photolytic removal takes place (14-34 km, Laube et al., 2010a). This is corroborated by the mean mixing ratio measured of (550 ± 50) ppt, very similar to surface measurements. Therefore these values can reasonably be considered as representative of the well-mixed and undisturbed troposphere. The CARIBIC flight sample set was measured using the same instrument as for the firn samples reported here.

The relative stability of $\delta^{13}C$ in the top 30 m of the firn implies little seasonality, which is expected given the long atmospheric lifetime of CFC-12. Below 63 m (the lock-in depth at NEEM; Buizert et al., 2011), where firn diffusivity decreases rapidly

Table 4.1. Firn air $\delta^{13}C$ and mixing ratio depth measurement series 1, 2 and mean.

Depth (m)	$\delta^{13}C$ Meas. 1[a]	$\delta^{13}C$ Meas. 2	$\delta^{13}C$ Mean[b]	[Meas. 1][c]	[Meas. 2]	[Mean][d]
10.5	-40.2	-41.3	-40.75	530	570	550
20.4	-42.5	-42	-42.25	536	540	538
30.2	-43.2	-43.1	-43.15	550	540	545
39.2	-43.8	-44.9	-44.35	527	527	527
50.7	-42.4	-41.2	-41.8	539	555	547
60.3	-44	-46.3	-45.15	530	527	528.5
62	-43.8	-46.4	-45.1	531	545	538
63.8	-44.4	-45.4	-44.9	460	473	466.5
66.8	-52.3	-53.3	-52.8	309	318	313.5
69.4	-78.3	-86.6	-82.45	168	169	168.5
71.9	-[e]	-	-	10	17	13.5

a – ‰ vs. VPDB

b – 98% confidence interval = 2.3 ‰

c – ppt = 10^{-12} mol / mol

d – 98% confidence interval = 10 ppt

e – $\delta^{13}C$ not measurable; peak area below acceptable threshold

and older air is found (see Fig. 4.5), CFC-12 becomes increasingly depleted in ^{13}C with depth. Measurements indicate a large $^{13}C/^{12}C$ depletion of 40 to 50 ‰ for the lowest measured sample (69.4 m) with respect to the surface. The $\delta^{13}C$ separation of the repeat measurements at the deepest point is larger than for the other sampling depths (Table 4.1 and Fig. 4.4). Both measurements at this depth had a signal above the instrument linearity threshold mentioned in section 4.2.2, at 0.59 and 0.55 Vs respectively, excluding instrument nonlinearity effects. However, the neighboring methyl chloride (see Fig. 4.2) peaks for these samples were relatively large and therefore the uncertainties associated with shoulder overlap induce the larger error in these measurements. The observed isotope depletions are much larger in magnitude than the expected firn fractionation effects (see discussion below). Thus, they most likely reflect that real changes exist in the isotope history in the atmosphere.

4.3.2 Atmospheric trend reconstruction

In order to interpret these data in terms of temporal variation we use a forward model of trace gas transport in firn proposed by Witrant et al., (2011). It takes into account diffusion and gravitational fractionation, which play a significant role in the measured isotope ratio of compounds in the firn versus that observed in the atmosphere (Trudinger et al., 1997). Thermal fractionation due to varying temperature with depth is not taken into account in the model, but this is of no detriment to the results as a whole as all but one of the measured samples are from below 15 m depth. Thermal fractionation is generally considered to be important in the upper 10–15 m only due to temperature gradients (Severinghaus et al., 2001). Similarly, eddy diffusion in the upper firn should be negligible as this affects only the uppermost levels of the firn (to 20 m at NEEM), and was noted to be small in magnitude at this site and would only serve to reduce fractionation (Buizert et al., 2011; Witrant et al., 2011).

The physical parameters (e.g. diffusivity) for the NEEM firn sampling site were reconstructed from a suite of gases with known histories (Buizert et al., 2011). More specifically, two gases in particular (CO_2 and CH_4) measured at CSIRO were used for the NEEM 2009 firn air experiment to tune the diffusivity profile. Because of the relative coarseness and the magnitude of scatter of our mixing ratio data, no independent CFC-12 mixing ratio scenario was modeled from our data. Instead a best estimate CFC-12 scenario based on atmospheric measurements combined with atmospheric chemistry model results is used (Martinerie et al., 2009; Buizert et al., 2011).

Figure 4.5 shows the age distributions for CFC-12 calculated by the forward model: mean, 15^{th} percentile and 85^{th} percentile ($\pm 1\sigma$). As expected, below 60 m the mean age with depth increases rapidly. In the so-called lock in zone, the transition from firn

to ice begins and further vertical diffusion slows, as firn is compacted by the weight above it. From samples collected in 2008, Buizert et al. (2011) identified the lock-in zone between 63 and 78 m at the NEEM site. At the bottom of this layer, permeability is zero, and no further trace gas transport can occur.

The recently developed scenario reconstruction method based on the separation of the effects of the major and minor isotopologues (Wang et al., 2011) is not suitable for use here as it has difficulty in reconciling large gradients in isotope ratio, leading to inconsistent results. Instead, we systematically explore scenarios with "smooth" variations of $\delta^{13}C$ (e.g. Bräunlich et al., 2001). Where both methods are suitable, they provide consistent results (Laube et al., 2010b). A large number of hypothetical scenarios are run with the forward model. Atmospheric scenarios with polynomial parameterizations of $\delta^{13}C$ as a function of time were run in monthly time steps from 1933 (the start of CFC-12 emissions) to 2009. In detail, we use 3rd and 4th degree polynomials with coefficients varying randomly within pre-defined limits (see below).

In order to reduce computing time, modeling proceeded in two steps for each polynomial setup. First, generated polynomials were evaluated with predetermined maximum and minimum values with an intentionally large interval to exclude unfeasible scenarios: scenarios with 2009 $\delta^{13}C$ values outside the range -43 to -38 ‰ and any scenarios with $\delta^{13}C$ values outside the range -400 to -30 ‰ are excluded. Selected scenarios were subsequently tested through the forward model, which is computationally expensive. In total, 50 000 000 and 78 125 000 individual scenarios using 3rd and 4th degree polynomials were evaluated, respectively. The results of the firn modeling can be found in Fig. 4.6 for both the 3rd and 4th degree results. The best scenario is the one leading to the smallest root mean squared deviation (RMSD)

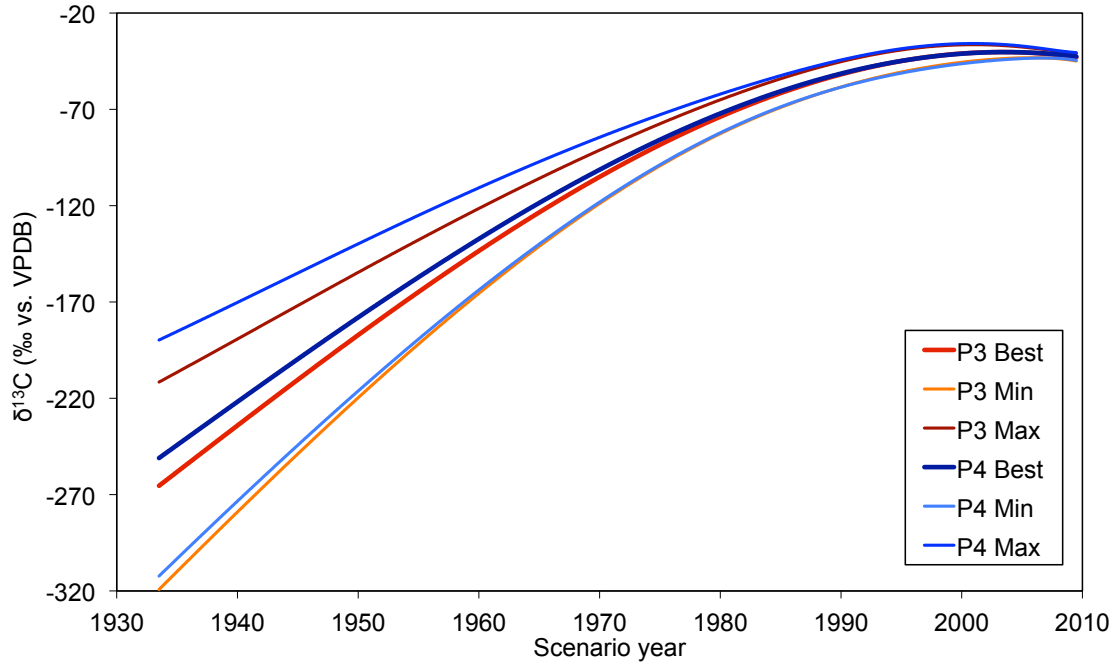

Figure 4.6. Reconstructed $\delta^{13}C$ scenarios for CFC-12 from 1933 to 2009; Best scenarios, maxima, and minima. P3 and P4 indicate 3rd and 4th degree polynomial firn model results, respectively.

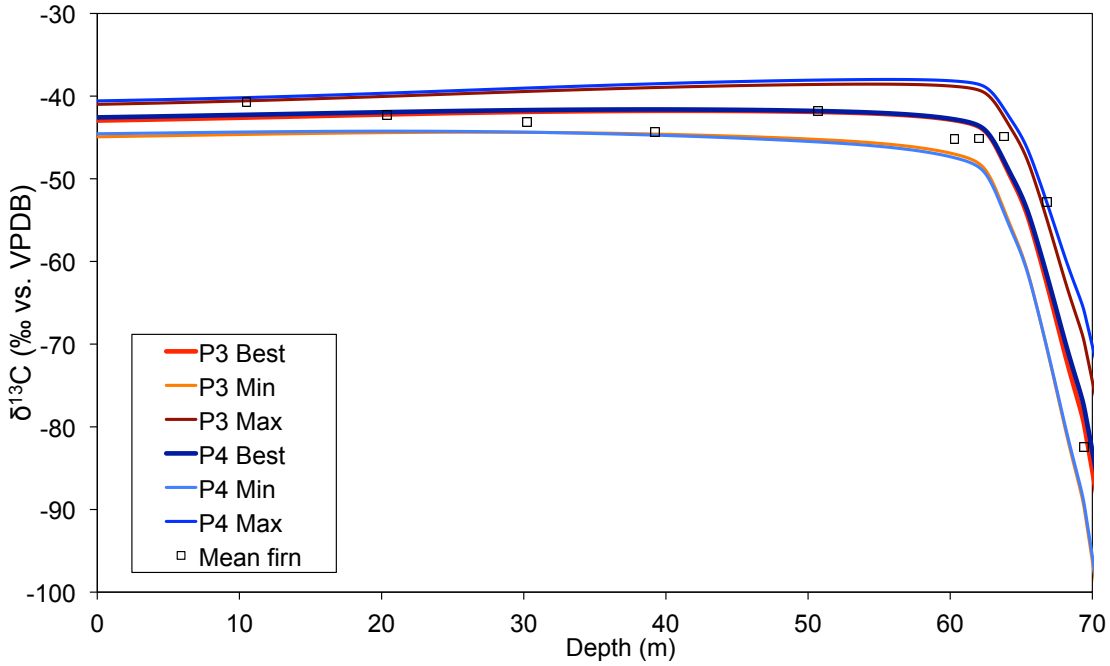

Figure 4.7. 3rd and 4th degree polynomial forward model results and mean firn data with depth. The envelopes show the overall minimum and maximum values of all selected scenarios.

between modeled and observed $\delta^{13}C$ (mean of two measurements at each depth) in the firn, which is shown in Fig. 4.7. Best RMSDs are 3.7 ‰ and 3.6 ‰ with the 3rd and 4th degree polynomial setups respectively. The envelopes shown on Figs. 4.6 and 4.7 show the overall minimum and maximum values of all selected scenarios (6809 and 8280 selected scenarios for 3rd and 4th degree polynomials, respectively).

In Fig. 4.6, an increase of $\delta^{13}C$ with time is seen, at approximately 5 ‰ per year from model start to 1960, but thereafter increasing less rapidly and leveling out to 0 ‰ per year by 2000, and remaining more or less constant until model end date. The best solutions obtained with the 3rd and 4th degree polynomials are consistent. Envelopes are somewhat larger for the 4th degree as compared to the 3rd degree polynomial scenarios. This is expected, as the 4th degree polynomial has an additional degree of freedom.

To assess the magnitude of induced fractionation from diffusion and gravitational effects in the firn, we run the forward model with a constant atmospheric $\delta^{13}C$ value with time of -40 ‰ (see e.g. Trudinger et al., 1997). The results (Fig. 4.8) show that the fractionation with depth due to diffusion and gravitational effects is limited to less than 1 ‰. This is not unexpected as the high molecular weight of CFC-12 leads to small fractional mass differences between the two isotopologues (0.8 %), and thus reduces the magnitude of these effects. By contrast, for $\delta^{13}C(CH_4)$, where the fractional mass difference is much larger (6 %), diffusion and gravitational effects are more significant (Bräunlich et al., 2001; Sapart et al., 2012, manuscript in preparation). Since the effect of fractionation in firn is small compared to observed variations of $\delta^{13}C$ of CFC-12 with depth, large variations of atmospheric $\delta^{13}C$ (CFC-12) must have occurred in the past.

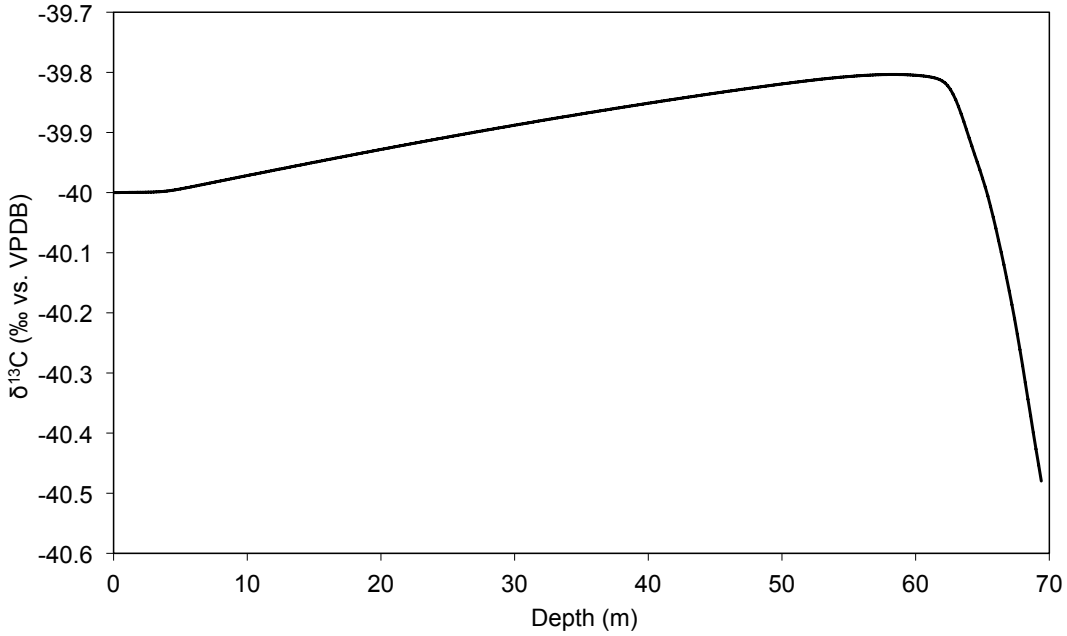

Figure 4.8. Modeled fractionation effects from diffusion and gravitation based on a constant atmospheric δ^{13}C (-40‰) with time scenario input to the forward model.

Besides fractionation, the transport of gases through the firn also induces mixing by molecular diffusion: concentration gradients between the top of the firn and the bottom of the diffusive zone are smoothed (Bräunlich et al., 2001; Buizert et al., 2011). Therefore, the strong δ^{13}C depletion at the deepest level in the firn where mixing ratios are low implies extreme depletions in the atmosphere (to -265 and -250 ‰ for the 3rd and 4th degree best scenarios, respectively).

4.3.3 Isotope mass-balance interpretation

In order to aid interpretation of atmospheric trends of δ^{13}C as indicated by the scenario in terms of CFC-12 production (unknown δ^{13}C source signature) and loss (photochemical fractionation measured as enrichment), we use an isotope mass-balance calculation (Eq. 4.2 - 4.6, Röckmann et al., 2003). The overall mass balance for CFC-12 is:

$$\frac{dn}{dt} = P - Jn \qquad (4.2)$$

where n is the number of moles of the compound in the atmosphere, and P is the magnitude of the emission rate of CFC-12 to the atmosphere. J, the stratospheric photolysis (first order) rate constant, is equal to $1/\tau$ where τ is the atmospheric lifetime.

Additionally, the heavy isotopologue equivalent of eq. 4.2 describes the contributions of the source and the sink to the atmospheric stable isotope signature as follows (Röckmann et al., 2003):

$$\frac{d[(1+\delta)n]}{dt} = P(1+\delta_{\mathrm{P}}) - Jn(1+\delta)(1+\varepsilon) \tag{4.3}$$

where δ and δ_{P} are the atmospheric and emission stable carbon isotope ratios of the CFC-12, respectively; ε is the fractionation inherent in the sink.

We expand Eq. 4.3 to:

$$\frac{dn}{dt} + \delta\frac{dn}{dt} + n\frac{d\delta}{dt} = P(1+\delta_{\mathrm{P}}) - Jn(1+\delta+\varepsilon+\delta\varepsilon) \tag{4.4}$$

Substituting eq. 4.2 we derive:

$$n\frac{d\delta}{dt} = P(\delta_{\mathrm{P}} - \delta) - Jn(1+\delta)\varepsilon \tag{4.5}$$

Solving for δ_{P} gives:

$$\delta_{\mathrm{P}} = \frac{\left[n\frac{d\delta}{dt} + Jn(1+\delta)\varepsilon\right]}{P} + \delta \tag{4.6}$$

To initialize the calculation based on this equation, n is based on mean atmospheric mixing ratio reconstructed from emissions estimates verified with ALE/GAGE/AGAGE data where available (Walker et al., 2009). P is back calculated from dn/dt. J is based on an atmospheric lifetime of 100 years (Forster et al., 2007). For δ, the 4th degree-polynomial best-fit scenario is used. $d\delta/dt$ is the CFC-12 atmospheric isotope ratio change per timestep.

Finally, ε is estimated at -35 ‰, approximately half of the laboratory measured isotopic fractionation at stratospheric temperatures (Zuiderweg et al., 2012). The magnitude of the fractionation directly observed in photolysis experiments is suppressed by the effect of mixing in the stratosphere. It has been shown through the stable isotope measurement of stratospheric samples that apparent (observed) fractionations in $\delta^{13}C$ of CH_4 and $\delta^{15}N$ and $\delta^{18}O$ in N_2O (which is similarly removed through UV photolysis) are approximately half of fractionations obtained from laboratory experiments (Röckmann et al., 2003; Kaiser et al., 2006; Röckmann et al., 2011).

The parameterization was run in yearly intervals, from 1955 to 2000. The start date was chosen because it is the mean age plus 1σ of the deepest sample. Results from the mass balance calculation are shown in Fig. 4.9. The reconstructed stable carbon isotope ratio δ_P of the CFC-12 source changes considerably during the period concerned; it starts very depleted near 1950 and increases strongly. The increase slows down with time and during the last 10 years of the parameterization δ_P begins to decrease. However, this decrease may not be significant given the small changes in the mixing ratio and the correspondingly large uncertainties in the net emissions.

In order to illustrate the influence of the sink fractionation effect in the model, the mass balance model was run to simulate the atmospheric $\delta^{13}C$ assuming a constant source delta, δ_P, of -45 ‰, the median value during the period 1955-2000. *P, L,* and ε are the same as above, and the starting (1955) $\delta^{13}C$ is set as -45 ‰. The resulting trend (Fig. 4.9, in green) shows that our firn air measurements can be explained only if we assume that the isotope signature of the sources changed significantly over time. Furthermore, modeling of a hypothetical scenario with *P* set to 0 (thus indicating atmospheric trends in the future when atmospheric release has ceased and the sink

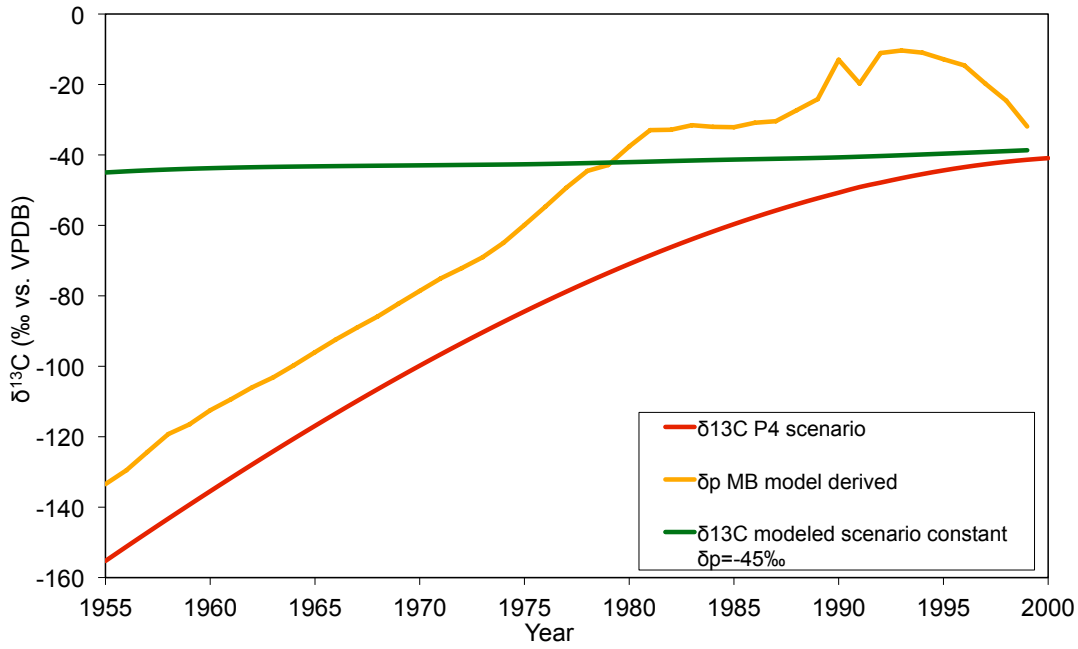

Figure 4.9. Temporal evolution of reconstructed atmospheric $\delta^{13}C$ values (‰, red, best fit 4th degree polynomial from firn air modeling) which are used as mass balance model input to calculate $\delta^{13}C$ of the CFC-12 source (δ_p, orange); mass balance calculated scenario with constant δ_p = -45‰ and initial (1955) δ of -45 ‰. (green).

fractionation drives CFC $\delta^{13}C$ evolution) indicated a systematic increase of only 0.29 ‰ per year.

The consistent increase in δ_P from the mass balance calculation prior to 1990 can potentially be explained by technological and industrial chemistry changes in the synthesis of CFC-12. Monocarbon chlorofluorocarbons may be synthesized by the following generalized reaction, either in the liquid, or more recently, in the gas phase at high temperatures and pressures:

$$CCl_4 + HF \xrightarrow{\text{catalyst}} CCl_3F + CCl_2F_2 + CClF_3 + HCl \qquad \text{(R4.3)}$$

The catalysts used for this reaction included $SbCl_5$ (first industrialization), or, more recently, various metallic and carbon compounds that promote chlorine-fluorine

exchange. By contrast, the first CFC synthesis experiments in the 1890s used SbF_3Br_2 or SbF_3Cl_2 as a reagent (Daudt and Youker 1935; Siegemund et al., 2003).

In addition to the above, the synthesis of the primary feedstock of CFC production, CCl_4, has changed significantly. Initially, synthesis was accomplished through the chlorination of CS_2. This was replaced within the last 50 years by the sequential chlorination of methane, which is a less polluting, though more technically challenging, process. Despite this, the older process was still in use, though at relatively small scale, in several locations (Rossberg et al., 2003).

The release of CFC to the atmosphere undergoes variable time delays due to its diverse uses (e.g. McCulloch et al., 2003). Produced CFC was released promptly (within a short time scale, 1 to 4.5 years) into the atmosphere through aerosol propellant use. On the other hand, the delay in CFC release to the atmosphere from non-hermetically sealed refrigeration and leakage from hermetically sealed refrigeration is difficult to quantify, with mean manufacturing to complete release times (total refrigerant release) approaching 10 years or more. As the production (and consequently sale and usage) of CFC is now restricted, release to the atmosphere in more recent times is most likely leakage-based, which clouds the global source picture considerably due to the introduced time lag. Moreover, leakage is a continuous process unless refrigerant is released through damage, thus the aggregate effect of leakage of CFC manufactured at different times and locations (with varying $\delta^{13}C$ values) can have a long-lasting impact. This can only be resolved by refining emissions functions by directly measuring leakage rates and surveying produced CFC for $\delta^{13}C$.

4.4 Conclusion

We have presented $\delta^{13}C$ (CF_2Cl_2) results from firn air collected in 2009 at the NEEM site in Greenland, the reconstructed atmospheric trend of which implies very depleted $\delta^{13}C$ values in the middle of the last century, and a rapid enrichment (nearly 80 ‰) to the present day value near -40 ‰. Mass balance modeling indicates that changes in production processes of this compound must be responsible for most of this enrichment: indeed, process changes in the synthesis of both CFC-12 itself and the feedstock used in CFC production have occurred over the last 80 years, due to technological advances. Furthermore, mass balance calculations indicate that in the future, when the release of the CFC to the atmosphere has ceased, the fractionation due to the photochemical sink will enrich the atmospheric reservoir continuously.

Acknowledgements

NEEM is directed and organized by the Center of Ice and Climate at the Niels Bohr Institute and US NSF, Office of Polar Programs. It is supported by funding agencies and institutions in Belgium (FNRS-CFB and FWO), Canada (NRCan/GSC), China (CAS), Denmark (FIST), France (IPEV, CNRS/INSU, CEA and ANR), Germany (AWI), Iceland (RannIs), Japan (NIPR), Korea (KOPRI), The Netherlands (NWO/ALW), Sweden (VR), Switzerland (SNF), United Kingdom (NERC) and the USA (US NSF, Office of Polar Programs).

Additional thanks to Zoe Courville of USACE Engineer Research and Development Center, Cold Regions Research and Engineering Laboratory, Hanover, USA for participation in the NEEM firn air sampling campaign.

References

Advanced Global Atmospheric Gases Experiment (AGAGE) data. Available online: http://agage.eas.gatech.edu/data.htm, 2011.

Archbold, M. E., Redeker, K. R., Davis, S., Elliot, T., and Kalin, R. M.: A method for carbon stable isotope analysis of methyl halides and chlorofluorocarbons at pptv concentrations, *Rapid Commun. Mass Sp.,* **19**, 337–340, doi:10.1002/rcm.17, 2005.

Bahlmann, E., Weinberg, I., Seifert, R., Tubbesing, C., and Michaelis, W.: A high volume sampling system for isotope determination of volatile halocarbons and hydrocarbons, *Atmos. Meas. Tech.*, **4**, 2073-2086, doi:10.5194/amt-4-2073-2011, 2011.

Bender, M. L., Sowers, T., Barnola, J. M., and Chappellaz, J.: Changes in the O_2/N_2 ratio of the atmosphere during recent decades reflected in the composition of air in the firn at Vostok Station, Antarctica. *Geophys. Res. Lett.*, **21(3),** 189–192, doi:10.1029/93GL03548, 1994.

Bock, M., Schmitt, J., Behrens, M., Möller, L., Schneider, R., Sapart, C. and Fischer, H.: A gas chromatography/pyrolysis/isotope ratio mass spectrometry system for high-precision δD measurements of atmospheric methane extracted from ice cores. *Rapid Comm. in Mass Spec.*, **24**, 621–633. doi: 10.1002/rcm.4429, 2010.

Bräunlich, M., Aballain, O., Marik, T., Jöckel, P., Brenninkmeijer, C. A. M., Chappellaz, J., Barnola, J.-M., Mulvaney, R., and Sturges, W. T.: Changes in the global atmospheric methane budget over the last decades inferred from 13C and D isotopic analysis of Antarctic firn air, J. Geophys. Res., 106, 20,465–20,481, doi:10.1029/2001JD900190, 2001.

Brenninkmeijer, C. A. M., Janssen, C., Kaiser, J., Röckmann, T., Rhee, T. S., and Assonov, S. S.: Isotope effects in the chemistry of atmospheric trace gases, *Chem. Rev.*, **103**, 5125-5162, 2003.

Buizert, C., Martinerie, P., Petrenko, V. V., Severinghaus, J. P., Trudinger, C. M., Witrant, E., Rosen, J. L., Orsi, A. J., Rubino, M., Etheridge, D. M., Steele, L. P., Hogan, C., Laube, J. C., Sturges, W. T., Levchenko, V. A., Smith, A. M., Levin, I., Conway, T. J., Dlugokencky, E. J., Lang, P. M., Kawamura, K., Jenk, T. M., White, J. W. C., Sowers, T., Schwander, J. and Blunier, T.: Gas transport in firn: multiple-tracer characterisation and model intercomparison for NEEM, Northern Greenland, *Atmos. Chem. Phys. Discuss.,* **11**, 15975 - 16021, 2011

Butler, J. H., Battle, M., Bender, M. L., Monzka, S. A., Clarke, A. D., Saltzman, E. S., Sucher, C. M., Severinghaus, J. P., and Elkins, J. W.: A record of atmospheric halocarbons during the twentieth century from polar firn air. *Nature*, **399**, 749 - 755, 1999.

Daudt, H. W. and Youker, M. A.: Patent No. 2,005,706, Organic Fluorine Compound. *United States Patent Office*, 1935.

Chen, N. H. and Othmer, D. F.: New Generalized Equation for Gas Diffusion Coefficient. *J. Chem. Eng. Data*, **7**, 1, 37–41, doi: 10.1021/je60012a011, 1962.

Etheridge, D. M., Steele, L. P., Francey, R. J., and Langenfelds, R. L.: Atmospheric methane between 1000 A.D. and present: Evidence of anthropogenic emissions and climatic variability, *J. Geophys. Res.*, **103(D13),** 15,979–15,993, doi:10.1029/98JD00923, 1998.

Etheridge, D., Rubino, M., Courteaud, J., Patrenko, V., and Courville, Z.: The NEEM 2009 firn air program: field report on sampling and analysis activities. Available: http://neem.dk, 2009.

Forster, P., Ramaswamy, V., Artaxo, P., Berntsen, T., Betts, R., Fahey, D. W., Haywood, J., Lean, J., Lowe, D.C., Myhre, G., Nganga, J., Prinn, R., Raga, G., Schulz, M. and Van Dorland, R. Changes in Atmospheric Constituents and in Radiative Forcing. *Climate Change 2007: The Physical Science Basis. Contribution of Working Group I to the Fourth Assessment Report of the Intergovernmental Panel on Climate Change* [Solomon, S., Qin, D., Manning, M., Chen, Z., Marquis, M., Averyt, K.B., Tignor, M., and Miller, H.L. (eds.)]. Cambridge University Press, Cambridge, United Kingdom and New York, NY, USA, 2007.

Francey, R. J., Manning, M. R., Allison, C. E., Coram, S. A., Etheridge, D. M., Langenfelds, R. L., Lowe, D. C., and Steele, L. P.: A history of $\delta^{13}C$ in atmospheric CH_4 from the Cape Grim Air Archive and Antarctic firn air. *J. Geophys. Res.*, **104(D19),** 23,631–23,643, doi:10.1029/1999JD900357, 1999.

Goldstein, A. H. and Shaw, S. L.: Isotopes of volatile organic compounds: an emerging approach for studying atmospheric budgets and chemistry. *Chem. Rev.*, **103**, 5025–5048, 2003.

Kaiser, J., Engel, A., Borchers, R., and Röckmann, T.: Probing stratospheric transport and chemistry with new balloon and aircraft observations of the meridional and vertical N_2O isotope distribution. *Atmos. Chem. Phys*., **6**, 4273-4324, SRef-ID: 1680-7375/acpd/2006-6-4273, 2006.

Laube, J. C., Kaiser, J., Sturges, W. T., Bönisch, H., and Engel, A.: Chlorine Isotope Fractionation in the Stratosphere. *Science*, **329(5996)**, 1167, DOI:10.1126/science.1191809, 2010a.

Laube, J. C., Martinerie, P., Witrant, E., Blunier, T., Schwander, J., Brenninkmeijer, C. A. M., Schuck, T. J., Bolder, M., Röckmann, T., van der Veen, C., Bonisch, H., Engel, A., Mills, G. P., Newland, M. J., Oram, D. E., Reeves, C. E., and Sturges, W.

T.: Accelerating growth of HFC-227ea (1,1,1,2,3,3,3-heptafluoropropane) in the atmosphere, *Atmos. Chem. Phys.*, **10**, 5903-5910, 2010b.

Mak, J.E. and Brenninkmeijer, C.A.M.: Compressed air sample technology for isotopic analysis of atmospheric carbon monoxide, *J. Atmos. Ocean Tech.,* **11(2)**, 425-431, 1994.

Martinerie, P., Nourtier-Mazauric, E., Barnola, J.-M., Sturges, W. T., Worton, D. R., Atlas, E., Gohar, L. K., Shine, K. P., and Brasseur, G. P.: Long-lived halocarbon trends and budgets from atmospheric chemistry modelling constrained with measurements in polar firn. *Atmos. Chem. Phys.,* **9,** 3911-3934, doi:10.5194/acp-9-3911-2009, 2009.

McCulloch, A., Midgley, P. M., and Ashford, P.: Releases of refrigerant gases (CFC-12, HCFC-22 and HFC-134a) to the atmosphere. *Atmos. Env.*, **37**, 7, 889-902, doi:10.1016/S1352-2310(02)00975-5, 2003.

Mead, M. I., Khan, M. A. H., Bull, I. D., White, I. R., Nickless, G., and Shallcross , D. E.: Stable carbon isotope analysis of selected halocarbons at parts per trillion concentration in an urban location. *Environ. Chem.* **5**, 340, doi:10.1071/EN08037, 2008.

Molina, M. J. and Rowland, F. S.: Stratospheric sink for chlorofluoromethanes: Chlorine atom catalyzed destruction of ozone. *Nature,* **249**, 810-814, 1974.

Monteil, G., Houweling, S., Dlugockenky, E. J., Maenhout, G., Vaughn, B. H., White, J. W. C., and Rockmann, T.: Interpreting methane variations in the past two decades using measurements of CH_4 mixing ratio and isotopic composition, *Atmos. Chem. Phys.*, **11**, 9141-9153, doi:10.5194/acp-11-9141-2011, 2011.

Redeker, K. R., Davis, S., and Kalin, R. M.: Isotope values of atmospheric halocarbons and hydrocarbons from Irish urban, rural, and marine locations, *J. Geophys. Res.*, **112**, D16307, doi:10.1029/2006JD007784, 2007.

Röckmann, T., Kaiser, J., Brenninkmeijer, C. A. M.: the isotopic fingerprint of the pre-industrial and the anthropogenic N_2O source. *Atmos. Chem. Phys.*, **3**, 315-323, 2003.

Röckmann, T., Brass, M., Borchers, R., and Engel, A.: The isotopic composition of methane in the stratosphere: high-altitude balloon sample measurements, *Atmos. Chem. Phys.*, **11**, 13287-13304, doi:10.5194/acp-11-13287-2011, 2011.

Rommelaere, V., Arnaud, L., and Barnola, J.-M.: Reconstructing recent atmospheric trace gas concentrations from polar firn and bubbly ice data by inverse methods, *J. Geophys. Res.*, **102(D25)**, 30,069–30,083, doi:10.1029/97JD02653, 1997.

Rossberg, M., Lendle, W., Pfleiderer, G., Tögel, A., Dreher, E., Langer, E., Rassaerts, H., Kleinschmidt, P., Strack, P., Cook, R., Beck, U., Lipper, K., Torkelson, T. R., Löser, E., Beutel, K. K., and Mann, T.: Chlorinated Hydrocarbons. *Ullmann's Encyclopedia of Industrial Chemistry*, 6th edition, Wiley-VCH, 2003.

Schmitt, J., Schneider, R., and Fischer, H.: A sublimation technique for high-precision measurements of $\delta^{13}CO_2$ and mixing ratios of CO_2 and N_2O from air trapped in ice cores, *Atmos. Meas. Tech.*, **4**, 1445-1461, doi:10.5194/amt-4-1445-2011.

Schwander, J., Barnola, J. M., Andrie, C., Leuenberger, M., Ludin, A., Raynaud, D., and Stauffer, B.: The age of the air in the firn and the ice at Summit, Greenland, *J. Geophys. Res.-Atmos.*, **98**, 2831–2838, 1993.

Seinfeld, J. H. and Pandis, S. N.: *Atmospheric Chemistry and Physics: from Air Pollution to Climate Change*, John Wiley and Sons, New York, 1326 pp., 1998.

Severinghaus, J. P., Grachev, A., and Battle, M.: Thermal fractionation of air in polar firn by seasonal temperature gradients, *Geochem. Geophys. Geosyst*., **2**, 1048, doi:10.1029/2000GC000146, 2001.

Severinghaus, J. P., Albert, M. R., Courville, Z. R., Fahnestock, M. A., Kawamura, K., Montzka, S. A., Mühle, J., Scambos, T. A., Shields, E., Shuman, C. A., Suwa, M., Tans, P., and Weiss, R. F.: Deep air convection in the firn at a zero-accumulation site, central Antarctica, *Earth and Planet. Sci. Lett.*, **293**, 359-367, doi:10.1016/j.epsl.2010.03.003, 2010.

Siegemund, G., Schwertfeger, W., Feiring, A., Smart, B., Behr, F., Vogel, H., and McKusick, B.: Organic Fluorine Compounds. *Ullmann´s Encyclopedia of Industrial Chemistry*, 6th edition, Wiley-VCH, 2003.

Sowers, T., Rodebaugh, A., Yoshida, N., and Toyoda, S.: Extending records of the isotopic composition of atmospheric N_2O back to 1900 a.d. from air trapped in snow at South Pole, in: 1st international symposium on isotopomers, (Ed) Yoshida, N., Yokohama, Japan, 2001.

Sturrock, G. A., Etheridge, D. M., Trudinger, C. M., Fraser, P. J., and Smith, A. M.: Atmospheric histories of halocarbons from analysis of Antarctic firn air: Major Montreal Protocol species, *J. Geophys. Res.*, **107(D24)**, 4765, doi:10.1029/2002JD002548, 2002.

Trudinger, C. M., Enting, L. G., Etheridge, D. M., Francey, R. J., Levchenko, V. A., Steele, L. P., Raynaud, D., and Arnaud, L.: Modeling air movement and bubble trapping in firn, *J. Geophys. Res.*, **102(D6)**, 6747–6763, doi:10.1029/96JD03382, 1997.

United Nations Environment Program (UNEP) Ozone Secretariat data. Available http://ozone.unep.org/, 2011.

Walker, S. J., Weiss, R. F., and Salameh, P. K.: Reconstructed histories of the annual mean atmospheric mole fractions for the halocarbons CFC-11, CFC-12, CFC-113 and Carbon Tetrachloride. Available: http://bluemoon.ucsd.edu/pub/cfchist/, 2009.

Wang, Z., Chappellaz, J., Martinerie, P., Park, K., Petrenko, V., Witrant, E., Blunier, T., Brenninkmeijer, C. A. M., and Mak, J. E.: The isotopic record of Northern Hemisphere atmospheric carbon monoxide since 1950, implications for the CO budget, Atmos. Chem. Phys. Discuss., 11, 30627-30663, doi:10.5194/acpd-11-30627-2011, 2011.

Witrant, E., Martinerie, P., Hogan, C., Laube, J. C., Kawamura, K., Capron, E., Montzka, S. A., Dlugokencky, E. J., Etheridge, D., Blunier, T., and Sturges, W. T.: A new multi-gas constrained model of trace gas non-homogeneous transport in firn: evaluation and behavior at eleven polar sites, Atmos. Chem. Phys. Discuss., 11, 23029-23080, doi:10.5194/acpd-11-23029-2011, 2011.

World Meteorological Organization (WMO), *Global Ozone Research and Monitoring Project Report No. 52: Scientific Assesment of Ozone Depletion 2010*, available: http://ozone.unep.org, 2010.

Zuiderweg, A., Holzinger, R. and Röckmann, T.: Analytical system for stable carbon isotope measurements of low molecular weight (C_2-C_6) hydrocarbons. *Atmos. Meas. Tech.,* **4**, 1161-1175, DOI: 10.5194/amt-4-1161-2011, 2011.

Zuiderweg, A., Kaiser, J., Laube, J. C., Röckmann, T., and Holzinger, R.: Stable carbon isotope fractionation in the UV photolysis of CFC-11 and CFC-12, *Atmos. Chem. Phys.*, **12**, 4379-4385, doi:10.5194/acp-12-4379-2012, 2012.

Zuiderweg, A.: Measurement of stable carbon isotope ratios of non-methane hydrocarbons and halocarbons. Thesis, Utrecht University, The Netherlands, 2012.

Chapter 5: Appendices

Abstract

In the following appendices additional data is presented to support and complete chapter 4.

Appendix A contains measurements of CFC-12 from CARIBIC I project flight 26 (return). The samples, collected at 9.4-10.7 km altitude through the CARIBIC instrument container whole air sampler, were measured for CFC-12 mixing ratio and $\delta^{13}C$ on the non-methane hydrocarbon instrument detailed in chapter 2. Mean mixing ratio and $\delta^{13}C$ values from these samples were (532.7 ± 53) ppt and (-44.7 ± 0.65) ‰ vs. VPDB. As these values were measured at an upper troposphere/lower stratosphere altitude well below the lowest atmospheric photolysis height of CFC-12 and exhibit mixing ratio values similar to those measured in the troposphere, it is reasonable to assume that these are representative of the well mixed remote troposphere, and provide a reference point for comparison to measured urban and remote values.

Appendix B provides mixing ratio and $\delta^{13}C$ data of 7 non-methane hydrocarbons measured from the NEEM (Greenland) 2009 firn air sample set analyzed in chapter 4 for CFC-12. These samples were similarly measured on the Utrecht NMHC $\delta^{13}C$ instrument. This data has not been published as of yet but is included here for completeness. Notably, maxima in mixing ratio and minima in $\delta^{13}C$ values occur near 70 m depth for nearly all compounds, suggesting large-scale fresh emission at that depth. Carbon monoxide data from NEEM 2008 samples show a co-located maximum at this depth, which had been dated to 1975 through firn air modeling; the referenced publication proposes that these maxima were due to the increase of automobile traffic up until this date; thereafter the increased adoption of catalytic

converters is proposed as the cause of the decrease to present day levels. Whether the respective maxima and minima in the mixing ratio and $\delta^{13}C$ values are truly coincident in time with the CO maximum is a matter for further investigation by applying firn air modeling. The source of the fresh emission responsible for these features is also a subject for further study.

Appendix A: CARIBIC project flight 26 (return) CFC-12 mixing ratio and $\delta^{13}C$ data.

The results of measurement of a series of 12 samples obtained as part of the CARIBIC I project (Brenninkmeijer et al., 1999) are presented here. These samples are from flight 26 return (Male, Maldives, to Dusseldorf, Germany) on August 17th, 2000. These data are presented here as supporting data to ch. 4.

These samples were sourced from the whole air sampler installed in the CARIBIC I instrument container in the aircraft used, a specially modified LTU B767ER. The 300 L samples obtained were cryogenically distilled (Brenninkmeijer and Röckmann, 1996) to remove bulk gases and sealed in break seal ampoules. The contents of these ampoules have been shown to be stable over long periods of time and thus are valid for analysis (Pupek et al., 2005). A significant portion of these concentrates was used for analysis (e.g. Assonov et al., 2009); with the remnants resealed in glass break seal ampoules of 10 mL volume, two for each sample, providing for two independent measurements.

After breaking the seal, the contents of each ampoule was individually cryogenically extracted onto a stainless steel trap; thereafter the sample was desorbed and introduced to the system described in Ch. 2. CFC calibration procedures are described

Table A.1. CARIBIC $\delta^{13}C$ (‰ vs. VPDB) and mixing ratio (ppt) data from flight 26.

Flight Sample Number	Latitude (°N)	Longitude (°E)	Altitude AMSL[a] (m)	$\delta^{13}C$[b] mean (‰)	[Mean] (ppt)
1	9.55	69.52	9458	-44.5	526.3
2	13.78	66.02	9460	-45.6	526.4
3	18.03	62.39	9460	-44.9	484.2
4	22.47	59.10	9460	-44.4	557.5
5	26.31	54.99	9460	-45.1	553.2
6	31.19	52.32	9460	-44.5	520.7
7	35.99	49.50	9460	-44.8	504.8
8	38.42	43.79	9460	-44.3	601.0
9	41.53	38.52	9460	-45.6	496.9
10	43.47	32.10	10677	-44.3	520.3
11	46.01	25.13	10677	-44.6	564.4
12	47.79	17.59	10677	-43.9	534.6
			Mean	-44.7	532.7

a- Above mean sea level (meters)
b- $\delta^{13}C$ error = 0.65 ‰; all data vs. VPDB
c- Mixing Ratio error = 10%

in Ch. 3. $\delta^{13}C$ results from this instrument are presented in per mill difference against the international Vienna Pee Dee Belemnite standard (VPDB). All measured peaks were well separated and had a peak area larger than 1 Vs, well in excess of the minimum instrument linearity limit of 0.5 Vs (see chapter 2).

Table A.1 Presents means of $\delta^{13}C$ and mixing ratio for the sample series. Hereafter fig. A.1 contains the results of the two sets of measurements. Mean values for mixing ratio and $\delta^{13}C$ are (532.7 ± 10 %) ppt and (-44.7 ± 0.65) ‰ vs. VPDB respectively. These samples were taken at altitudes 9.4-10.7 km above mean sea level (AMSL); well below the level where atmospheric removal of CFC-12 by photolytic destruction takes place (19-34 km, Laube et al., 2010), and mixing ratio measurements are comparable to surface values (AGAGE 2012). As such, these UTLS samples may be taken as being representative of the well-mixed remote troposphere and can be used as a reference point to compare other $\delta^{13}C$ values. For example, Bahlmann et al.

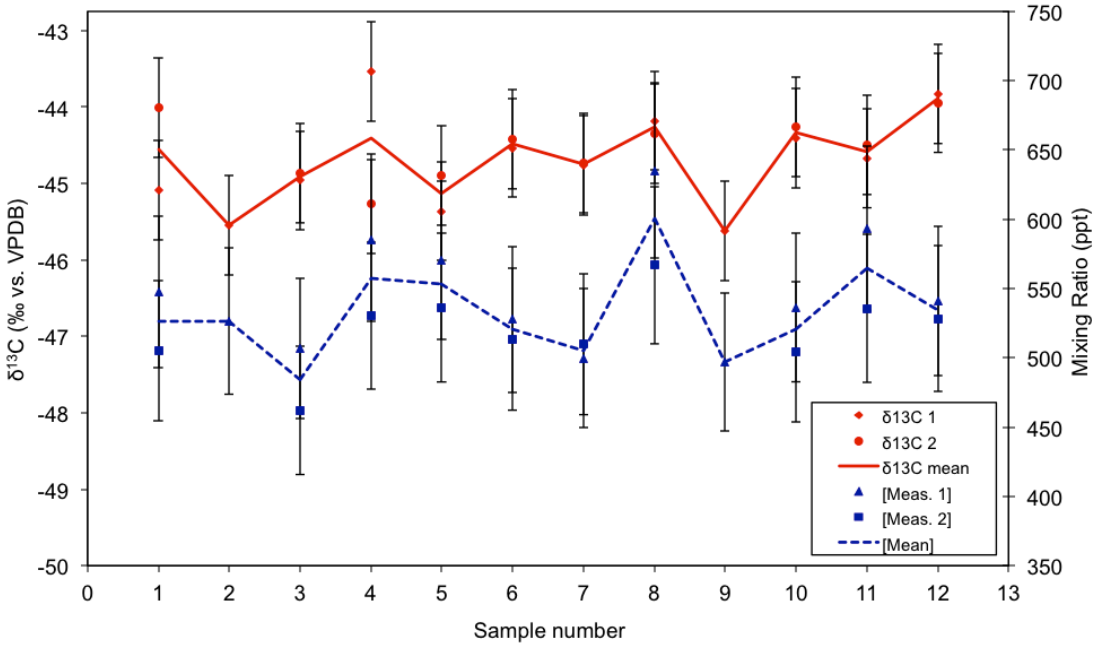

Figure A.1. CARIBIC $\delta^{13}C$ (‰ vs. VPDB) and mixing ratio measurements, series 1 and 2 and means. Errors as above.

(2011) report (-41.2 ± 0.2) ‰ from the North Sea island of Sylt, Germany, and measured values from NEEM (Greenland) project 2009 firn air samples reported in chapter 4 have near-surface (recent) values between -40 and -45 ‰ vs. VPDB.

Urban CFC-12 $\delta^{13}C$ values have been noted to be more enriched than those from remote locations (Archbold et al., 2005; Redeker et al., 2007). The reason for this difference is unknown. Urban emission is known to continue at low levels in the developing world and China (McCulloch et al., 2003; WMO 2010; UNEP 2011), but as chlorofluorocarbon compounds are strongly regulated in Western Europe this result is rather unexpected. CFC-12 based refrigeration and propellant use has been phased out and emissions should have been curtailed (WMO 2010; UNEP 2011).

Appendix B: NEEM 2009 Firn Air Hydrocarbon Data

A series of 12 large volume firn air samples were obtained from the S2 firn borehole at the North Greenland Emian Ice Drilling (NEEM) site (77°25.898´N, 51°06.448´W, 2484m above sea level), collected as part of the summer 2009 firn air program. These samples were extracted from the borehole through a firn air sampling system described in detail in Etheridge et al., (2009) and stored in 5 L Luxfer cylinders at 120 bar.

The contents of the sample cylinders were measured twice for mixing ratio and $\delta^{13}C$ using the instrument and calibration procedures described in chapters 2 and 4. $\delta^{13}C$ results from this instrument are presented in per mill difference against the international Vienna Pee Dee Belemnite standard (VPDB). Mixing ratio measurements have 10% error, and $\delta^{13}C$ error levels are described in table B.1.

Presented here are the 7 most complete hydrocarbon compound series as a supplement to data collected and analyzed in ch. 4. These selected compounds had peak area values above the instrument critical linearity threshold of 0.5 Vs above which instrument calibration is valid. Tables B.2 and B.3 contain mean mixing ratio and $\delta^{13}C$ data per depth. In each table the data point with the greatest $\delta^{13}C$ depletion (in table B.2) and highest mixing ratio (in table 3) for each compound are printed in bold. Following, plots (figs. B.1-7) of the vertical profiles of mixing ratio and $\delta^{13}C$ of each compound are presented for independent measurements 1 and 2. Qualitatively, it is notable that in nearly all samples presented here that the highest mixing ratios and the most depleted $\delta^{13}C$ values are nearly collocated at depths between 66.8-71.9 m. The co-occurrence of high mixing ratio and depleted $\delta^{13}C$ values suggest large-scale

Table B.1. $\delta^{13}C$ error levels

Compound	Error (‰)
Acetylene	0.44
Ethane	0.28
Propane	0.40
Isobutane	0.54
n-Butane	0.48
Hexane	1[a]
Benzene	0.48

a- Estimate, no direct calibration available

Table B.2. Mixing ratio mean data in ppt. σ = 10%

Depth (m)	Acetylene	Ethane	Propane	Isobutane	n-Butane	Hexane	Benzene
10.5	92.1	1017.7	249.4	49.6	83.5	7.2	**58.9**
20.4	130.7	1277.5	422.0	88.0	125.3	-	-
30.2	260.9	1403.5	524.5	92.0	180.6	14.4	78.5
39.2	215.9	1337.6	500.7	96.9	158.8	-	-
50.7	191.4	1340.2	530.2	105.7	194.8	19.0	118.6
60.3	203.8	1376.4	512.9	96.8	198.0	29.7	70.3
62.0	218.8	1370.9	530.4	106.1	201.0	-	-
63.8	243.0	1486.5	595.1	118.1	239.3	-	-
66.8	324.7	1710.8	702.9	129.5	290.5	**183.5**	157.5
69.4	661.9	1959.3	753.1	**115.9**	**327.5**	27.2	53.7
71.9	**1078.7**[a]	**1779.1**	**577.4**	90.3	201.7	-	-
73.6	607.1	1589.8	518.2	78.5	184.8	11.1	109.3

a – Bold indicates most depleted $\delta^{13}C$

Table B.3. $\delta^{13}C$ mean data in ‰ vs. VPDB. σ as defined above.

Depth (m)	Acetylene	Ethane	Propane	Isobutane	n-Butane	Hexane	Benzene
10.5	12.2	-24.1	-28.9	-27.9	-30.2	-31.4	-27.9
20.4	5.5	-25.6	-28.2	-31.6	-28.2	-	-
30.2	-14.2	-27.6	-29.6	-29.1	-30.4	-31.7	-24.3
39.2	-9.6	-27.2	-29.6	-31.3	-28.8	-	-
50.7	1.5	-25.8	-28.1	-28.7	-28.3	-28.3	-22.8
60.3	1.1	-26.4	-28.5	-28.4	-28.7	-37.9	-25.6
62.0	-1.6	-26.5	-29.3	-29.7	-29.0	-	-
63.8	1.0	-26.2	-28.8	-29.5	-28.9	-	-
66.8	-2.7	-27.3	-30.1	**-29.8**	-29.9	**-46.3**	**-27.4**
69.4	-16.0	**-30.6**	**-31.4**	-29.9	**-30.4**	-30.3	-22.4
71.9	**-21.3**[a]	-30.9	-31.5	-29.7	-29.1	-	-
73.6	-15.4	-29.8	-30.6	-25.9	-28.9	-31.3	-24.9

a – Bold indicates highest mixing ratio

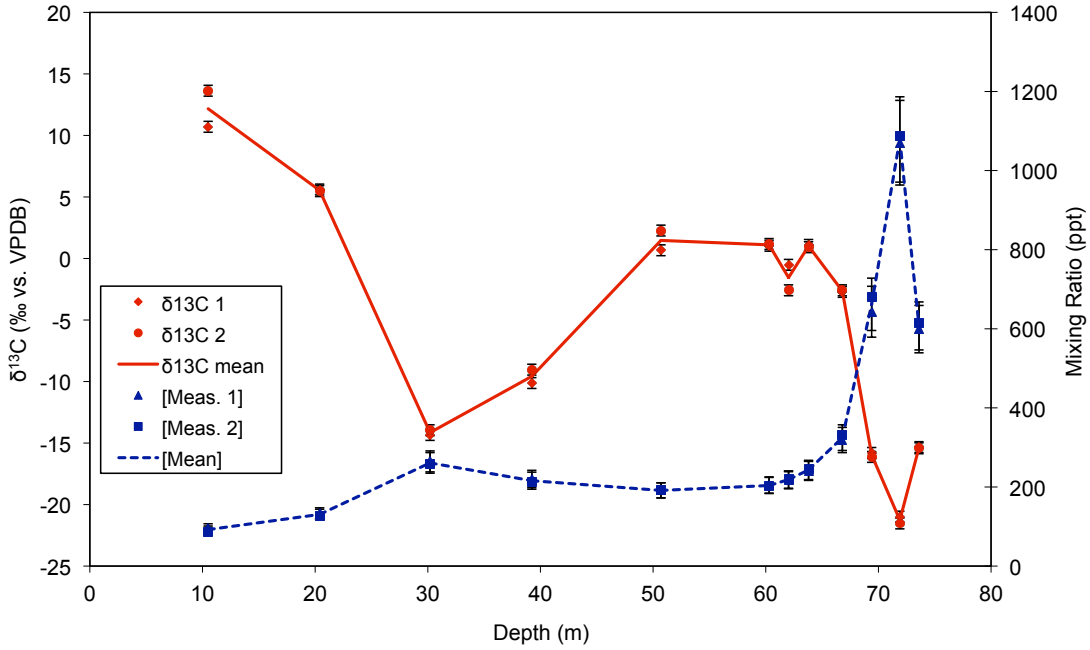

Figure B.1. Acetylene $\delta^{13}C$ (‰, vs. VPDB) and Mixing ratio (ppt) series with depth, measurements 1 and 2.

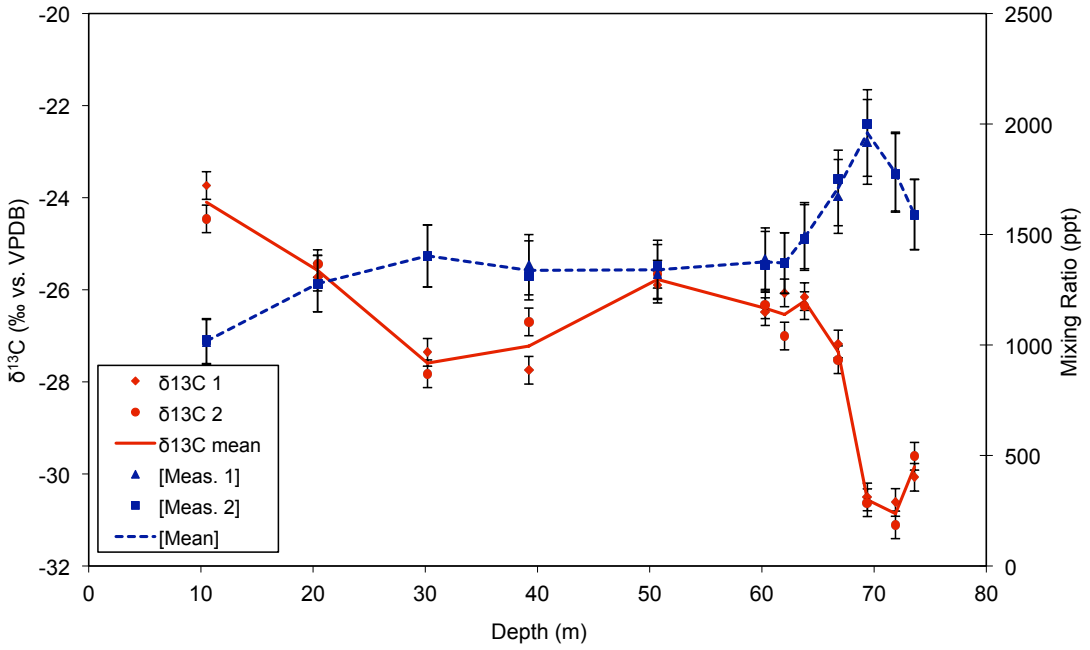

Figure B.2. Ethane $\delta^{13}C$ (‰, vs. VPDB) and Mixing ratio (ppt) series with depth, measurements 1 and 2.

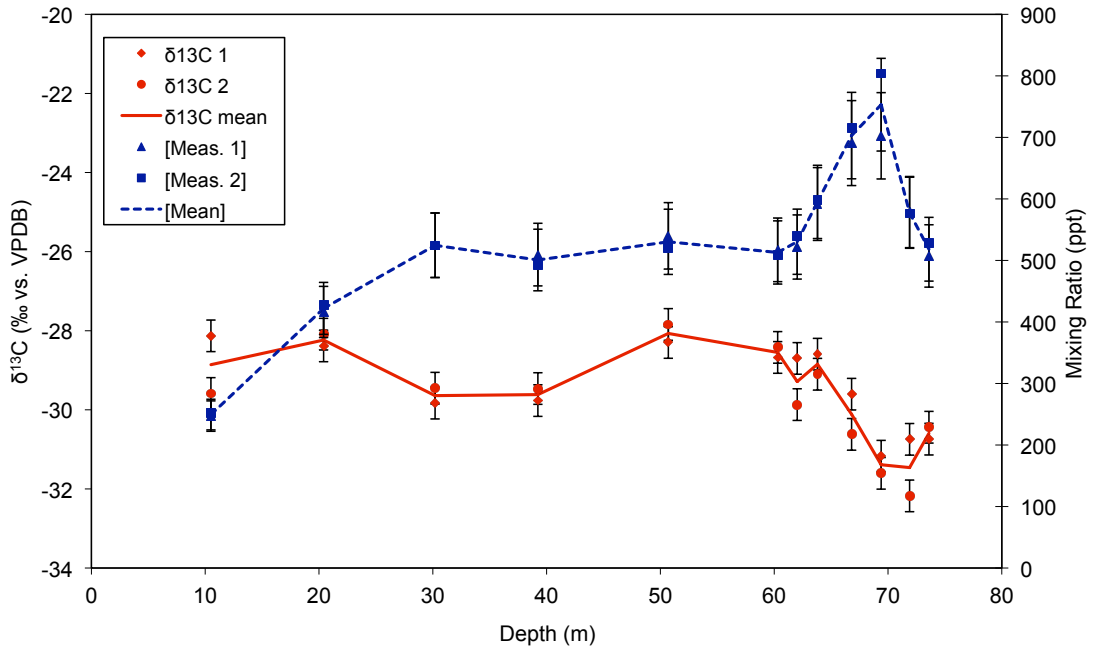

Figure B.3. Propane $\delta^{13}C$ (‰, vs. VPDB) and Mixing ratio (ppt) series with depth, measurements 1 and 2.

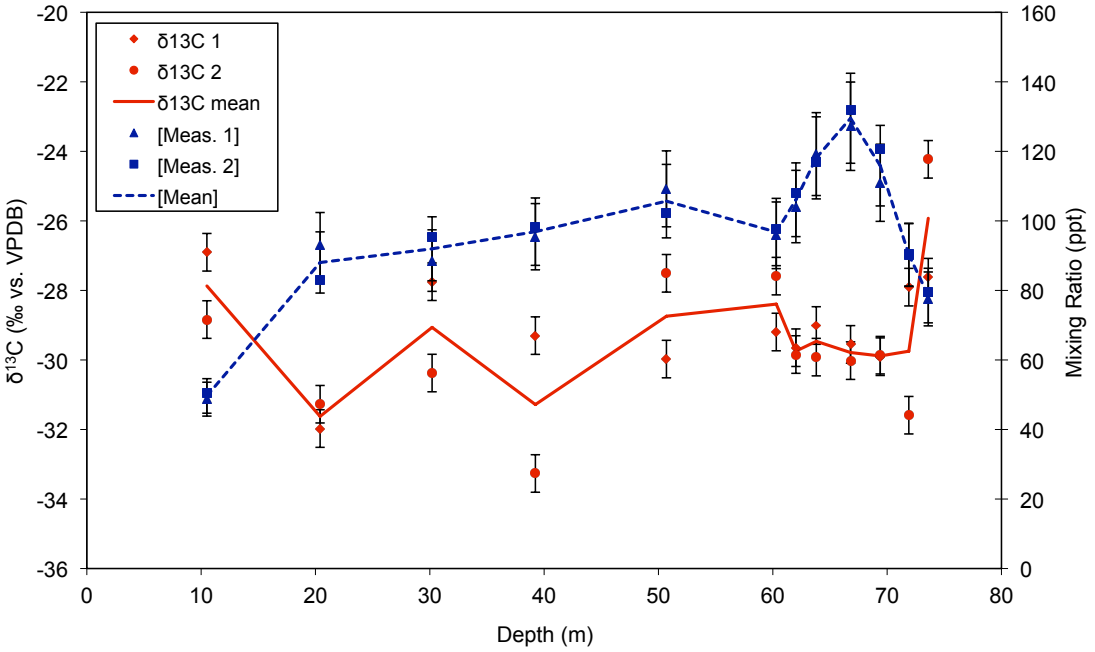

Figure B.4. Isobutane $\delta^{13}C$ (‰, vs. VPDB) and Mixing ratio (ppt) series with depth, measurements 1 and 2.

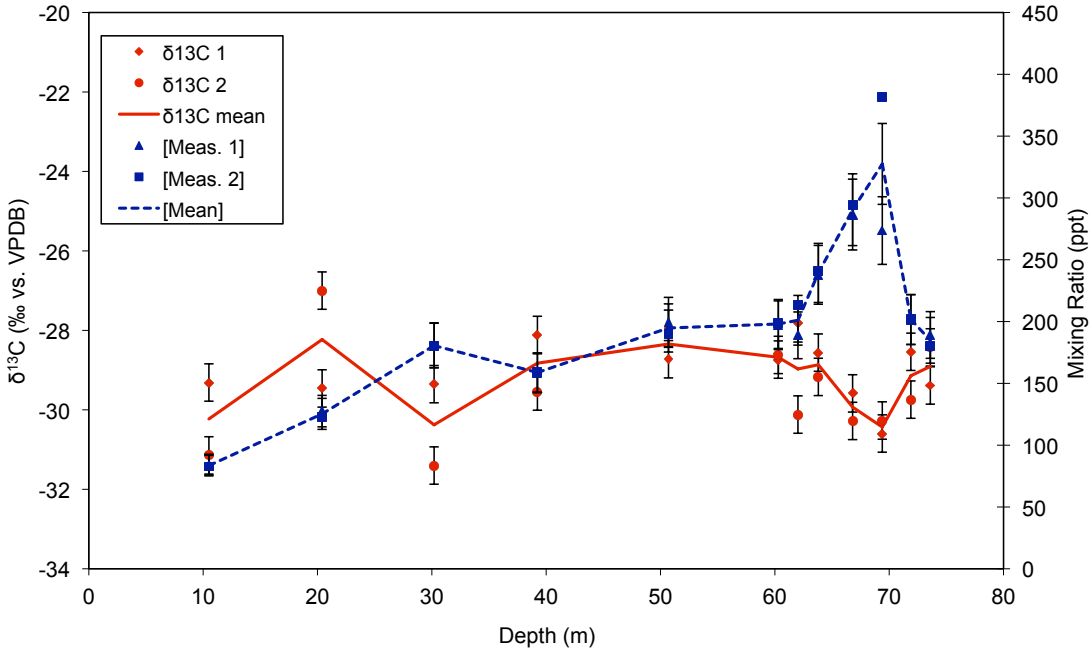

Figure B.5. n-Butane $\delta^{13}C$ (‰, vs. VPDB) and Mixing ratio (ppt) series with depth measurements 1 and 2.

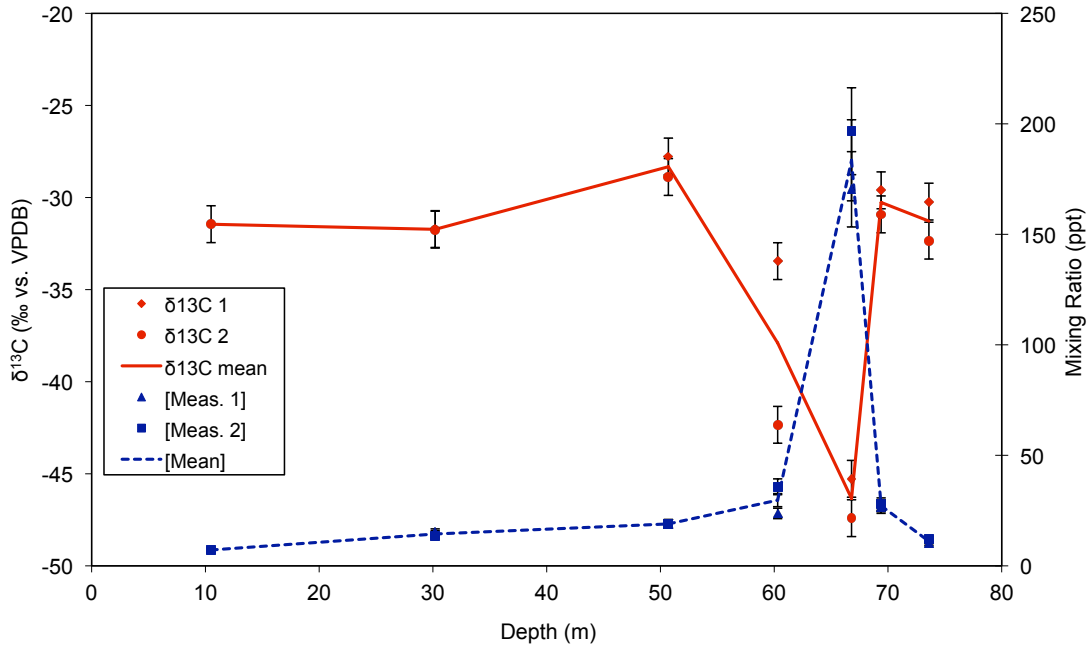

Figure B.6. Hexane $\delta^{13}C$ (‰, vs. VPDB) and Mixing ratio (ppt) series with depth, measurements 1 and 2.

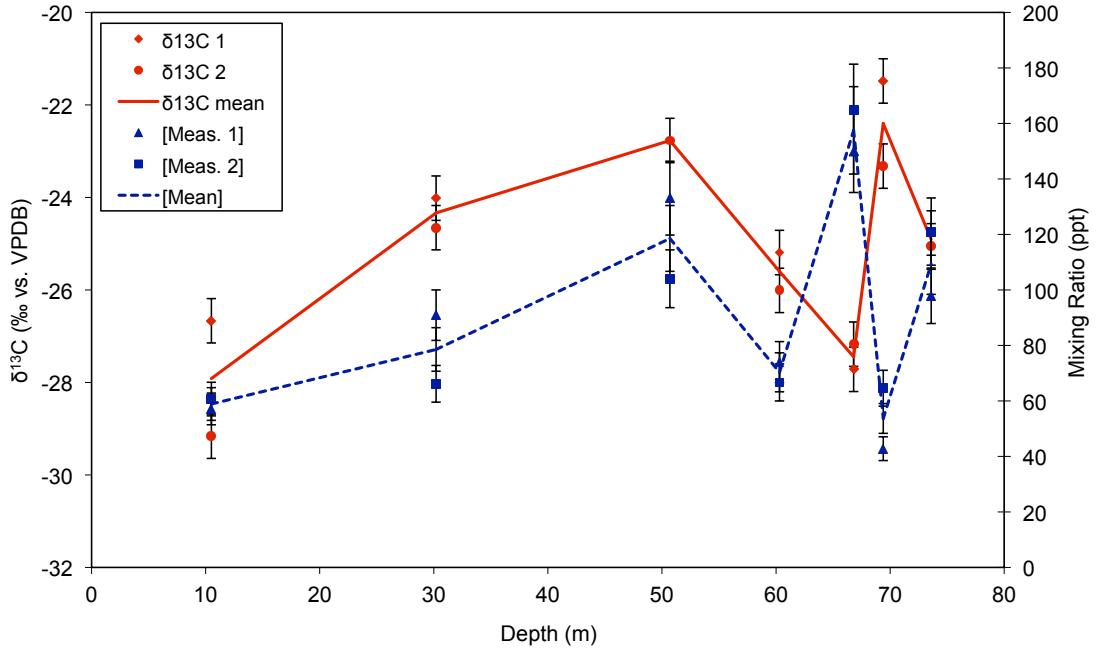

Figure B.7. Benzene $\delta^{13}C$ (‰, vs. VPDB) and Mixing ratio (ppt) series with depth, measurements 1 and 2.

minimally OH-aged emission of the compounds concerned (Rudolph and Czuba 2000).

Wang et al. (2011) note mixing ratio peaks in the carbon monoxide record from NEEM 2008 samples at 70 m depth. Firn air modeling similar to that used in chapter 4 estimates 1975 as the date for the CO maximum seen. The rise in CO from 145 to 150 ppb prior to this date is ascribed to the increase of automobile use prior to 1975. The decrease to 130 ppb that follows after that date is speculated to be caused by the adoption of catalytic converters that catalyze the further oxidation of CO to CO_2 and also reduce the emission of uncombusted hydrocarbons to improve urban air quality (Wang et al., 2011).

Whether the NMHC mixing ratio peaks and depleted $\delta^{13}C$ values in the firn air data reported are truly coincident with the CO peak noted in the firn is a matter for detailed further study. At the very least, firn air modeling with appropriate diffusion constants and accounting for seasonality (as the upper 30 m of the firn is affected by

seasonal variations) and diffusive mixing ratio and $\delta^{13}C$ effects is vital for further interpretation. Also, whether the cause for the peak and subsequent decrease in NMHC mixing ratio is truly the result of automotive catalytic converter installation is certainly up for debate; alternatively, large scale biomass burning in the taiga regions of northern Canada could also be responsible as this is transported towards Greenland (Forster et al., 2001). The black and organic carbon content of compacted Greenland snow and ice of equivalent age may serve to be useful to evaluate the source of these emissions (Bond et al., 2007).

References

Advanced Global Atmospheric Gases Experiment (AGAGE) data. Available online: http://agage.eas.gatech.edu/data.htm, 2012.

Archbold, M. E., Redeker, K. R., Davis, S., Elliot, T., and Kalin, R. M.: A method for carbon stable isotope analysis of methyl halides and chlorofluorocarbons at pptv concentrations, *Rapid Commun. Mass Sp.,* **19**, 337–340, doi:10.1002/rcm.17, 2005.

Assonov, S. S., Brenninkmeijer, C. A. M., Koeppel, C. and Röckmann, T.: CO_2 isotope analyses using large air samples collected on intercontinental flights by the CARIBIC Boeing 767. *Rapid Comm. in Mass Spec.*, **23**, 822–830, doi:10.1002/rcm.3946, 2009.

Bahlmann, E., Weinberg, I., Seifert, R., Tubbesing, C., and Michaelis, W.: A high volume sampling system for isotope determination of volatile halocarbons and hydrocarbons, *Atmos. Meas. Tech.*, **4**, 2073-2086, doi:10.5194/amt-4-2073-2011, 2011.

Bond, T. C., Bhardwaj, E., Dong, R., Jogani, R., Jung, S., Roden, C., Streets, D. G., and Trautmann, N. M.: Historical emissions of black and organic carbon aerosol from energy-related combustion, 1850–2000, *Global Biogeochem. Cycles*, **21**, GB2018, doi:10.1029/2006GB002840, 2007.

Brenninkmeijer, C. A. M., and Röckmann, T.: Russian Doll Type Cryogenic Traps: Improved Design and Isotope Separation Effects, *Anal. Chem.,* **68**, 3050-3053, 1996.

Brenninkmeijer, C. A. M., Crutzen, P. J., Fischer, H., Güsten, H., Hans, W., Heinrich, G., Heintzenberg, J., Hermann, M., Immelmann, T., Kersting, D., Maiss, M., Nolle, M., Pitscheider, A., Pohlkamp, H., Scharffe, D., Specht, K., and Wiedensohler, A.: CARIBIC—Civil Aircraft for Global Measurement of Trace Gases and Aerosols in

the Tropopause Region. *J. Atmos. Oceanic Technol.*, **16**, 1373–1383, doi: 10.1175/1520-0426, 1999.

Etheridge, D., Rubino, M., Courteaud, J., Patrenko, V., and Courville, Z.: *The NEEM 2009 firn air program: field report on sampling and analysis activities.* Available: http://neem.dk, 2009.

Forster, C., Wandinger, U., Wotawa, G., James, P., Mattis, I., Althausen, D., Simmonds, P., O'Doherty, S., Kleefeld, C., Jennings, S. G., Schneider, J., Trickl, T., Kreipl, S., Jäger, H., and Stohl, A.: Transport of boreal forest fire emissions from Canada to Europe, *J. Geophys. Res.*, **106**, 22887–22906, 2001.

Laube, J. C., Kaiser, J., Sturges, W. T., Bönisch, H., and Engel, A.: Chlorine Isotope Fractionation in the Stratosphere. *Science*, **329(5996)**, 1167, DOI:10.1126/science.1191809, 2010.

Pupek, M., Assonov, S. S., Mühle, J., Rhee, T. S., Oram, D., Koeppel, C., Slemr, F. and Brenninkmeijer, C. A. M.: Isotope analysis of hydrocarbons: trapping, recovering and archiving hydrocarbons and halocarbons separated from ambient air. *Rapid Comm. in Mass Spec.*, **19**, 455–460, doi:10.1002/rcm.1812, 2005.

Redeker, K. R., Davis, S., and Kalin, R. M.: Isotope values of atmospheric halocarbons and hydrocarbons from Irish urban, rural, and marine locations, *J. Geophys. Res.*, **112**, D16307, doi:10.1029/2006JD007784, 2007.

Rudolph, J. and Czuba, E.: On the use of isotopic composition measurements of volatile organic compounds to determine the "photochemical age" of an air mass, *Geophys. Res. Lett.,* **27, 23**, 3865–3868, 2000.

United Nations Environment Program (UNEP) Ozone Secretariat data. Available http://ozone.unep.org/, 2011.

Wang, Z., Chappellaz, J., Martinerie, P., Park, K., Petrenko, V., Witrant, E., Blunier, T., Brenninkmeijer, C. A. M., and Mak, J. E.: The isotopic record of Northern Hemisphere atmospheric carbon monoxide since 1950, implications for the CO budget, *Atmos. Chem. Phys. Discuss.*, **11**, 30627-30663, doi:10.5194/acpd-11-30627-2011, 2011.

World Meteorological Organization (WMO), *Global Ozone Research and Monitoring Project Report No. 52: Scientific Assesment of Ozone Depletion 2010*, available: http://ozone.unep.org, 2010.

Future Perspectives

The completion of an instrument capable of measuring both mixing and stable carbon isotope ratios of hydrocarbons and halocarbons is an important development for the Utrecht Atmospheric Physics and Chemistry Group laboratory, as it allows for broad opportunities for measurement in isotope sciences. Now that this instrument has been tested and successfully applied, measurement possibilities abound, both within the original framework of the instrument and requiring its adaptation for new roles.

For example, the first applications of the instrument may be expanded upon. Additional research into hydro- and halocarbon stable isotope ratio content in urban situations may further the understanding of diurnal and seasonal variation of the anthropogenic emission of these compounds. This could be accomplished through an expanded regular on-line sampling campaign in Utrecht, along the lines of what was accomplished for chapter 2. Alternatively, sample collection and off-line analysis from e.g. the CABAUW tower site 20 km to the southeast of Utrecht in a rural area, which already hosts the infrastructure for an extended cylinder sampling campaign, might be worthwhile for study as a comparison.

Complete analysis of CARIBIC I project concentrates, as mentioned in chapter 5, is also a great opportunity, giving insight into global remote troposphere NMHC isotope distributions. The samples from flights to diverse locations such as Southern Africa or sub-tropical regions of Central and South America remain available and viable for analysis. In particular, analysis of equator-crossing flights, such as flight 30, from Munich, Germany to Cape Town, South Africa v.v. may be particularly valuable in this regard (see http://www.caribic-atmospheric.com/). This flight crosses several regions with intense biomass burning for energy use, and signals of fresh emission

may be clearly present in the samples. Also, as the aircraft samples are obtained from 9-11 km altitudes during all flights, crossing of the tropopause could have occurred, and stratospheric air might be sampled as a result. If so, departures from tropospheric $\delta^{13}C$ values might be expected, giving insight to the magnitude of stratosphere-troposphere transport and removal processes at high altitudes.

Another point of interest is further study of historical samples such as air that has been trapped in firn (see chapter 4) or stored flask samples. Analyzing samples from different geographic locations, including e.g. Antarctic samples could give clues to global surface trends and better examine the true cause of the large fresh hydrocarbon emission present in NEEM samples at depth (see chapter 5).

Further analysis of chlorofluorocarbon effects could also be pursued. Further defining the fractionation inherent in the UV sink in terms of wavelength, pressure and temperature dependency through more reactor experiments with differing UV light sources, along the lines of that done in chapter 3 might be valuable. Exploring the cause of the as-yet-unexplained atmospheric $\delta^{13}C$ variation between urban and rural environments that is mentioned in chapter 4 also comes to mind. Atmospheric and source $\delta^{13}C$-CFC sampling may be a way forward to resolve this question. Also, stratospheric balloon sampling of CFC and subsequent analysis could potentially confirm the existence of the expected $\delta^{13}C$ gradient caused by the removal reactions.

In an entirely different direction, isotope studies of emissions of hydrocarbons directly from fresh and combusted plant material could contribute to the understanding of this contribution to the atmospheric budget of these compounds. Also, reactor studies of chemical reactions to establish diverse kinetic isotope effects at any number of temperatures and pressures could significantly contribute to the

current fractionation knowledgebase, similar to what has been accomplished in the Rudolph group at York University, Canada.

On the technical front, the instrument might still be further improved. First, an upgrade of the automation system might be considered to increase reliability and flexibility. The V25 hardware controller currently used (see chapter 2) is occasionally erratic in its behavior, requiring system resets to correct. Further, any change to the parameters of the system such as timing require edition of multiple command files, followed by a system restart. As a system restart commands all mass flow controllers to a zero setting for a short period, this action increases the chance of contamination affecting the following measurement. A modern hardware controller with features such as that afforded by e.g. LabVIEW would likely not have such drawbacks.

Secondly, the process timings for actions in the analysis procedure might be further optimized, in order to speed analysis times. Another technical improvement that might be undertaken is to devise a method to increase the instrument sensitivity, in order to decrease the necessary sample size for effective measurement. A possibility exists in the current system setup by selectively uncoupling the quadrupole mass spectrometer through use of a valve when it would not be needed for sample identification. This would allow the whole of the GC effluent to proceed to the isotope ratio mass spectrometer. Adjustments to carrier gas flow rates would have to be made to reduce the amount of sample lost through the open split. This would clearly increase the sensitivity of the system, though decreases in flow rates would lengthen GC elution times.

An important technical improvement that would allow the most groundbreaking research work in stable isotopes of non-methane hydrocarbons would be to convert the system to measure isotopes of hydrogen. Very few studies of δD in non-methane

hydrocarbons have been undertaken because of physical and technical challenges inherent in its measurement.

In principle it would seem simple to install a reduction oven to obtain molecular hydrogen from compounds in the place of the oxidation oven; however, there are complications. The minor stable isotope of hydrogen, deuterium, has a far lower mean abundance than ^{13}C: 0.015 % vs. 1.1%. Also, hydrogen has lower ionization efficiency in a mass spectrometer. On the other hand, there are many more hydrogen than carbon atoms in a hydrocarbon molecule: for an alkane NMHC species the formula is C_nH_{2n+2}. Nevertheless, measuring δD from ambient air would require samples more than ten times larger for acceptable signal due to low NMHC mixing ratios. Therefore any instrument sensitivity improvements would be of great use here as well.

Besides interest in new directions of isotope studies and determination of isotope effects in NMHC using stable hydrogen isotopes, a major point of interest lies in the contribution of non-methane hydrocarbons to the atmospheric molecular hydrogen budget. The oxidation of hydrocarbons results in the production of formaldehyde in the atmosphere. This is photolyzed by UV radiation to release hydrogen. The main interest in this reaction chain is to better understand the atmospheric molecular hydrogen budget. This is quite important at this moment in time as anthropogenic hydrogen release through spill and leakage is set to increase due to its likely adoption as a future energy carrier, overwhelming other sources. The future large increase in the mixing ratio of hydrogen may have impacts on other oxidative processes (as OH is the main H_2 sink) as well. Therefore, measuring the stable hydrogen isotope ratio of NMHC and studying how this transfers to molecular hydrogen would be a significant development.

The isotope measurement community is actively pursuing all these subjects to various degrees, and progress will forever continue on, with advances in technology and creativity in applications. Clearly the current instrument provides many opportunities to contribute to significant research, and technical advances in instrumentation can open new doorways to exciting possibilities. The Utrecht University NMHC $\delta^{13}C$ instrument is a valuable asset in the continuing studies of atmospheric chemistry: the compounds; their sources, sinks, properties and transformations; and the relative contribution of humanity to climate change and atmospheric pollution.

Acknowledgements

Without any doubt, my heartfelt thanks go to my supervisors Rupert and Thomas. In the end we got there! Thank you both for the opportunity and of course for all your support: from the very beginning when I was just starting out not knowing anything in atmospheric chemistry, through the protracted but ultimately successful production of this work. Most importantly however, thank you for your patience and wise advice despite all the difficult times.

For my colleagues at IMAU and in the APCG group in particular, it's been a privilege to work amongst you, though of course I haven't been around much lately. For all the help and advice I have benefitted from over the last 6 years, I truly thank you.

To all my dear friends all around the world: Catalina, Axel, and Vincent; Itzel and Julien; Ivan; Joseph; Carlos; Mauro; Motoki; Leticia, Stefan, and Thiago; Arjen; Hector; Esteban; Dewi; Célia; Guillaume; Christiana and Theofanis; Carina; Marianne; Susu; Helena and Ricard; Laia; Rene; Michal; Chino; Marja, Abram, and Arwin; Leonie and Pim; Shanna and many others: thank you for all the good times during my work and all the support for the difficult times, and of course thanks for giving me a swift kick in the backside when needed! Cheers!

Y a Margarita, Costy, Mark y Frani: Muchísimas gracias por brindarme constantemente todo su apoyo y ánimo! Ahora es muy importante recibirlos en la nueva casa y celebrar juntos nuestro nuevo comienzo con un gran asado. Vengan tan pronto como puedan, los espero con inmensas ansias!!! Abrazos.

Of course to my family: Lieve vader, moeder, zus: hartelijk dank voor alles! Het is zo'n opluchting voor mij en natuurlijk voor jullie ook dat ik het gehaald heb. Zonder

jullie steun was het nooit gelukt. Love you! Ook voor Maria, Gert, Arda, Tekla, en Tjip: het feest kan beginnen! Proost en tot snel!

A mi pololа Catalina, estoy en deuda contigo de manera inmensurable por tu paciencia, persistencia e infinito apoyo durante todos los retrasos y frustraciones que sufrí (sufrimos). Jamás lo hubiera logrado de otra manera, por lo que un millon-millon de gracias no son para nada suficientes, y ésto no lo olvidaré durante el resto de mi vida. Ahora continuamos con mejores cosas, un buen comienzo es la nueva casa en que estamos viviendo, para que disfrutemos juntos :-) Besos! Salud!

Curriculum Vitae

Adriaan T. Zuiderweg was born on May 27th 1979 in Nijmegen, The Netherlands. During his early years, his family moved several times, eventually emigrating to the United States. After graduation from Huron High School (Ann Arbor, class of 1997), he enrolled at the University of Michigan, attaining his Bachelor of Sciences in Atmospheric Science in May 2002, with a focus on mesoscale storm system phenomena and weather forecasting. Thereafter, he entered post-graduate study at Florida State University School of Meteorology (Tallahassee, Florida, US), obtaining the degree of Master of Science (Meteorology) in April 2006 with his thesis "Microwave Radiative Transfer Modeling of Ice in the Atmosphere", concentrating on radiative transfer and satellite remote sensing of the atmosphere under the supervision of Dr. Guosheng Liu. Seeking new challenges in late 2006, he returned to The Netherlands to accept a Ph.D. position at Universiteit Utrecht Institute of Marine and Atmospheric Research (IMAU), which resulted in the present work. He is currently employed at Mitutoyo Research Center Europe in Best, The Netherlands, in the position of Researcher, and resides in Utrecht together with his girlfriend Catalina.